OAK RIDGE NATIONAL LABORATORY LIBRARIES
3 4456 0599456 9

CENTRAL RESEARCH LIBRARY
ORNL-Annual 1971-72
cy 2

Oak Ridge National Laboratory

1971-72

OAK RIDGE NATIONAL LABORATORY
CENTRAL RESEARCH LIBRARY
DOCUMENT COLLECTION
LIBRARY LOAN COPY
DO NOT TRANSFER TO ANOTHER PERSON
If you wish someone else to see this document, send in name with document and the library will arrange a loan.
UCN-7969
(3 3-67)

Oak Ridge National Laboratory Annual Report 1971-72

Operated by Union Carbide Corporation for the U. S. Atomic Energy Commission

Editor: Barbara Lyon
Consulting Editor: A. H. Snell

Published with the assistance
of the Technical Publications, Graphic Arts, Photography,
and Reproduction Departments of the Information Division
Oak Ridge National Laboratory, P.O. Box X, Oak Ridge, Tennessee 37830

Photographs of animals and flowers found on the ORNL reservation were taken
by Jay Story and Fred Taylor of the Environmental Sciences Division

CHIPMUNK

Foreword:

Once again our Annual Report displays the many imaginative variations that ORNL plays each year on several basic themes: nuclear and nonnuclear energy systems, the environment, biomedical research and development, basic physical research. These are broad and divergent fields: they do not admit of simple or quick resolutions. A reader who follows these Annual Reports from year to year will notice steady movement toward clarifying some of the problems that face us, and may also find a number of flashes of scientific beauty. This year's report, as usual, represents only a sampling of the work at ORNL during the past year. I hope that these short essays and reports will encourage interested readers to go more deeply, and broadly, into the complex and diversified scientific and technical achievements of ORNL.

Though the report is necessarily incomplete, I find it an impressive account of work expertly performed by many dedicated people. I hope it conveys to the reader some of this spirit that makes ORNL so exciting a place in which science and technology continue to advance.

Alvin M. Weinberg

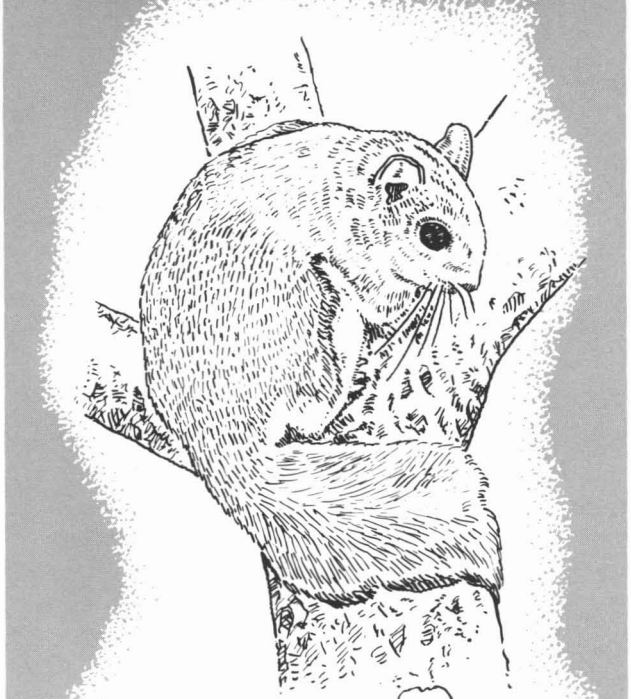

CONTENTS

FOREWORD 3
NUCLEAR ENERGY 6
Reactor Development 7
Nuclear Safety 22
Fusion Research 24
RESEARCH AND DEVELOPMENT 26
Physics 27
Chemistry 35
Mathematics 41
Life Sciences 43

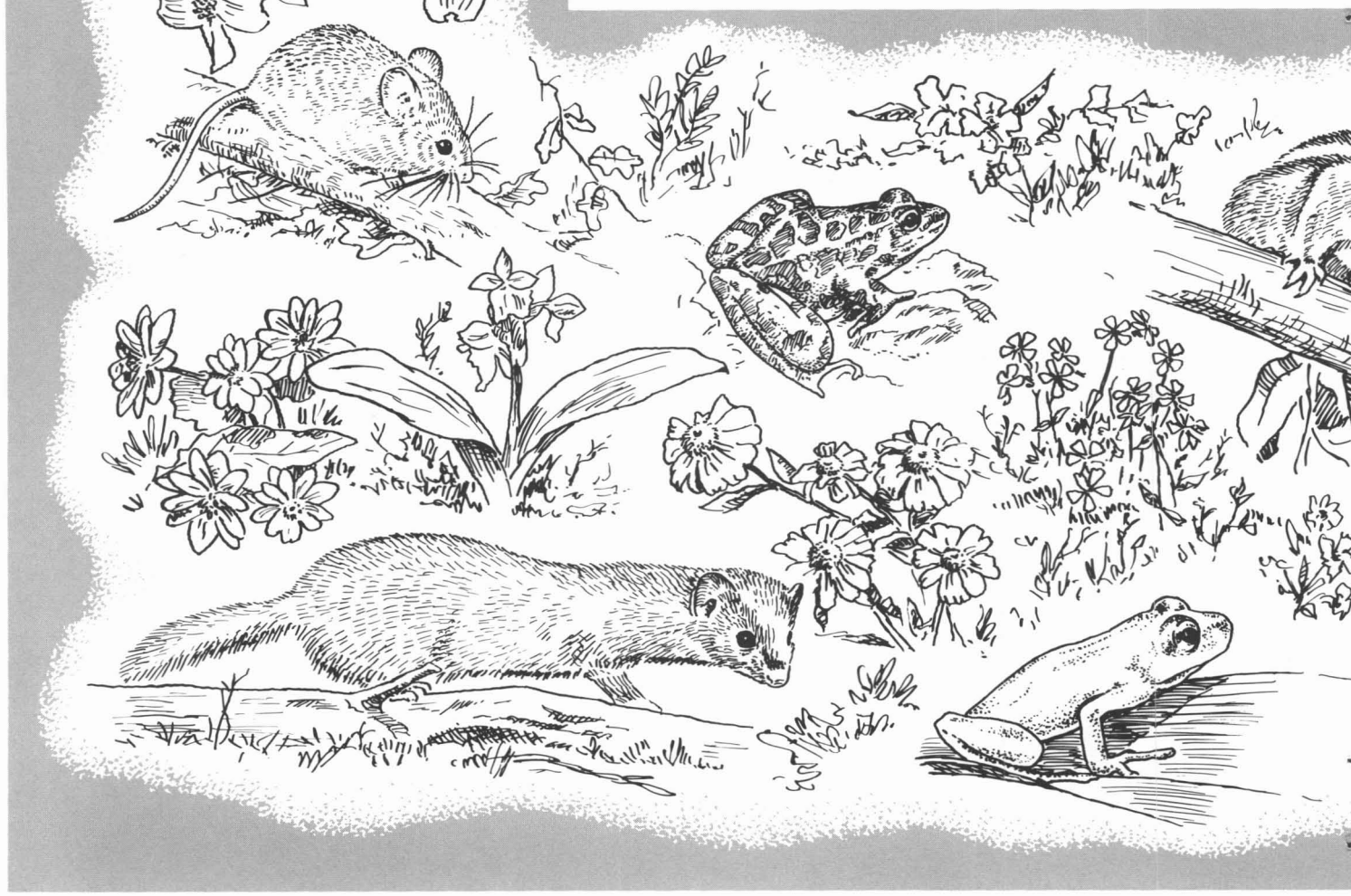

Instruments 52
Materials 54
ENVIRONMENT 58
NSF Environment—Energy Studies 59
Toxic Element Studies 61
Water Research 66
Environmental Impact Statements 70
CIVIL DEFENSE PROJECT 72
Hasty Winter Shelters 73
MEETINGS 76

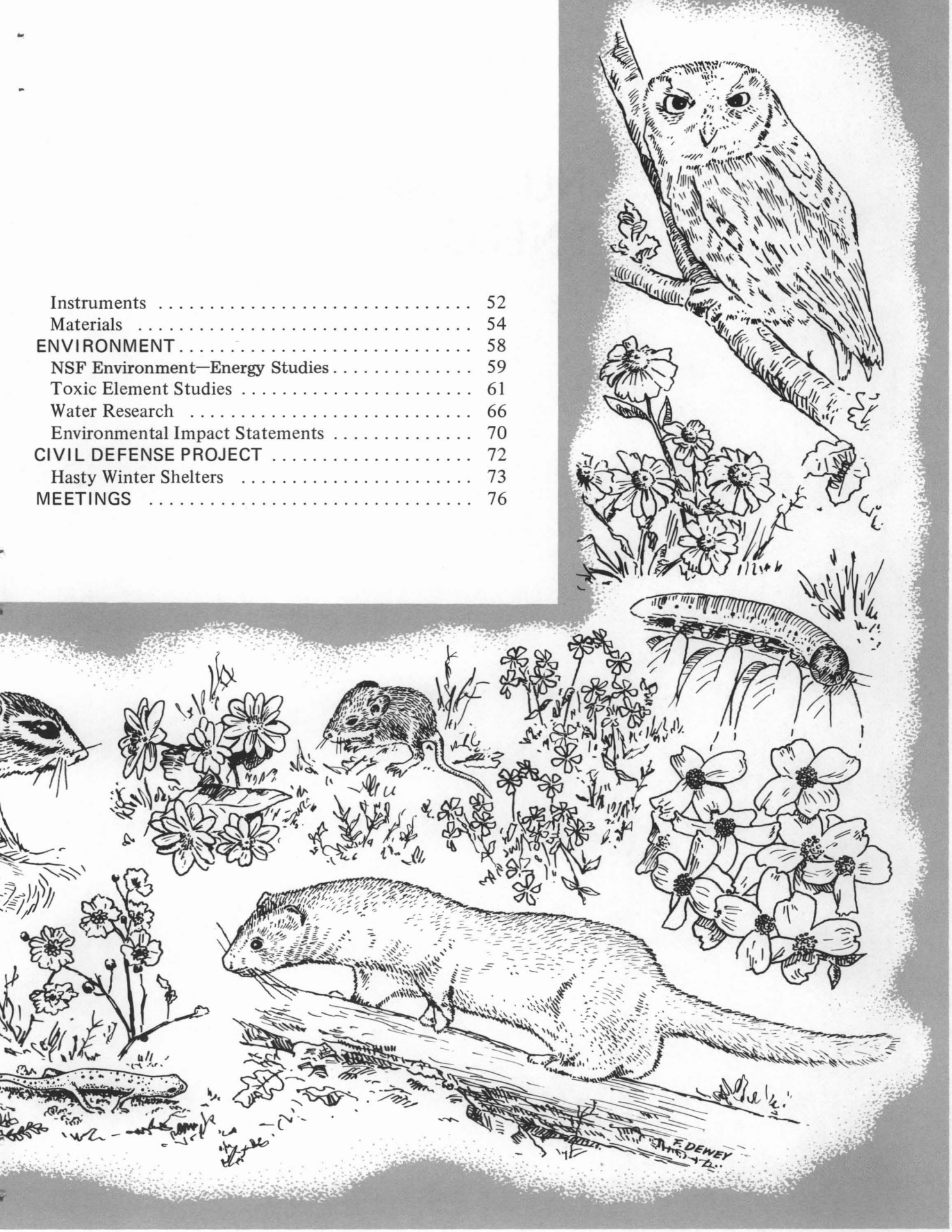

NUCLEAR ENERGY

Reactor Development

WILDLIFE AT ORNL SERVICEBERRY

Liquid-Metal Fast Breeder

Oak Ridge National Laboratory continues to play an active role in this country's highest priority civilian power reactor program, aimed at the timely introduction of LMFBR's. Roughly one-half of the Laboratory's reactor development effort is devoted to this cause, principally in the technical areas of fuels and materials, physics, fuel recycle, components, instrumentation and controls, safety, and core design. We have emphasized during the past year those aspects of the programs that are relevant to the Fast-Flux Test Facility (scheduled for criticality in June 1974) and the first demonstration plant (1978—1980). Some examples of activities and accomplishments in the areas of materials, components, shielding, and instrumentation and controls are presented here.

High-Temperature Structural Mechanics

Many of the structural components for liquid-metal-cooled fast breeder reactors (LMFBR's) will be designed to operate at temperatures and strain levels considerably higher than comparable parts in the more conventional water-cooled nuclear reactors. Under LMFBR conditions, structural materials tend to creep under load; progressive distortion takes place as temperatures oscillate ("thermal ratcheting"); large strains tend to concentrate in critical regions such as structural discontinuities; and fatigue and creep damage become complex, nonlinear phenomena involving temperature, time, and stress-strain relations. All of these effects are grouped under the general heading of inelastic materials behavior. Conventional design techniques, however, and the corresponding safety codes and standards are based largely on the laws of linear elasticity, which state that stresses and strains are uniquely determined by linear mathematical relations. Conventional methods are thus clearly inadequate for the design of LMFBR structural components.

The main purpose of the ORNL program on structural design methods and criteria for LMFBR's is to investigate the behavior of inelastic materials at elevated temperatures and to develop proven structural analysis methods for use in design. One of the items under investigation last year was the elastic-plastic behavior of type 304 stainless steel at high temperatures (up to 1200°F). This type of behavior is characterized by stresses above the yield strength and strains related to the stresses by nonlinear physical laws that depend

on temperature but not on time. The plastic parts of the strains are not recovered upon unloading, and their magnitudes depend heavily on the loading history of the structure.

In order to describe the mathematical relationships between stresses and strains (constitutive equations) for an elastic-plastic material, three fundamental ingredients are needed. These are (1) the initial yield condition in terms of all nine components of the stress tensor; (2) the flow rule, which defines an increment of nonrecoverable plastic strain in terms of the temperature and stress state and the changes in these variables from one loading condition to a subsequent condition; and (3) the hardening law, which describes the manner in which the initial yield condition changes as the material is stressed beyond the yield strength. Using these three rules and the general mathematical theory of plasticity, unique relations between stresses and strains can be expressed in terms of a plastic potential function called the yield function. The yield function describes a surface that can be represented as a convex hypersurface in nine-dimensional stress space where each dimensional direction in the hyperspace is denoted by one of the stress components in the stress tensor. Experiments, like the one shown in the photograph, are being conducted at temperatures that range from room temperature to 1200°F to obtain measured strains (using high-temperature strain gages) in terms of predetermined loading paths within the stress space. Thin-walled tubular specimens of

Ken Liu tests the behavior, under extremely high temperatures, of a leading contender for LMFBR structural material.

stainless steel, 1.25 in. in diameter, with a wall thickness of 50 mils (0.050 in.), are alternately pulled and pushed (uniaxial tension-compression tests) at stress levels up to ±45,000 psi. The specimens may also be pressurized and twisted in either direction, or loaded with arbitrary combinations of tension, torsion, and pressure, so that material behavior in several of the stress space dimensions can be investigated simulaneously.

From the room-temperature data we have deduced that the size of the yield surface remains essentially constant, independent of the loading path or the past loading history, but that it shifts in position as a function of the load. In addition, uniaxial data obtained at various temperature levels indicate that the size of the initial yield surface decreases as the temperature increases and is a function of the temperature alone. These two pieces of information enormously simplify the task of developing the required constitutive equations for LMFBR design application. Experiments are being conducted with combined stress states (tension and torsion, etc.) to determine the precise shape of the yield surface as a function of temperature and loading history.

The Sodium Shielding Experiment

The increasing use of reactors for power production is making it essential, for both economic and engineering reasons, that the radiation shields built around the reactors be carefully designed as integral parts of the systems and that extravagant ad hoc shield additions be avoided. The shield design for any new reactor plant must rely heavily on calculations that predict how radiation will interact with the materials in the various components of the system. Such calculations are extremely complicated and unfortunately are frequently based on tenuous interaction data. Confidence in a calculational technique often cannot be gained unless large uncertainties are removed through experiments which guide methods development and improvement of data.

During 1971, ORNL staff members performing shield calculations for the proposed LMFBR's were confronted with a need to reduce the uncertainty regarding the transport of neutrons through sodium. In the LMFBR systems a large thickness of liquid sodium will be present above the reactor core and will greatly influence the characteristics of the radiation incident on the shield. An experiment was called for — one in which a sample of sodium could be positioned adjacent to a reactor and accurate information obtained for verification of the calculational methods and interaction data. Such experiments are routine at the Tower Shielding Facility, but for the results to be reliable the samples must be effectively full scale. In this case full scale meant a 15-ft-thick sodium sample with lateral dimensions large enough to prevent leakage of the neutrons from the sides. Safely fabricating and transporting a "pure" sample of this size — 40 tons of sodium — was one of the more interesting tasks faced by ORNL engineers during the year.

As eventually fabricated, the sample consisted of four 11-ft-diam cylindrical aluminum tanks filled with frozen sodium; two were 5 ft thick and two were $2\frac{1}{2}$ ft thick. The 11,000 gal of sodium arrived in

A tank containing 40 tons of frozen sodium stands waiting to be evaluated for its shielding properties at ORNL's Tower Shielding Facility.

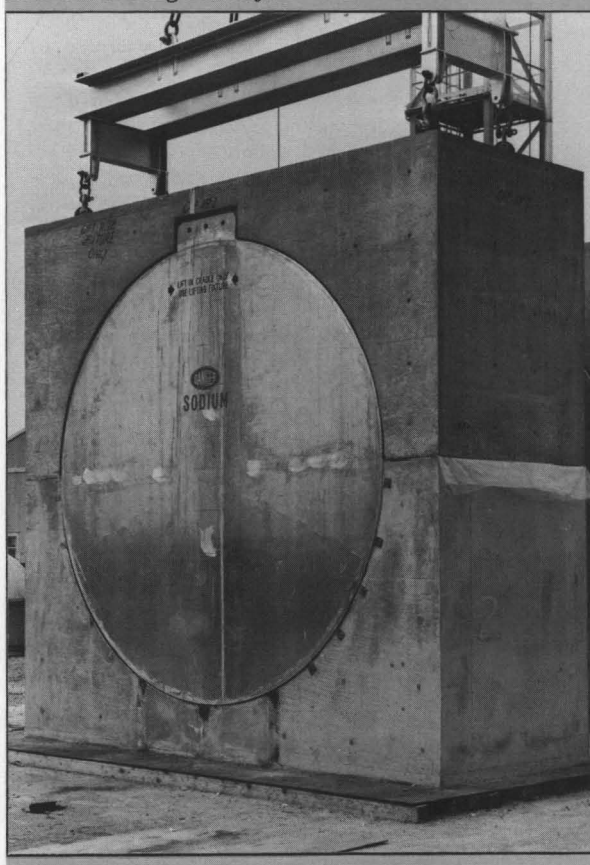

200 55-gal drums, and it was transferred into the four tanks by successively surrounding four drums at a time with a heater that melted the sodium and allowed it to flow into one of the tanks located in a nearby pit. Steel plates on the flat faces of the tanks served as structural braces during the time that the sodium was liquid. These plates also incorporated heating elements to ensure that some portion of the sodium in the tank remained in a liquid state until the filling was complete. The arrangement of the heaters facilitated zonal cooling and subsequent backfilling to compensate for shrinkage. Later checks revealed that the density of the sodium was constant throughout each tank and was the same in all four tanks.

When delivered to the site of the experiment, each tank was placed in a concrete cradle and capped with concrete. Only the flat faces of the tanks remained exposed, and these were placed in juxtaposition to obtain the desired sample thickness.

During the experiment, both the energies of the emerging neutrons and their directions of emergence were determined. Comparing the experimental data with corresponding results from the calculations led to the proper techniques being established for calculating neutron penetration through large thicknesses of sodium, and these can now be integrated into LMFBR shield design methods.

Ductility Studies on SS

Effect of an ORNL modification of type 316 stainless steel on irradiation stability. The curves plotted are creep curves showing the stretch of a specimen subjected to a steady stress of 45,000 psi at 550°C. The preferred behavior is that the material yield for a prolonged period before fracture. Curve A shows the satisfactory normal behavior of type 316 stainless steel, a proposed LMFBR fuel cladding alloy. Curve B shows the loss of ductility exhibited by this alloy after irradiation to a fast neutron fluence of 3×10^{22} neutrons/cm^2. Curve C shows the ORNL alloy modified with 0.2% titanium after comparable irradiation; its performance with respect to fracture ductility effectively matches that of the unirradiated standard alloy.

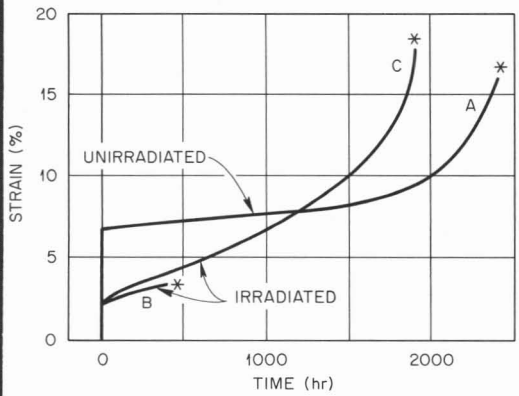

Subcriticality System Tested

A subcriticality measurement system for LMFBR's developed at ORNL, using new measurement methods and improved instrumentation, proved to be successful in tests performed in the Southwest Experimental Fast Oxide Reactor (SEFOR) near Fayetteville, Arkansas, in 1971. The system employs the modified neutron source multiplication method, which is calibrated, with the reactor near criticality, by either the inverse-kinetics rod-drop technique or the neutron noise analysis technique.

The subcriticality of a nuclear reactor is a measure of how far the reactor is from a self-sustaining chain reaction, the so-called "critical" condition. During refueling and maintenance operations, it is imperative for safety reasons that the reactor be kept far from its critical condition, because the normal protection system of the plant must be made inoperable to allow access to the reactor. With a reliable, continuous measurement of subcriticality, coupled with the proper administrative control procedures, the reactor operator can guarantee that the reactor is being kept far below criticality at all times during refueling and maintenance, thus ensuring the safety of the plant during these operations. Moreover, with an effective subcriticality measurement system, considerable economic savings are effected by permitting the relaxation of severely restrictive and time-consuming refueling schemes that would be necessary in its absence.

The successful test of the measurement system in SEFOR represents a significant improvement in the safety and economics of future LMFBR plants.

Molten-Salt Breeder

The development of a breeder reactor in which the nuclear fuel is dissolved in molten salt continues to be a goal of the Oak Ridge National Laboratory. One reason for the attractiveness of the molten-salt breeder is its promise of low fuel cycle costs and low electric power generation costs through the use of a high-temperature fluid fuel. In a reactor with circulating molten salt fuel, gaseous fission products can be removed continuously by a simple physical separation, and a chemical "kidney" can be used to remove other fission products. The elimination of fuel element fabrication and the simplification of processing open the way to low fuel costs.

The past year brought progress in several areas of MSBR development, notably in fuel processing. Continuous processing, although not required for simple molten-salt power reactors, is an essential part of the ultimate molten-salt breeder, where rapid separation of protactinium and the rare-earth fission products from the fuel salt is necessary in order to achieve satisfactory breeding performance.

WILDLIFE AT ORNL TICKSEED

Protactinium Removal

We are developing two methods for the removal of protactinium from MSBR fuel salt — reductive extraction and oxide precipitation.

The reductive extraction process, which is the one we include in our reference plant designs, exploits the tendency for protactinium to go from the fuel salt into molten bismuth in exchange for lithium dissolved in the bismuth. The distribution coefficients are quite favorable, and operation for the past two years of a small-scale reductive extraction development facility has shown that protactinium separation can be accomplished in equipment of reasonable size. Now a facility is being designed for studies using salt and bismuth flow rates about 25% of those required for removing protactinium from a 1000-MW(e) MSBR.

A bothersome requirement of the reductive extraction method for protactinium removal is that most of the uranium must be removed from the fuel salt prior to the removal of protactinium in order to avoid the use of undesirably large quantities of lithium-7 reductant. We have, therefore, continued to seek a method that removes the protactinium but leaves the uranium. Work carried out during 1971 indicates that we may have found such a process. Addition of oxide ion to fuel salt in the state in which it circulates in the reactor will precipitate protactinium as protactinium dioxide containing appreciable quantities of uranium dioxide and thorium dioxide in solid solution. We have found, however, that if the redox potential of the salt is first shifted sufficiently to put the protactinium in the 5+ valence state, protactinium pentoxide, Pa_2O_5, forms. This is much less soluble than the other oxides and precipitates as a pure phase. Whether or not this is a practicable method for removing protactinium will depend on engineering

A simplified flowsheet for the fluorination—reductive extraction—metal transfer process proposed for continuous removal of protactinium and the rare earths from molten salt breeder fuel. A 1-gpm stream of salt from the reactor goes first to a fluorinator, where most of the uranium is removed as gaseous uranium hexafluoride. The salt then passes through an extractor, where the protactinium and the remaining uranium are transferred into a countercurrent bismuth stream. The extracted materials are then transferred to a secondary salt by hydrofluorinating the bismuth in the presence of the salt. This salt is held in a tank to allow decay of the protactinium to uranium-233, which is removed by fluorination. Lithium is added to the bismuth leaving the hydrofluorinator to provide the metal stream that is fed to the extractor.

Fuel salt leaving the extractor, essentially free of uranium and protactinium, is fed to the rare-earth removal system, where a fraction of each of the rare earths and the thorium is extracted into a downflowing bismuth stream. Contact of the bismuth stream with molten lithium chloride in a second contactor results in the preferential transfer of the rare earths to the lithium chloride. Finally, the rare earths are extracted from the lithium chloride into bismuth containing a relatively high concentration of lithium.

The uranium is put back into the salt returning to the reactor by introducing uranium hexafluoride into the salt leaving the rare-earth removal system and reducing it to uranium tetrafluoride with hydrogen.

questions that are yet to be investigated, such as the difficulty of separating the precipitate from the salt and the handling of solids that contain intense heat sources. Studies are being pursued to characterize the oxide precipitate, to determine the quantity of uranium that may precipitate simultaneously with the protactinium, and to develop equipment suitable for removing protactinium from fuel salt by this method.

Rare-Earth Removal

Rare earths can also be removed from MSBR fuel salt by reductive extraction into bismuth. Unfortunately, thorium comes out in about the same ratio as the rare earths, so the problem was to get rid of the rare earths without discarding too much thorium. About two years ago, we observed that rare earths and thorium distribute quite differently between bismuth and molten halides such as lithium chloride, so that effective thorium—rare-earth separation factors ranging from more than 10^4 to about 10^8 for the various rare earths are possible. On this basis, we have devised a vastly improved rare-earth removal method, known as the metal transfer process, which allows removal of rare earths in relatively simple equipment with only negligible discard of valuable constituents of the fuel salt. We have recently successfully demonstrated all steps of the metal transfer process, including thorium-lanthanum decontamination by a factor of about 10^5. We are currently operating an engineering experiment in which the salt and bismuth flow rates are about 1% of those that will be required in a rare-earth removal system for a 1000-MW(e) MSBR, and we are designing an experiment that will circulate salt and bismuth at 5 to 10% of the MSBR rates.

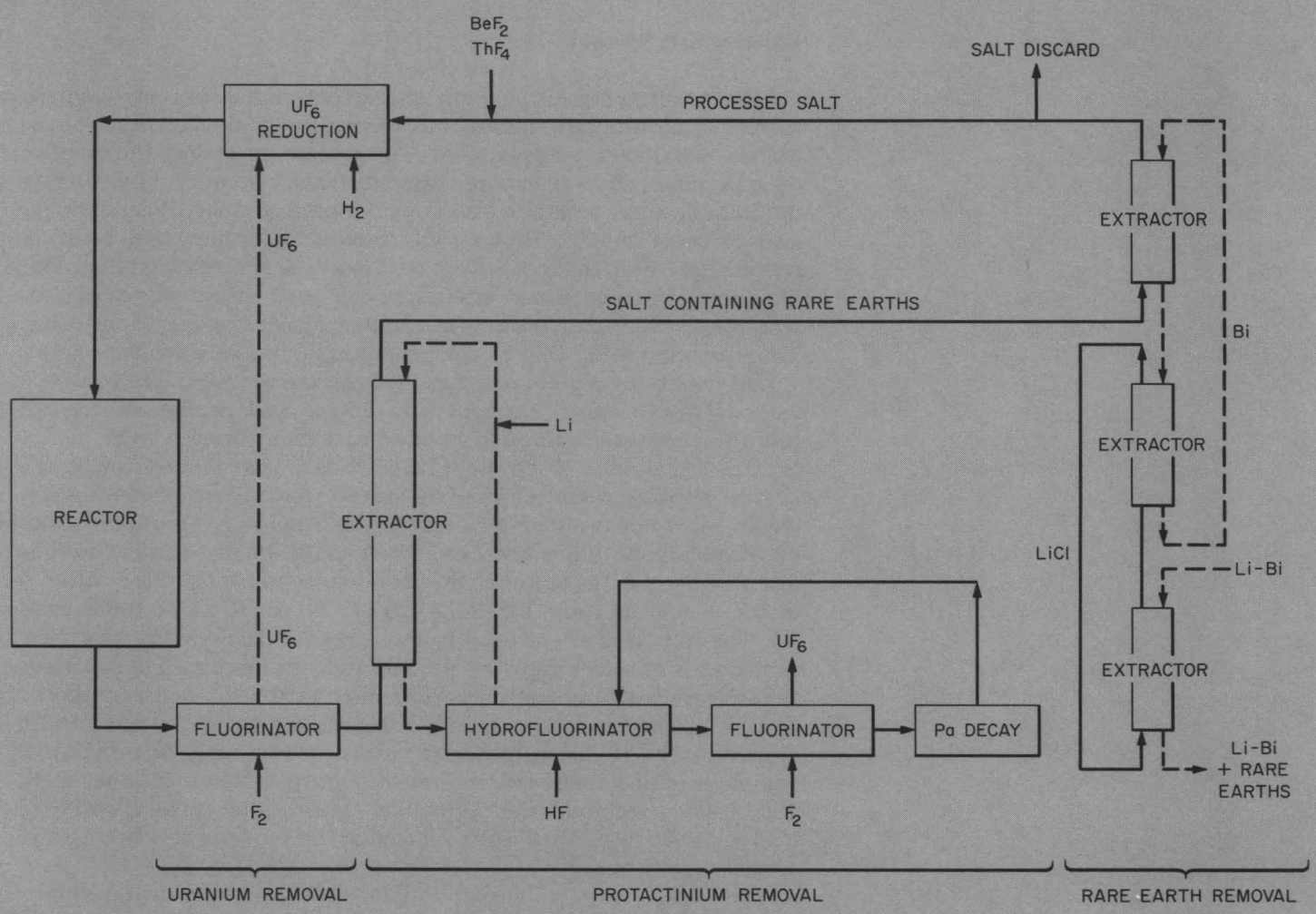

Successful Fabrication of Molybdenum

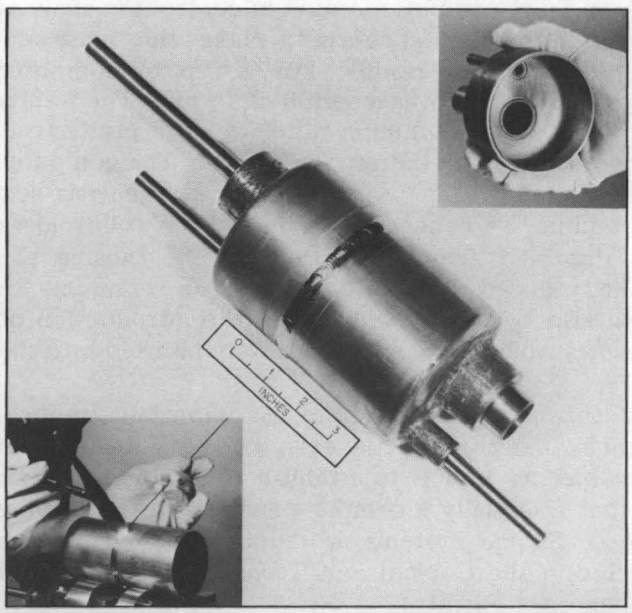

Molybdenum equipment for MSBR processing. For MSBR processing to be successful it is essential that practical materials, compatible with bismuth that contains reductant, be developed. Both molybdenum and graphite are quite resistant to attack by molten bismuth, but the difficulty of fabricating these materials into the shapes required for chemical processing systems has so far restricted their use. During the past year, significant advances in the fabrication of molybdenum were made as ORNL began building an all-molybdenum system in which bismuth and molten salt will be countercurrently contacted. It was found that commercially available molybdenum tubing, which is normally brittle at room temperature, can be made ductile by the removal of impurities from the inside surface of the tubing and can be welded successfully either by the tungsten-arc welding technique (shown in the lower left figure) or by the electron beam technique (upper right).

The equipment shown in the center was made by the electron beam method from tubing of various diameters, welding it to molybdenum sections made by back extrusion. The two half sections were then joined by manual tungsten-arc welding. The unavoidable increase in the grain size of the molybdenum in the weld area makes the material nonductile at room temperature, but by brazing a molybdenum band over the weld-affected zone, a practical system can be fabricated. These and other advances indicate that practical materials will be available for MSBR chemical processing systems.

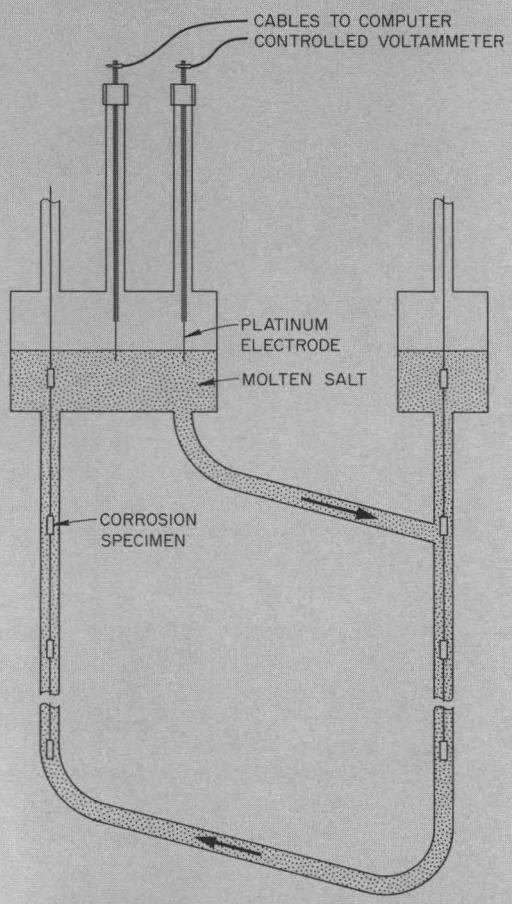

This schematic drawing shows how a flowing salt system can be examined for its corrosive effects on specific material without interrupting the flow.

Flowing Salt System

The desirability of making in-line determinations of dissolved species in molten salt streams was recognized at the inception of the Molten-Salt Reactor Experiment. For reactor operation, the practice of sampling and analyzing discrete samples not only creates undesirable time delays in obtaining required compositional data but also presents the likelihood that these samples may not be truly representative of the reactor salt stream at the time of sampling. This likelihood was confirmed later by experience with analyses of salts from the MSRE, reaffirming the importance of in-line monitoring. The operating efficiency of the proposed molten-salt breeder reactor would clearly be enhanced by immediate knowledge of the composition of reactor salts, both in the reactor and in the reactor salt reprocessing system, through a continuous monitoring system.

The Analytical Chemistry Division last year demonstrated the first successful chemical analysis system for a flowing molten salt stream in a corrosion test facility for determining the effect of salt on Hastelloy N under both oxidizing and reducing conditions. The test facility is a Hastelloy N thermal convection loop filled with 6.5 kg of the MSRE salt, $LiF\text{-}BeF_2\text{-}ZrF_4\text{-}UF_4$ (65.4-29.1-5.0-0.5 mole %). The salt flow in the loop is about 4 to 5 lin fpm. The analytical transducers consist simply of platinum electrodes installed in a surge tank where the temperature is controlled at 650°C. As the potential of one of the electrodes is varied linearly with time by means of a voltammeter, a current-potential curve is obtained, the shape of which is dependent on the electroactive species in the melt. Established voltammetric principles allow the current-potential curves to be translated into concentrations of these electroactive species.

The ratio of the concentrations of uranium in the melt in the 3+ and 4+ oxidation states was selected to be monitored, since it reflects the oxidation-reduction condition of the salt. This ratio has been monitored over a period of several months on a completely automated basis. A PDP-8/I computer is used to control the analysis system, analyze the experimental output, make the necessary calculations, and print out the results. For a typical computer program, five analyses are made over a period of 10 min. The results are combined to give an average uranium ratio, which is printed out along with a relative standard deviation for the set. The computer then enters a preset timing loop to await the next analysis set. Increases in the uranium 3+ concentration have been followed as chromium slowly dissolved from the Hastelloy N, causing the uranium 4+ to be reduced. Precipitous drops in uranium 3+ concentrations have also been observed due to the introduction of oxidizing contaminants when metal specimens were inserted into the melt.

The success of this monitoring system has important implications. Since other electroactive species exist in the salts, such as chromium 2+, the objective now is to establish conditions for their determination, so that essentially a complete analysis of the flowing salt can be obtained. Similar systems are to be installed on two MSRP engineering loops, the Coolant Salt Technology Facility and the Gas System Technology Facility.

High-Temperature Gas-Cooled Reactor

Gas-cooled reactors are promising and versatile energy sources, and we are involved in several development areas concerning them. Work highlighted here concerns development of prestressed concrete reactor vessels, development of HTGR fuels, head-end off-gas processing, and fuel refabrication.

Concrete Reactor Vessels

Prestressed concrete pressure vessels are used in nuclear systems as both primary and containment vessels. The problem of predicting the long-term behavior of these types of structures is being attacked at ORNL in an experiment that simulates an operating primary vessel for a gas-cooled reactor.

The circumferential tensioning system of a prestressed concrete pressure vessel model utilizes 40 wraps of strand, each developing a force of approximately 40,000 lb, to contain the internal pressure load within the structure.

WILDLIFE AT ORNL HEPATICA

Concrete is a complex multiphase material that has been used successfully for centuries. However, the first practical application of prestressed concrete was developed less than 50 years ago, and prestressed concrete pressure vessels were first put into operation by the French in 1958. Concrete is a brittle material with a low tensile strength, and it is utilized in a pressure vessel application by being placed in a state of precompression with prestressing steel, so that design membrane loads are taken with the concrete remaining in net compression. In pressure vessels the concrete may be subjected to operating temperatures that accentuate the creep phenomena of the material, which complicates predictions of structural behavior.

The current experiment utilizes the 7-ft-diam barrel of a right cylindrical pressure vessel. This model segment has been prestressed axially and circumferentially with high-strength strands of steel, each loaded to 36,000 lb of initial tension. A combined system of pressure-tight steel liners and heat exchangers serves to heat and cool the concrete to induce a temperature gradient and to form a leak-tight volume that can be pressurized. Prestressing, internal pressure, and thermal crossfall have been applied in a sequence that duplicates the regimes that an actual structure would be subjected to during startup and operation.

In order to verify the adequacy of design and analysis methods, time-dependent finite-element creep analyses have been performed, and the results are being compared with experimental behavior. A large number of devices have been built into the experiment to obtain data on strain, stress, deformation, temperature, and concrete conditions.

In addition to the evaluation of normal operating conditions, overload tests will be performed by simulating high temperatures in a segment of the structure followed by sudden cooldown to demonstrate the capability of the model to endure thermal shock. After a test program expected to last some three years the model will be disassembled for complete examination and inspection.

Off-Gas Cleanup in Fuel Processing

Removal of radioactive components from effluent gases produced in the reprocessing of all reactor fuels is an important consideration in determining the acceptability of the reprocessing plants. The reprocessing of graphite matrix fuel blocks used in the HTGR, as contrasted with the more common metal-clad fuel elements of other reactor types, poses a problem in off-gas cleanup not encountered heretofore. Crushing and burning the graphite matrix to permit recovery of the uranium and thorium in the fuel produces large amounts of carbon dioxide containing a few percent of lighter gases such as nitrogen and oxygen, trace amounts of entrained particulates, and 10 to 20 ppm of krypton-85, which is the radioactive contaminant of special concern in this report.

Several processes for removing krypton-85 and other noble gases from various gas streams exist in current technology. However, these processes are not applicable to an off-gas stream that is primarily carbon dioxide because of the many similarities between krypton

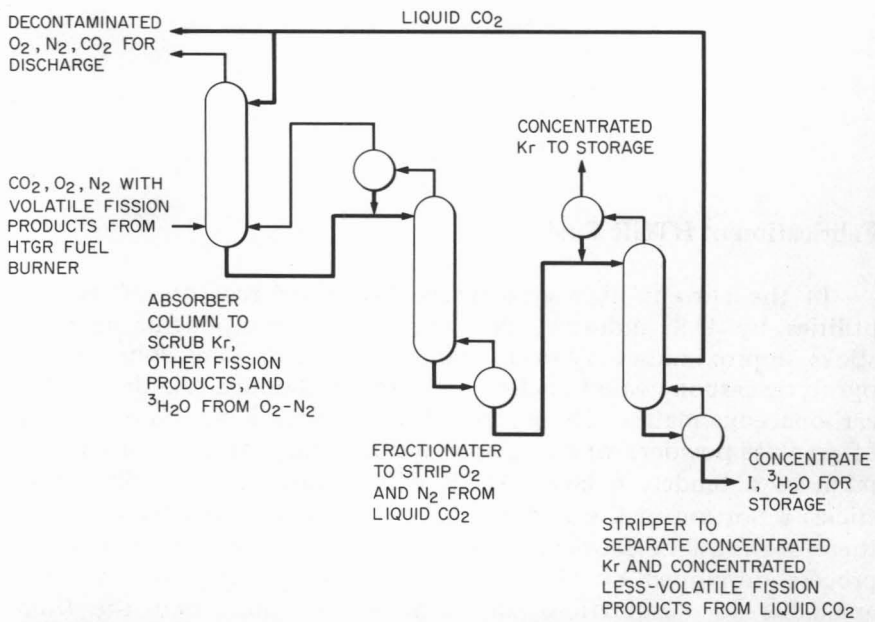

The KALC (krypton absorption in liquid carbon dioxide) process for decontaminating off-gases from fuel processing. The KALC process separates the constituents of fuel reprocessing off-gases by using the differences in gas solubilities in liquid carbon dioxide. KALC is particularly suitable for off-gases from burning graphite HTGR fuels. The high carbon dioxide content is troublesome for other off-gas treatments, but supplies the absorbent for the KALC process.

and carbon dioxide in the physical properties (such as adsorption and solubility) that provide the basis for previously developed separation schemes. Capitalizing on this similarity, the relatively high solubility of krypton in carbon dioxide provides the basis for separating krypton from the light gases (oxygen, nitrogen, and carbon monoxide) present in the HTGR off-gas, while a subsequent fractionation step separates the krypton from the liquid carbon dioxide solvent. This procedure, known as KALC (from krypton absorption by liquid carbon dioxide), has the added advantage that the absorbent is one of the species already present in the gas mixture, thus avoiding the introduction of a new component. Furthermore, the KALC process may also provide a means of concentrating and removing tritium (as the oxide), iodine, and particulate matter during the various scrubbing and fractionation steps. The KALC process operates as follows: (1) incoming carbon dioxide, krypton, and light gases are chilled and scrubbed free of krypton with liquid carbon dioxide, most of the light gases (along with some carbon dioxide) being discharged; (2) the liquid carbon dioxide, which now contains all the krypton and the balance of the light gases, is fractionated to remove these remaining light gases, which are recycled to the scrubber because they contain some krypton; (3) the krypton-rich carbon dioxide is further fractionated to boil off the krypton, which is sent to storage for ultimate disposal; (4) the remaining liquid carbon dioxide, now free of both light gases and krypton, provides the scrubber liquid for the first step plus an excess (corresponding to steady-state input of HTGR burner off-gas to the system) which is discharged. Xenon, which is also present in the burner off-gas to the extent of a few parts per million, will probably carry along with the krypton, but it is of relatively little significance, since its activity, which is short-lived, will have decayed out prior to reprocessing.

Pilot studies have demonstrated the feasibility of the KALC operations and encourage us to believe that with continued development and optimization, the KALC process will be an effective solution to the problem of removing krypton from off-gases generated during the head-end reprocessing of reactor fuels.

Fabrication of HTGR Fuel

In the current high-temperature gas-cooled reactors offered to utilities by U.S. industry, the primary fuel components are fuel sticks, approximately $^1/_2$ in. in diameter and 2 in. long, consisting of pyrolytic-carbon-coated nuclear fuel particles bonded together with a carbonaceous matrix. The matrix of a fuel stick is normally a blend of graphite powder, which serves as a filler, and petroleum or coal-tar pitch as a binder. A large HTGR will contain several million fuel sticks; a portion of the fuel will have been previously irradiated and therefore must be fabricated in a hot cell. A new fuel fabrication process developed by ORNL, the slug injection process, is more amenable to automation and remote operation than the fluid intrusion method currently used by industry.

In the slug injection process, the coated particles and a preformed and precisely measured slug of the pitch and graphite matrix are loaded into a mold. The mold is then heated to melt the matrix, and pressure is applied to force the matrix into the bed of particles. After cooling and removal from the mold, the stick is heated and the pitch is converted to coke and stabilized. By eliminating the need for a hot pitch reservoir and dispensing system, the slug injection technique simplifies the design of automatic equipment. This process simplification is a major advancement, particularly for fuel recycle, where the process needs to be carried out remotely. Thousands of sticks of excellent quality have been made in the laboratory by the slug injection process.

Another process that shows promise for HTGR fuel fabrication involves the old art of extrusion. In this process, pyrolytic-carbon-coated microspheres containing uranium and thorium are blended with graphite powder and a carbonaceous liquid binder to form a plastic mass. This mixture is then forced through a die of prescribed shape to form rods, which are subsequently "carbonized," that is, heated to drive off volatiles. This results in a solid, strong semigraphitic rod. These rods are then inserted into holes of graphite blocks, which comprise the core of the reactor. For a core loading of a typical 1100-MW(e) reactor, approximately 1.8×10^6 ft of 0.5-in.-diam fuel rods are required.

Elements made by the extrusion process have the advantages that the bonding matrix is continuous and the carbon density is about that of moderator graphite, the estimated thermal conductivity based on electrical resistivity measurements is high compared with fuel sticks containing a closely packed lattice of coated particles, and the elements can be formed to the full length of the hole in the fuel block at a rate of at least 10 fpm. Further, the extrusion process appears well suited to remote fabrication of recycle fuel. The application of this process is dependent on maintaining the above features while increasing the coated particle fraction in the fuel to 40 or 45 vol %; such values appear feasible.

WILDLIFE AT ORNL BLACK-EYED SUSAN

Slug injection process for making bonded bed fuel sticks. Matrix material in slug form is placed above the bed of coated fuel particles and then warm pressed into the bed to give a bonded fuel stick.

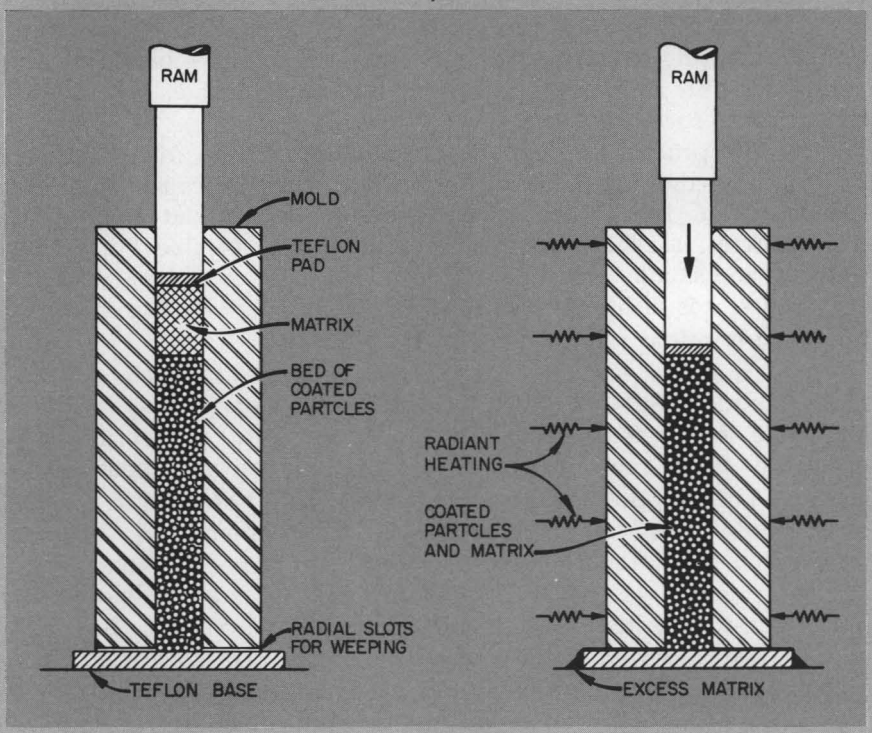

Fuel Technology

Preparation of Plutonium Dioxide Sols

A new method has been developed for preparing plutonium dioxide sols by procedures that are readily amenable to scale-up. This method combines the high quality and versatility of products prepared by precipitation and peptization with the advantages of continuous processing offered by solvent extraction.

Sol-gel technology is of interest for the fabrication of nuclear reactor fuels because it affords a promising method for the production of dense actinide oxides of controlled size and shape. The sols produced by this method can be converted to dense microspheres, shards, or sintered powders. The sols can also be mixed with uranium oxide or thorium oxide sols in any proportion and used to prepare microspheres, shards, or powders.

Plutonium oxide colloids prepared by any known method have a small crystallite size. This is significant, because plutonium oxide colloids of crystallite size 10 to 20 Å have only limited usefulness, whereas colloids composed of larger crystallites (50 to 100 Å) exhibit greatly improved versatility. The only previously demonstrated method for increasing the crystallite size involves thermal denitration, in which the sol is dried and baked at 250°C for approximately 2 hr. This process is difficult to control, because very uniform heating of the plutonium oxide solids is required for long periods of time and because overheating results in solids that will not resuspend to form a colloid.

The old process for preparing plutonium dioxide sols was based on this procedure, and the sols have been used to prepare kilogram quantities of both PuO_2 microspheres and mixed PuO_2-UO_2 microspheres, as well as similar amounts of sinterable PuO_2-UO_2 powders and smaller amounts of PuO_2-ThO_2 microspheres. Although the process has been operated routinely at a 250-g batch size, careful control is required and scale-up appears difficult.

In a more recent development we prepared high-nitrate plutonium dioxide sols by the APEX solvent extraction process, which is amenable to scale-up. In this process, nitrate is continuously extracted from plutonium nitrate solutions with normal hexyl alcohol. The sols produced by this process cannot be used to prepare pure plutonium dioxide microspheres. On the other hand, they can be blended with uranium dioxide sols to form mixed sols that can be used to prepare satisfactory UO_2-PuO_2 microspheres, providing the plutonium-to-uranium ratio in the mixed sols is limited to less than about 0.43. However, because of the very small crystallite size of the plutonium dioxide and the attendant requirement for a relatively high nitrate-to-metal ratio to maintain colloidal stability, the mixed

sols tend to gel prematurely and must be stored at approximately 5°C to achieve a shelf life longer than 8 hr.

The essential feature of the new sol preparation method involves seeding, in which a portion of a sol prepared by the APEX process is added to the plutonium nitrate feed solution during the initial extraction stage. This technique yields sols in which the primary crystallites are arranged in aggregated micelle structures, which are responsible for rapid denitration and crystallite growth when the sol is evaporated to dryness and heated.

Although various extraction techniques can be used and several process options are available to produce the desired micelle structure, the process consists of three principal operations:

1. the extraction of nitric acid from the acid plutonium nitrate feed with a long-chain alcohol (such as normal hexyl alcohol) until a plutonium oxide sol with a nitrate-to-plutonium mole ratio of about 1.0 is obtained,
2. the addition of sol to the feed solution before or during extraction, to create a micelle structure of aggregated crystallites,
3. thermal denitration, which consists in drying the sol and heating the dried solids in an appropriate atmosphere.

A significant process option involves double seeding, in which the product sol from a first seeding experiment is used as seed in a subsequent sol preparation. This technique increases the micelle size, which in turn produces larger crystallites in the final sol. A multiple seeding effect can also be obtained in a single run by incremental feed addition during continuous extraction. Using this procedure, the effect of double seeding is obtained because extraction is continued after each feed addition until colloidal plutonium is formed. Following extraction, the sol is evaporated to dryness and heated for a minimum of 15 min at 230°C in a dry sweep gas which removes volatile decomposition products. The final sol is prepared by resuspending the denitrated solids in water and evaporating to the desired plutonium concentration. As a result of the larger crystallites, low-nitrate sols (having a nitrate-to-plutonium mole ratio of 0.1 to 0.2) with average crystallite diameters of 60 to 70 Å are easily prepared. Because these sols denitrate very rapidly — in 10 to 15 min — and are insensitive to overheating (they can be baked at 230°C more than 6 hr without adverse effects), denitration can be accomplished by a variety of continuous processing methods. Therefore, all aspects of sol preparation by this method appear to be readily amenable to scale-up.

The new method has been studied extensively in the laboratory, but scaled-up runs with large quantities of plutonium have not been made. Sols prepared by mixing uranium dioxide sols with plutonium dioxide sols produced by this process can be stored at room temperature and later used to prepare high-quality UO_2-PuO_2 microspheres. The plutonium dioxide sols can also be used to prepare plutonium dioxide microspheres by techniques that have been demonstrated on an engineering scale for thorium oxide and ThO_2-UO_2 sols. These sols show promise of having all the versatility of application of sols prepared by the earlier methods. In addition, considerable advantages are gained in the method of preparation and ease of scale-up.

Nuclear Safety

Steel Pressure Vessels

In the presence of flaws the fracture behavior of thick steel plates and forgings, typical of the mammoth primary containment pressure vessels used in civilian water reactor power plants, is of great

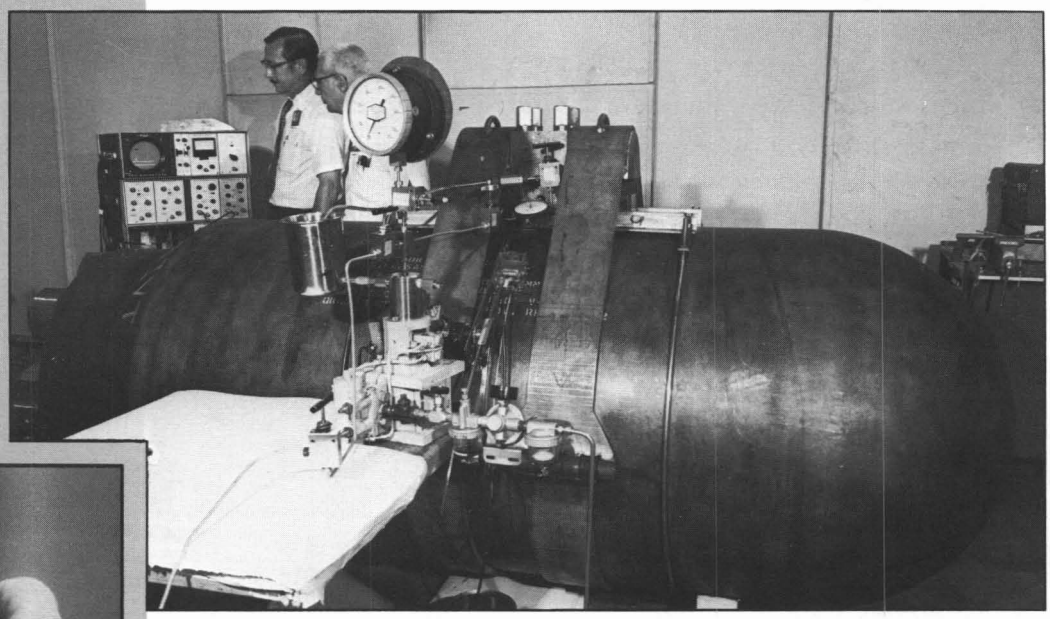

Pressure vessels 6 in. thick and containing mechanically induced sharp flaws are being tested throughout the toughness regimes to demonstrate both the inherent toughness of the steel and the ability to predict the conditions under which fracture will occur. Here we see a flaw being sharpened in one of the vessels prior to testing to failure. The vessel weighs about 20,000 lb.

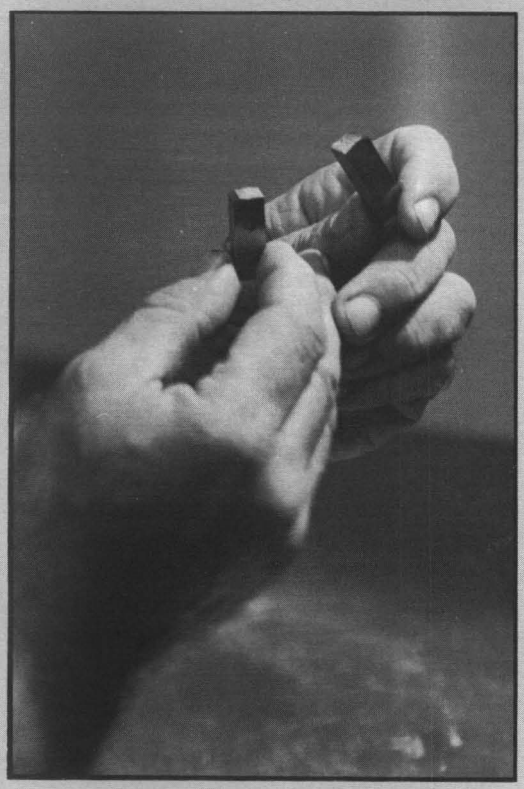

The determination of quantitative fracture toughness parameters from small laboratory specimens is of primary importance in establishing fracture characteristics for the many heats of steel and several product forms used in fabricating the primary containment system for water reactors.

importance in assuring the safety of these nuclear plants. The Heavy Section Steel Technology (HSST) Program at Oak Ridge National Laboratory is one of the major USAEC-sponsored programs in this field. Techniques for making the necessary assessments of thick plates are being developed and verified by the testing to fracture of series of specimens in increasing size, including pressure vessels up to 6 in. thick. The fracture analysis techniques being developed encompass both experimental and theoretical approaches, including the development of highly sophisticated finite-element elastic-plastic computer programs. Equally emphasized is the extension of linear elastic fracture mechanics into the elastic-plastic regimes. Particularly significant has been the rapidity of the development of the technology in the fracture mechanics areas. Considerable confidence has been developed in quantitative procedures for calculating gross plastic failures and, in less quantitative terms, for making conservative engineering fracture calculations throughout the toughness regimes.

Significant among the several recent accomplishments of the HSST Program has been the development of procedures for determining quantitative fracture-toughness values applicable to thick structures directly from small specimens, including those of such size as can be used in irradiation surveillance programs.

International Comparison of Dosimetry Systems

For several years, the Health Physics Division has conducted a program annually whereby the Health Physics Research Reactor is used as a pulsed source of mixed neutrons and gamma rays to test radiation dosimetry systems utilized in nuclear safety programs. Both personnel and area surveillance monitors are included. When the program began in 1964, most of the participating organizations were AEC contractor laboratories. The need for such a series of studies was manifested in the results of early experiments where the accuracy for mean values of individual components of the radiation fields varied from −50 to +150%. Results in this program have improved over the years to the point that values for dose are available to within ±25—30% in 24 hr and less than ±25% in 48 hr.

As a result of these studies, the International Atomic Energy Agency (IAEA) started a similar program, principally for laboratories from developing countries. The first in this series was held at the Centre d'Études Nucléaires de Valduc in France in June 1970. In May 1971, ORNL and the IAEA cosponsored the latest intercomparison study, in which the responses of accident dosimetry systems in use throughout the world were compared. Participants in this study included representatives from England (2), France (2), Italy, Poland, Czechoslovakia, Canada (2), Russia (4), Yugoslavia (2), Germany (2), and Hungary. The results of this set of experiments indicated that there was general accord as to the interpretation of the characteristics of three radiation fields with varied neutron spectra and a factor of 8 change in the ratio of neutron dose to gamma-ray dose. Values of absorbed dose and fluence were found to be in good agreement; individual measurements varied less than ±25% from the average of all values reported.

Fusion Research

ELMO Bumpy Torus

Research at Oak Ridge in the creation and heating of plasmas by high-frequency microwave power in mirror confinement devices has resulted in the routine production of plasmas in which the particle pressure is a significant fraction of the confining magnetic pressure. This can be advantageous for stability, since the plasma "digs its own hole" by displacing magnetic field. However, unlike other high-pressure plasmas, such as those produced in pinch experiments, the microwave-heated plasmas are sustained stably and in the steady state. During this past year, the unique methods developed at ORNL are finding application in a new area, that of toroidal confinement. Through a basic improvement in an old idea for toroidal magnetic confinement (the "bumpy torus"), this method of producing plasmas through microwave interactions promises a stable, steady-state confined toroidal plasma.

Single particles can be contained in a simple torus if the magnetic field is modulated spatially (i.e., is bumpy) — one way is to use discrete coils, separated by roughly a coil diameter and joined in a circle to form a torus. Because this shape theoretically permitted the unstable growth of large fluid-like plasma motions, even though single particles could be well confined, no major devices of this type have been investigated experimentally. But we have shown, first in simple mirrors and then later in one segment of a torus (the "canted mirror experiment"), that one can produce suitable high-pressure plasmas in each section of the torus, so that the hole-digging effect is sufficient to provide stable confinement for another plasma which circulates around the torus. Moreover, the high-pressure plasma acts through particle interactions to heat the toroidally confined plasma also; so the microwave power ultimately heats the whole system. A torus is being constructed to study these essential features.

The high-pressure plasmas that are produced directly by the microwave power are annular in shape, and the equilibrium and stability of the annuli have been studied theoretically. The problems were solved using the guiding-center equilibrium equations numerically on the computer for pressure models that were chosen to reproduce the experimental properties of the plasma as closely as possible. The equilibria obtained in this way permit one to study the known indices of stability as functions of the high plasma pressures. The findings indicate that only the outermost edge of the plasma is unstable to fluid-like interchanges at high plasma pressures, and it is this limited region that is experimentally observed to be stabilized by some form of line tying in the mirror experiments that have been performed. Thus, it is expected that a bumpy torus with a high ratio

of plasma pressure to magnetic pressure should be stable against all the known existing stability criteria and that it will be possible in the future to observe stable, steady-state high-pressure plasmas in toroidal confinement geometries.

The "bumpy torus" is a hybrid plasma confinement system now being built in the Thermonuclear Division. It combines the advantages of both mirror and toroidal confinement geometries. It is composed of 24 mirror sections, one of which is shown here, each canted enough so that all 24 form a torus. Within each mirror section, high-power microwaves are applied to create an annular plasma that strongly modifies the vacuum magnetic field produced by the external mirror coils. The microwaves heat the plasma to high temperatures. The combined field that results from the external coils and the plasma itself allows the plasma that is circulating around the torus to be confined stably against rapid losses, and through interaction with the applied microwave power, to become heated as well.

These novel principles are now being tested in the Thermonuclear Division. Realization of the expected performance will mean greatly reduced losses and the successful achievement of a stable, steady-state toroidal plasma capable of exerting pressures very nearly equal to those the magnetic field itself exerts on the plasma. This means that confinement could be obtained far more efficiently in much smaller devices than with other methods now being tried.

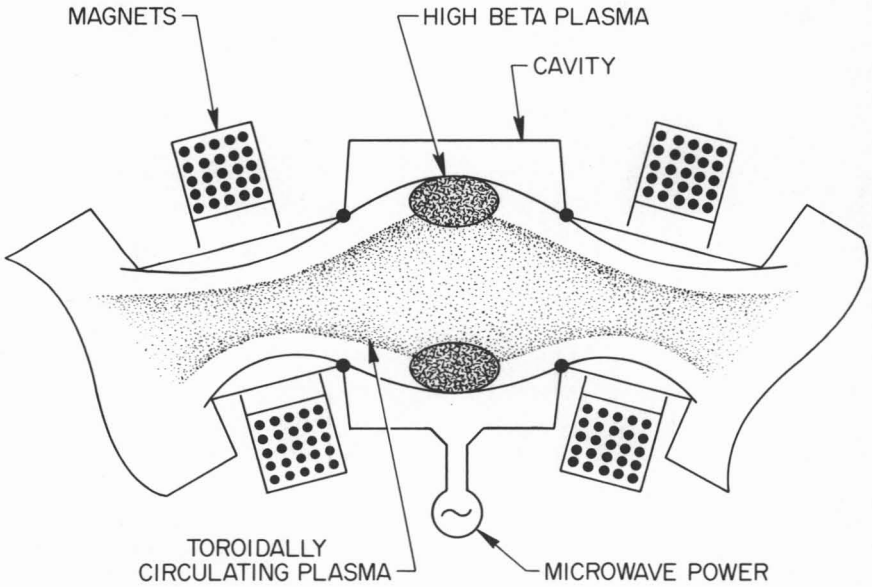

BUMPY TORUS INCLUDING CIRCULATING PLASMA

RESEARCH AND DEVELOPMENT

Physics

The Magnetically Pulsed Beam:

A New Technique for Neutron Inelastic Scattering

WILDLIFE AT ORNL SCREECH OWL

Neutron inelastic scattering gives us the best information available for determining the dynamic properties of materials. The inelastic scattering measurements provide direct information on the nature of the interatomic forces responsible for a material's strength. Also, since the neutron has a magnetic moment, inelastic scattering experiments can determine the nature of the magnetic forces responsible for magnetism in materials. Unfortunately, inelastic scattering cross sections are very small, and intense neutron beams are necessary in order to measure the energy change a neutron undergoes upon scattering from a sample material. Using the high-intensity neutron beams from the HFIR, a number of investigations have been made to determine both the magnetic and interatomic forces in several classes of materials. Until this year these measurements were performed at ORNL on a three-axis crystal spectrometer, where crystal reflections are used to determine the energies of the incoming and outgoing neutrons so that the energy change upon scattering can be determined. This technique is limited to taking measurements at only one scattering angle and one energy transfer at a given time.

In 1971 a new technique was developed in the Solid State Division by which the energy of the neutrons can be determined after the scattering process by measuring the time a neutron pulse takes to traverse a fixed path. Very short neutron pulses must be produced in order to obtain good energy resolution. These pulses are achieved by changing the magnetization state of a ferrite crystal. Ferrite crystals with the correct chemical composition have reflections where only the atomic magnetic moments of the crystal provide the scattering interaction. The scattering power of the crystal is then related to the direction of the atomic moments in the crystal. If these moments are aligned along a direction in the plane of scattering that makes equal angles with both the incoming and the outgoing neutron beam, the scattering interaction is zero, and no neutrons are reflected by the crystal. However, if the atomic moments are aligned along a direction perpendicular to this specific direction, the full reflected intensity is obtained. In the reflecting process, the crystal picks out a unique energy; thus one ferrite crystal serves both to determine the energy of the outgoing neutrons and to pulse the beam so that the energy of the scattered neutrons can be

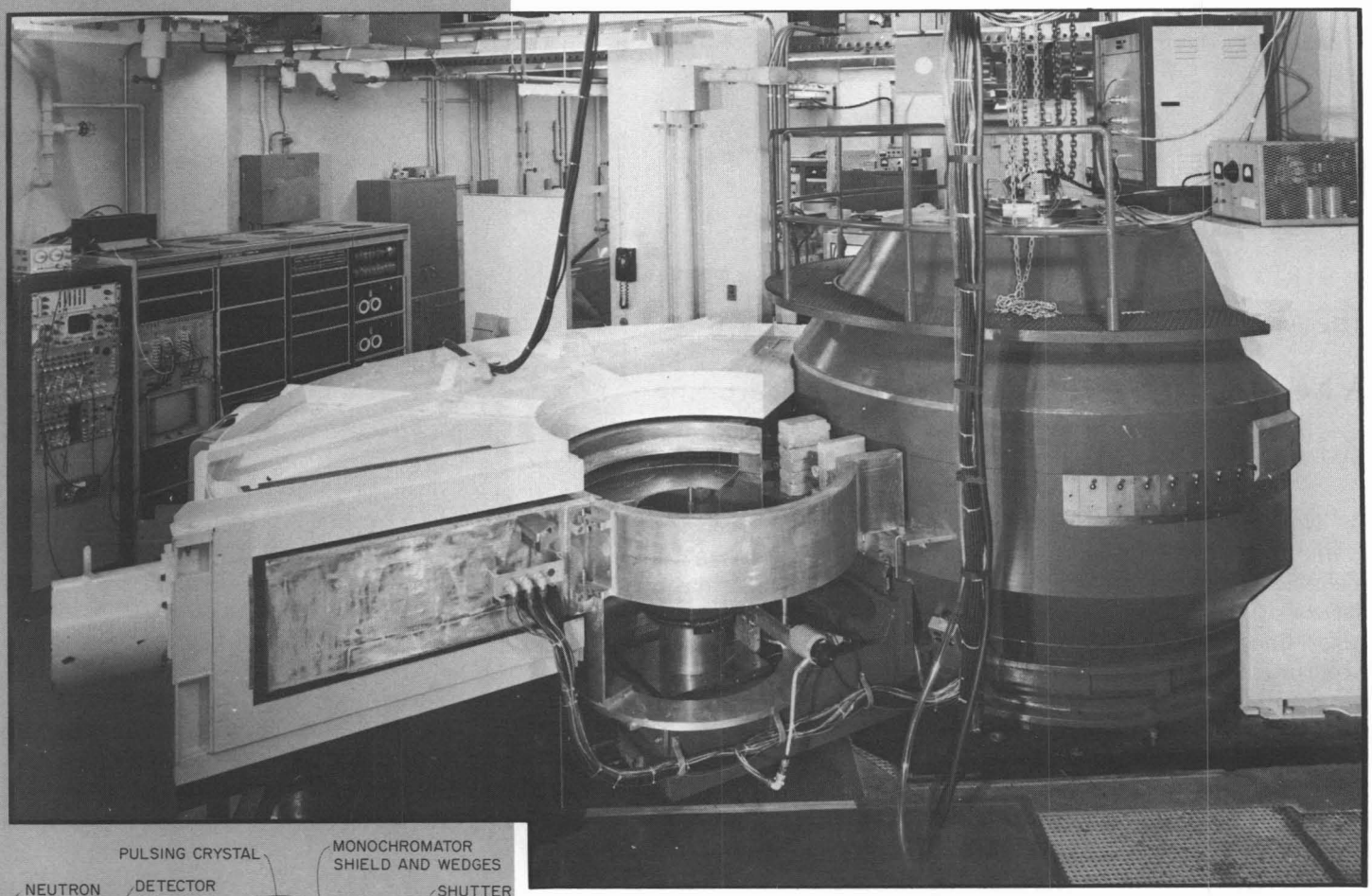

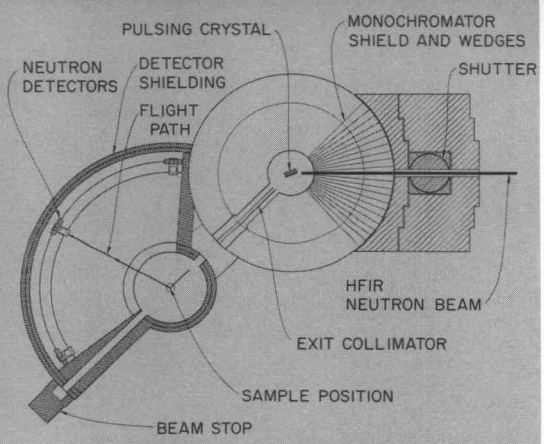

New inelastic scattering technique at the High Flux Isotope Reactor research facility.

measured by time of flight. The atomic moments in the ferrite crystal can be easily oriented by an external magnetic field, since the magnetic crystalline anisotropy is small. The crystal is normally magnetized in a direction such that the reflected intensity is zero; when a pulse of neutrons is desired, a coil is energized so that the magnetic moments are aligned in a direction to give the maximum reflected intensity. Since the ferrite is a good electrical insulator, eddy currents are small, and the magnetization direction can be changed very quickly, giving short pulses and thus good time resolution. The pulse can be made of any length and can occur at any time, making the instrument very flexible. Pulse lengths of about 1×10^{-5} sec are normally used.

The neutrons are timed over a path length of 1.5 m. A large shield surrounds the sample crystal, so that scattering angles from 5 to 130° can be used. At present, 15 detectors can be used simultaneously at any angle within this range. The detector position, sample position, and pulsing crystal take-off angle are all adjustable so that the optimum scattering geometry can be obtained for a given experiment.

Since the pulsing is accomplished magnetically, any series of pulses of any desired width may be produced, and the cross-correlation technique of obtaining scattering data can be used. In the standard time-of-flight technique a new pulse cannot be produced before the neutrons from the old pulse are counted, or confusion will

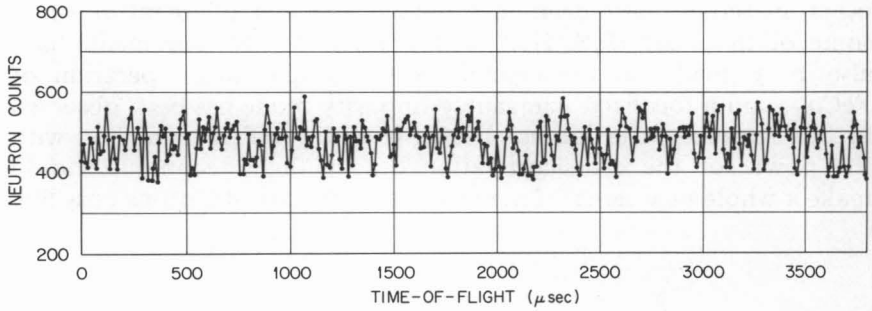

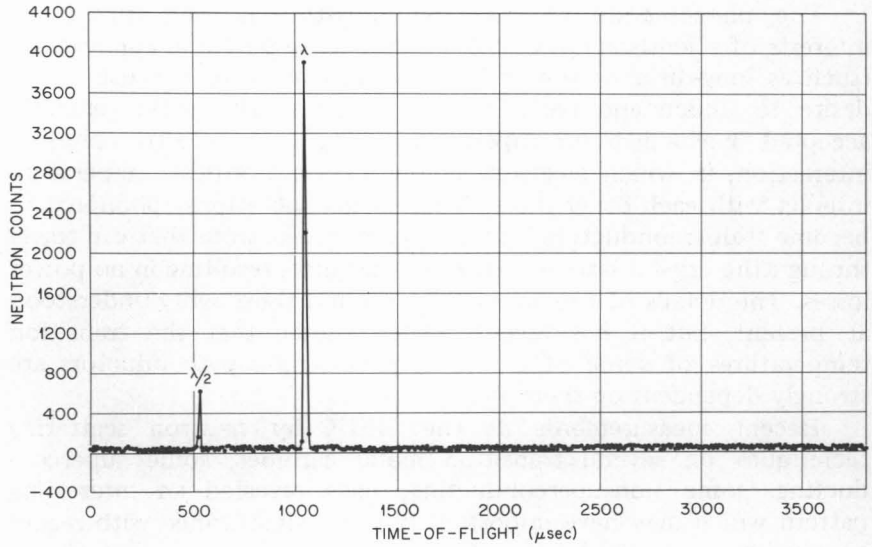

The time-of-flight spectrum of the direct beam falling on the sample (above) and the result of cross-correlating the spectrum to show the type of pulse produced by the pulsing crystal (below). A small amount of second-order (λ/2) intensity results from a higher order reflection in the pulsing crystal. With the cross-correlation technique the beam may be pulsed on as much as half the time, thereby giving a 50% duty cycle and a large increase in intensity over the standard technique.

arise about which pulse a given neutron belongs to. This limits the duty cycle to about 1% and gives very poor neutron economy. With the correlation technique a continuous series of pulses of varying widths is used, and the timing information is derived by matching the position in time of the neutron pulses counted with the original pulse sequence. From this matching, or cross correlation, the time of flight of the scattered neutron can be obtained and thus its energy determined.

The spectrometer is on line to its own PDP-15 computer. The computer sets the desired scattering angles by means of pulsed motors, outputs the sequence of pulses for the correlation technique to the pulsing crystal, and simultaneously collects time-of-flight data from 15 separate neutron detectors. When the experiment is finished, the computer cross-correlates the time-of-flight data and displays the result on a scope. The computer is then used to reduce and analyze the collected data. As many as 10,000 data points may be obtained simultaneously; thus the computer is a very important tool for handling the raw data.

The spectrometer has been running consistently since April 1971. Some of the experiments have been investigations of the crystal field splitting of the ground-state multiplet of a series of rare-earth compounds. The effect of the crystalline field is crucial in determining the magnetic properties of a material. Temperature-dependent measurements have been made in PrN, TmN, and TmBi. A number of

other materials have been investigated at room temperature only; some of these are HoS, HoN, PrSb, and TmSe. Measurements have also been made on the crystal field and spin wave spectrum of $FeCo_3$, and a localized manganese impurity mode has been observed in this material. The intense beams from the HFIR combined with the power of the cross-correlation time-of-flight technique should make a whole new series of neutron scattering investigations possible.

Phonon Spectra and Superconductivity

The phenomenon of superconductivity has long stirred the interests of scientists, not only for its immense potential applications (such as long-distance power transmission) but also because of the desire to understand basic laws of physics. The most generally accepted mechanism for superconductivity is the electron-phonon interaction, in which electrons below a certain critical temperature interact with each other through the lattice vibrations (phonons) to become "superconductors," that is, pairs of electrons that can travel through the crystal lattice with zero resistance, resulting in no power losses. The details of this interaction are not thoroughly understood at present, but it has recently been shown that the transition temperatures of some of the most promising superconductors are strongly dependent on their phonon spectra.

Recent measurements at the HFIR by neutron scattering techniques on several transition metal carbides, some superconducting, some nonsuperconducting, have revealed an interesting pattern which may have important physical significance with regard to elucidating the relation of the detailed phonon spectrum to superconducting properties of high-transition-temperature materials. Pronounced structure is observed in some of the phonon modes of superconducting TaC and NbC but is virtually absent in the same modes in nonsuperconducting HfC, ZrC, and $NbC_{0.76}$. Although the present theory of metals for these transition metal compounds is inadequate to predict their electronic and lattice dynamics in detail, there is little doubt that the observed anomalies in the phonon branches are due to strong electron-phonon interactions.

Most of the measurements were made at room temperature. Measurements made at 7.2°K in TaC indicate only minor changes in the phonon frequencies as a function of temperature, and there were no observed changes in the phonon spectra in going through the superconducting transition at about 10°K. The anomalies in the phonon dispersion curves are believed to be indicative of high transition temperatures in superconductors; thus these measurements appear to be only type of observation of low-temperature superconducting properties that can be made at room temperature.

(These transition metal carbides are of interest for other reasons as well. Even the ones that are nonsuperconducting exhibit metallic conductivity comparable with that of the elemental metals. They also are some of the highest melting compounds known and are extremely hard and chemically inert. Their bonding mechanisms are often described in terms of metallic, covalent, and ionic bonding, simultaneously. In fact a correlation may exist between the

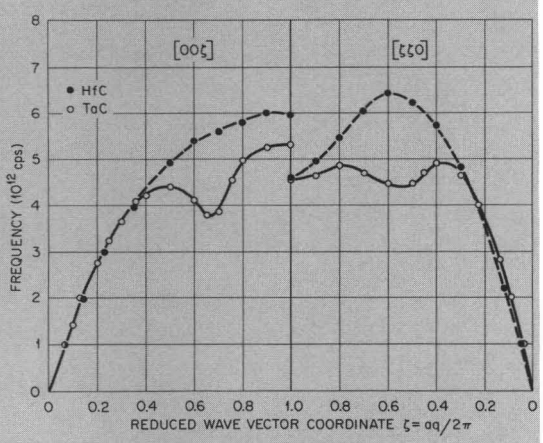

The longitudinal acoustic modes measured in TaC, a high-T_c superconductor with a high critical temperature, and HfC, a nonsuperconductor, by inelastic neutron scattering techniques at room temperature. The pronounced differences between their spectra are believed to be due to strong electron-phonon interactions and to be indicative of high-T_c superconductors.

superconducting and bonding properties. Lattice dynamics studies by neutron scattering are providing useful information about the electron-phonon interaction and the properties related to superconductivity. Insight into the various bonding mechanisms is an additional goal.)

Variations in Ionic X-Ray Intensity

When iodine ions in the energy range between 15 and 60 MeV strike a target atom with a certain violence, some inner-shell electrons of the moving ion are kicked out of their orbits. The time for such collisions is very short, something like 10^{-18} sec. Later the inner shell of the ion is reoccupied, and characteristic x rays are emitted.

In recent experiments, measurements were made on x-ray spectra from the L (second innermost) shell of electrons of iodine ions, arising from collisions with targets ranging from carbon to lead. They show a remarkable specificity in the production of vacancies in the L subshells of the iodine ion, although the subshells differ in energy only by 200 or 300 eV out of a total binding energy of about 5 keV and although the vacancies are produced by collisions of ions having energies of many million electron volts. The relative numbers of vacancies produced in the $2p_{1/2}$, $2p_{2/3}$, and $2s_{1/2}$ subshells were extracted from the observed x-ray spectra and were found to vary strongly with slight changes in the atomic number of the target element.

A plot was drawn of an x-ray intensity ratio corresponding to the relative probabilities for producing vacancies in the $2p_{3/2}$ subshell and in the $2p_{1/2}$ and $2s_{1/2}$ subshells together as a function of the atomic number of the target. It showed that there are two maxima

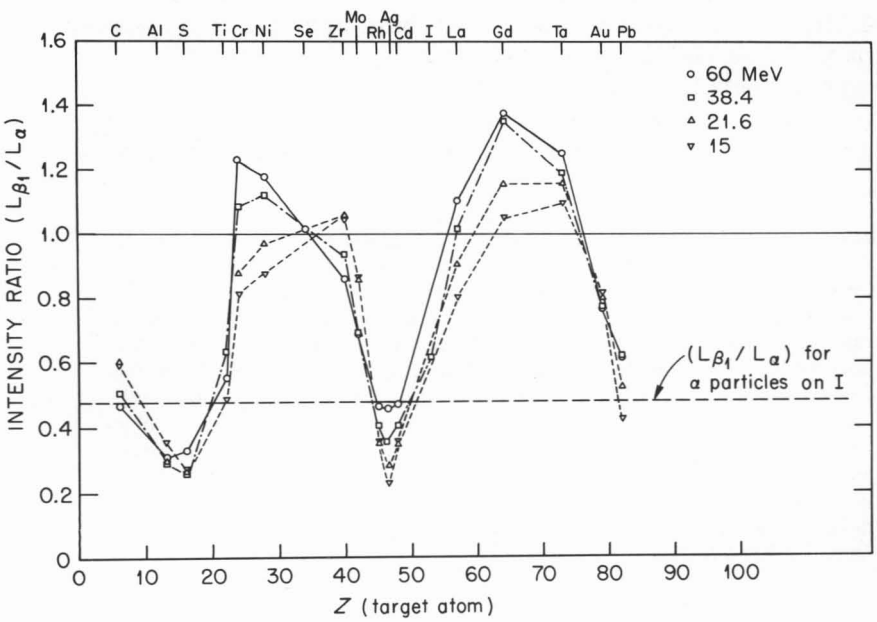

Ratio of $2p_{1/2}$ vacancy production to $2p_{3/2}$ vacancy production in atomic collisions of 15- to 60-MeV iodine ions incident on various targets compared with the "normal" vacancy ratio produced by simple charged particle interactions.

between carbon and lead, the ratios being about 1.4 and 1.2 at the maxima (gadolinium and chromium respectively) and about 0.2 at the minimum (silver). It seems likely that this very distinctive behavior will be explained in terms of a pseudomolecular interaction of extremely short duration between the projectile and the target atom, but the theory for this behavior is not yet available.

Radiation Damage in Graphite

Graphite has been extensively used in thermal fission reactors starting with the pile built by Fermi in 1942, in which the first self-sustaining nuclear chain reaction was realized. Present-day thermal reactor designs such as the molten-salt breeder reactor and the high-temperature gas-cooled reactor employ graphite as a reflector and moderator for the same reasons it was chosen for the first reactor. The nuclear properties of low thermal-neutron capture cross section and low atomic weight are essential for this application; however, the chemical and physical properties of graphite are also important in determining its use in reactors. An important factor in the economical performance of the MSBR and HTGR designs is the service life of the graphite, which is limited by radiation damage. It is of interest that in the same report in which Fermi described the success of the Chicago pile, E. P. Wigner called attention to the possible effects of fast particles on solids, pointing out that the collisions of fast neutrons with lattice atoms transferred sufficient energy to displace atoms from their equilibrium lattice sites. The possible effect of this process on the properties of a solid was unknown at that time, but studies since then have revealed that important changes can and do occur. The radiation damage process in graphite gives rise to dimensional changes and accompanying deterioration of mechanical properties that ultimately limit the service life.

The dimensional changes in graphite are related to its hexagonal crystal structure, in which the carbon atoms are tightly bound to each other in the basal plane, with only weak bonding between the planes. The collision of a fast neutron with a carbon atom in the crystal ejects the atom from its lattice site with considerable energy. In slowing down, the energetic atom makes collisions with lattice atoms, and the resulting displacement cascade will lead on the

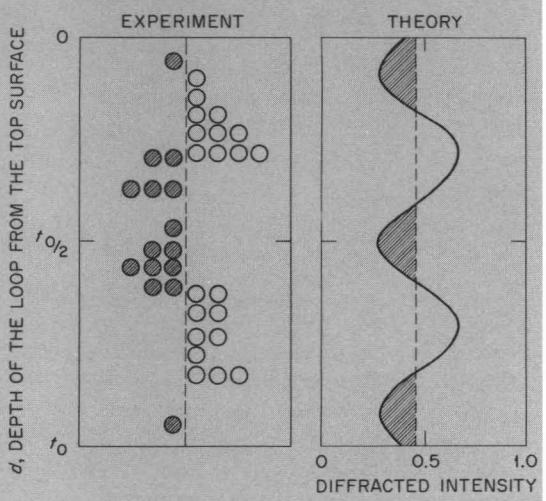

Stereo studies of the distribution of the damage in irradiated graphite single crystals have shown that the black and white spots are present in alternating layers parallel to the crystal surface. To understand this contrast behavior, the anisotropic elasticity theory was developed to find the local distortions around the defect clusters and the results applied to calculate the electron microscope image contrast using the dynamical theory of diffraction. The theory predicts that the intensity of the diffracted electrons varies periodically with the depth of the defect clusters in the specimen and that alternating layers of black and white spots are to be expected. These results and other observations of the contrast behavior provide identification as to the nature and structure of these defect clusters.

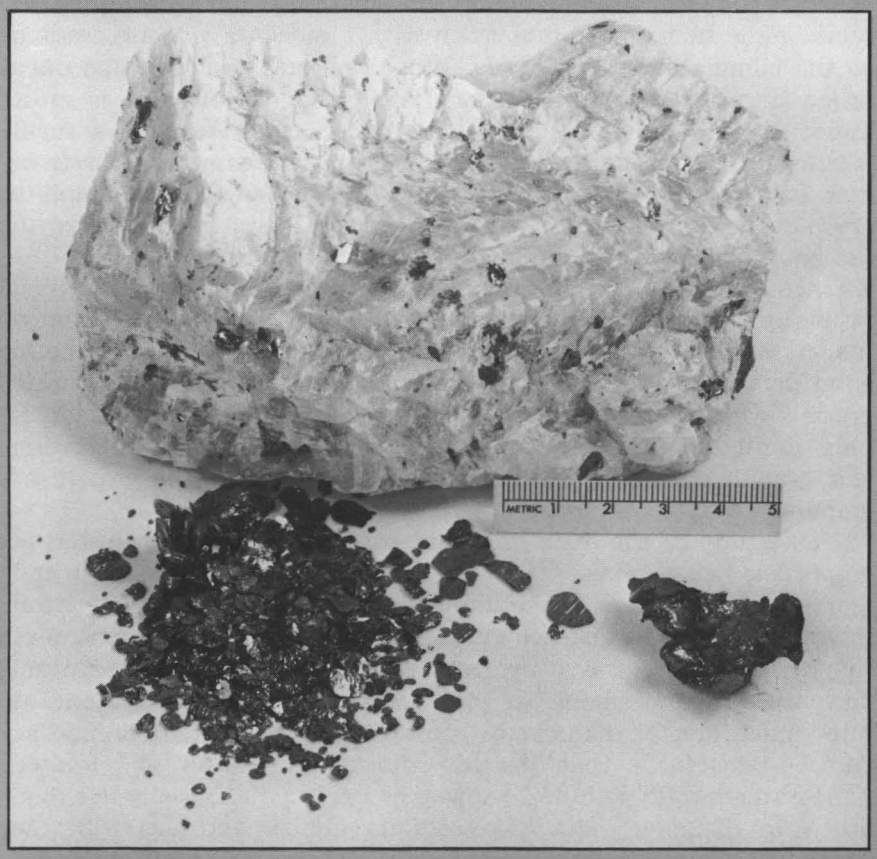

The Lead Hill graphite mine near Ticonderoga, New York, has been a prime source of research-grade graphite single crystals for over 50 years. The graphite is found near the interface of a magma intrusion into a limestone formation and is present in part as a seam of massive graphite (a sample is shown in inset) and in part as isolated crystals in a calcite matrix. Due to folding and deformation, the massive graphite is of little value for research purposes. The flakelike graphite crystals in rock like that shown in the inset are obtained by dissolving the rock in acid. Most of these crystals have also been heavily deformed, and only a small fraction will be perfect enough for research purposes. In 1970, ORNL's W. E. Atkinson, W. P. Eatherly, and T. S. Noggle (shown here) explored the Lead Hill mine and brought back over 500 lb of this graphite-bearing rock, from which about 10 to 20 g of research-grade single crystals will be obtained. To date, man-made graphite single crystals do not approach the perfection of these selected natural crystals.

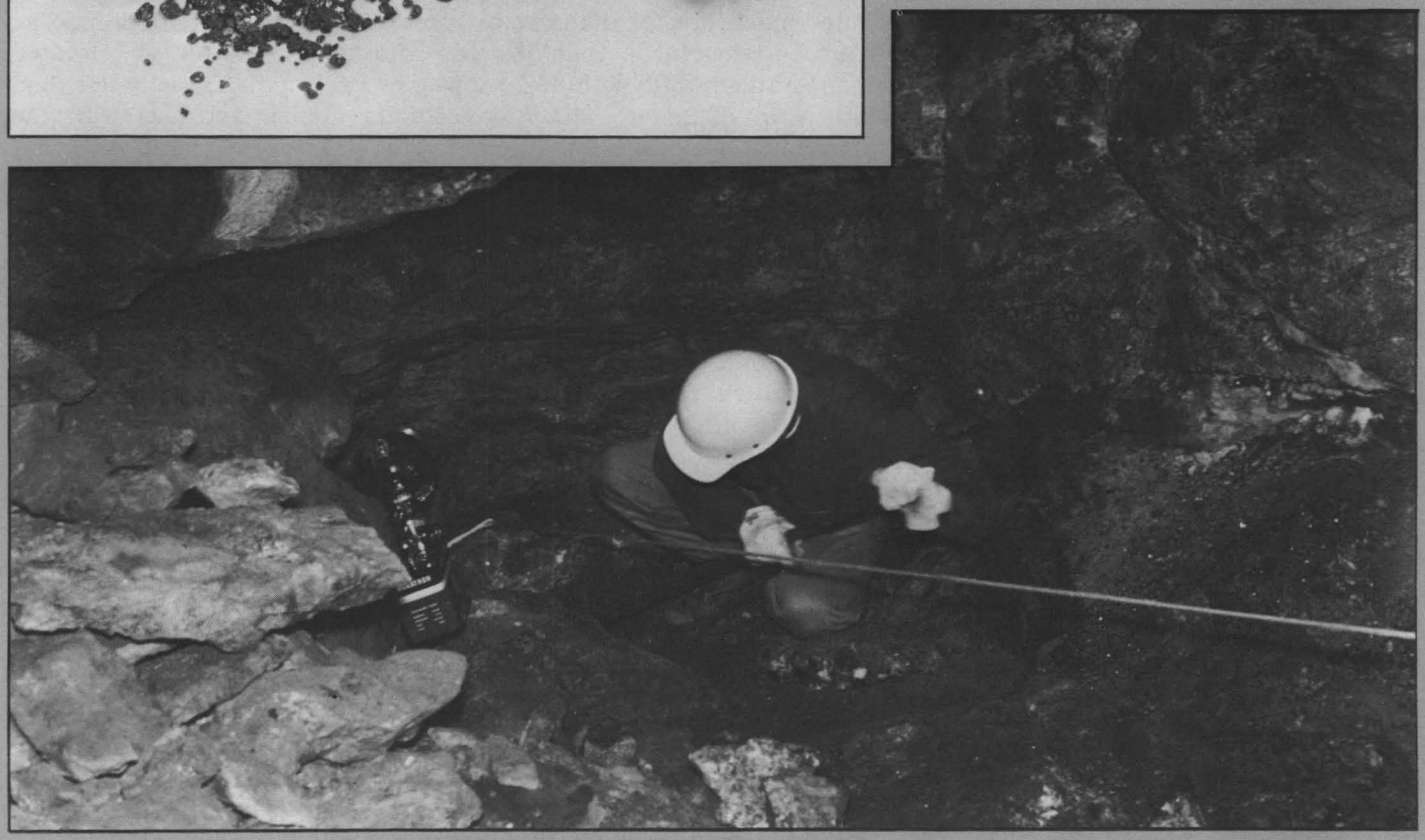

average to about 400 displaced atoms. The thermalization (slowing down) of a fission neutron requires 50 to 60 collisions and generates about 20,000 displaced atoms. At power reactor temperatures (300 to 600°C), these displaced atoms, called interstitials, diffuse freely between the basal planes until they encounter a defect in the crystal at which they can again be bound. Among the several possibilities for rebinding — such as recombination with a vacant lattice site, leading to the elimination of a vacancy-interstitial pair, and accretion onto dislocations or crystallite boundaries — the process that is most important for dimensional change is the aggregation of a small fraction of the interstitials into clusters, which become small areas of new atomic planes between the original basal planes of the graphite crystal. These interstitial clusters expand the crystal perpendicular to the basal plane, and in conjunction with the contraction due to the vacancies, they lead to a change in the shape of the crystal, seen primarily as growth perpendicular to the basal planes. This atomic model that accounts for the dimensional changes has developed in good part as a result of study of irradiated natural graphite single crystals with the transmission electron microscope. To date, there is only limited understanding of the factors affecting the nucleation and growth of the interstitial clusters and, in turn, the growth of graphite.

The study of the nucleation and growth of interstitial clusters in graphite is being carried out in the Solid State Division at ORNL and employs the electrons in the illuminating beam of a 200-kV electron microscope both to displace atoms and to form magnified images of the defect clusters resulting from the irradiation. The high beam current density attainable in the microscope displaces the atoms at rates much greater than can be attained in reactor irradiations. The damage structures that develop during irradiation at elevated temperatures (300 to 600°C) appear as small spots, initially less than 50 Å in diameter, which increase in number and size with the continued electron bombardment. This structure is identical to that previously observed in reactor-irradiated graphite. Moreover, the detailed appearance of these spots is sensitive to the diffraction of the electrons, and by tilting the specimen to change the diffraction conditions, changes appear that are in qualitative agreement with those expected for interstitial clusters. Because of the highly anisotropic nature of graphite, previous theoretical calculations based on isotropic elasticity theory could not be employed to arrive at a quantitative relationship between the microscope images and the defect configurations. Upon examination of the possibility of applying anisotropic elasticity to this problem, it was found that the hexagonal crystal structure of graphite results in simplification, which in turn led to tractable solutions. These results have been incorporated into diffraction theory calculations to obtain the theoretical image contrast, which is in good agreement with the experimental contrast.

The development of anisotropic elasticity theory for this particular problem has also led to a more general solution of the problem of calculating the stress and strain fields around dislocation loops in other materials. It is being employed to improve the theoretical calculations relating diffuse x-ray scattering to the radiation damage in irradiated metals and to the interactions between point defects (vacancies and interstitials) and defect clusters.

WILDLIFE AT ORNL WHITE VIOLET

WILDLIFE AT ORNL PINK KATYDID

Chemistry

Radiohalos and Unknown Alpha Radioactivity

As is sometimes the case in research, progress in one field of science must await discoveries in another field. Before the discovery of radioactivity near the turn of the century, mineralogists had something of a mystery on their hands. They had observed beautifully colored rings surrounding pointlike centers in thin sections of certain minerals when looking through the microscope. While there was some speculation about the origin of these halos, as they were named, the essential factor in the genesis of the tiny microscopic ring structures was not realized until radioactivity was discovered. It was then postulated that some of the newly discovered radioactive elements might occur in the halo inclusions. If so, perhaps the tiny concentric colored rings were formed by particles ejected into the surrounding mineral by radioactive atoms in the minute centers. This theory was formulated almost simultaneously by Joly in Ireland and Mügge in Germany in 1907 and has since proved to be correct. It was found that the radii of the rings, identified as the terminal points of the radioactively ejected particles (subsequently known as alpha particles — actually helium nuclei), corresponded to the ranges of the respective alpha particles in the mineral — that is, they were related to the energy of the alpha particles in the radioactive decay. The explanation for the different ring sizes became apparent when the elements uranium and thorium were discovered to be the initiators of radioactive chains wherein a series of successive radioactive decays take place. That is, each ring in the uranium and thorium halos could be associated with a specific member of the decay chain, emitting alpha particles of a particular energy. Thus, long before radioactivity was discovered, nature had provided a photographic "replica" of such a phenomenon, dating back to the earliest period of the earth's history.

Besides the well-known uranium and thorium halos, there exist other varieties that are not easily explained. There are halo types that exhibit rings much smaller (dwarf halos) and much larger (giant halos) than any corresponding to known alpha radioactivity. Are these peculiar halo types indications of the previous existence of elements not known today? This possibility is now being studied with a variety of analytical techniques.

Research into the origin of the dwarf halos has recently spawned new interest in the work, performed decades ago, of several European scientists. These investigators reported some results indicating evidence of a type of alpha radioactivity much lower in energy

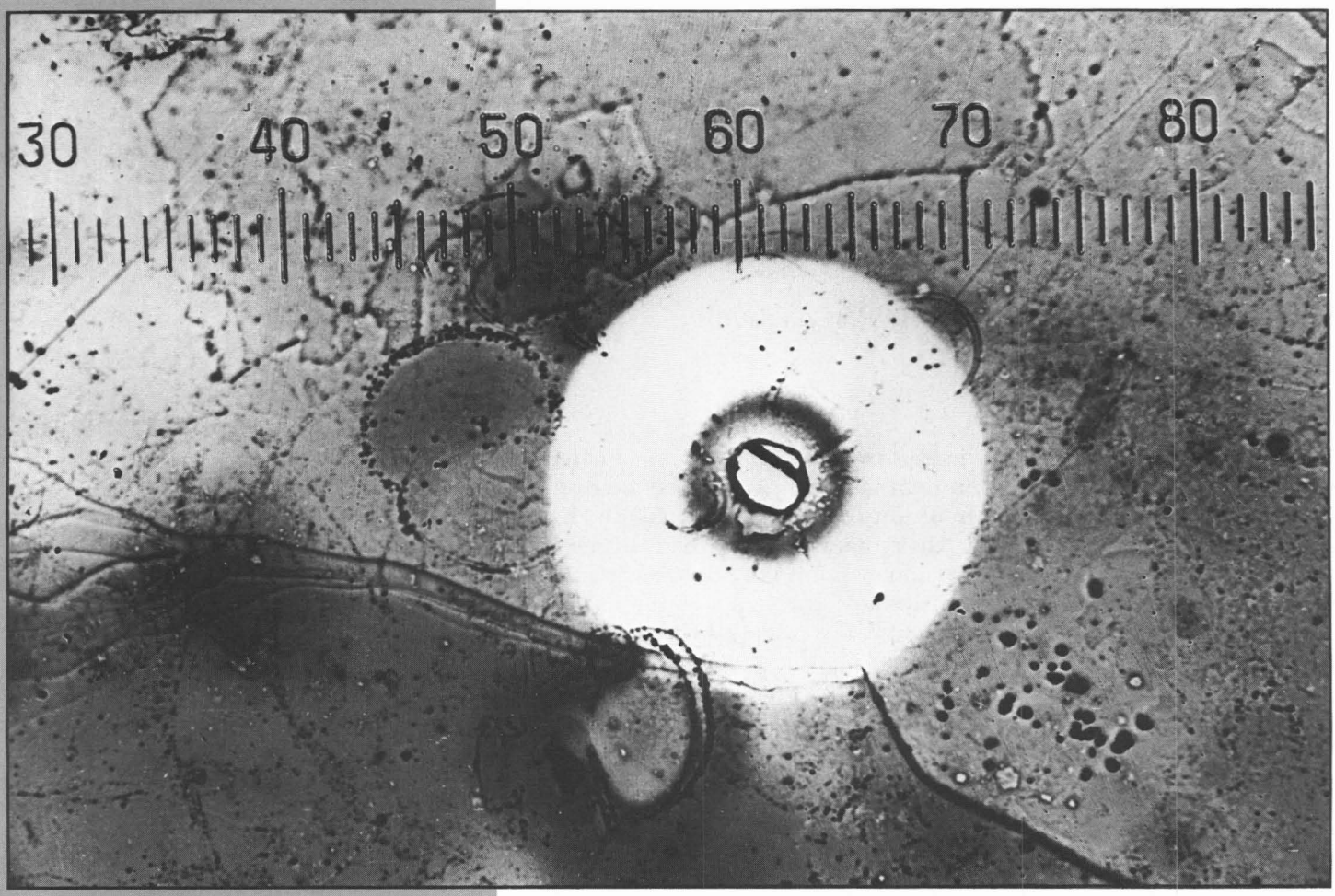

Certain terrestrial minerals, such as the mica from Madagascar shown here, often undergo visual coloration changes when subjected to radiation damage effects from radioactive sources such as uranium and thorium. The radiation from small radioactive inclusions often produces colored concentric spheres or halos, which, though invisible to the unaided eye, are visible when a thin section of the mineral is examined microscopically. While radioactive halos generally are produced by alpha radioactivity from the naturally occurring uranium or thorium series, the giant halo in this photomicrograph is something of an enigma, for there are no known radioactive elements possessing radiation with such high penetration distances. An intriguing possibility is that these extremely rare giant halos may be evidence of a type of radioactivity that existed in an earlier epoch of the earth's history but has since completely decayed. Each scale division is 0.01 mm.

than usually thought to exist in nature. Although World War II almost destroyed all traces of this research, one of the original investigators, F. Hernegger of the Radium Institute in Vienna, recalled certain facets of it to an ORNL staff member in Europe last year. As a result, ORNL researchers are working with some of the original ore samples found on the island of Elba, using autoradiographic and alpha-spectrometric techniques, in an attempt to pinpoint the exact nature of this elusive substance.

In addition, the giant halos have reopened interest in the question of the existence of unusually long-range alpha activity — another field that was lying dormant for lack of confirmation of some early experiments.

Significantly, the story does not end there. Other unusual halo types result from the decay of comparatively short-half-life radioactivity, and there is a question as to how this radioactivity got into the rocks. But at least the nuclides that produced these halos are known to originate with the isotopes of the element polonium. Confirmation of this identification came from analyzing the inclusions, or centers, of the polonium halos with a new type of mass analyzer, the ion microprobe mass spectrometer. This instrument works by focusing a small, intense beam of ions on a sample, thereby sputtering a portion of the halo nucleus directly into a mass analyzer for identification. It has already been used to discover a new type of

lead in the inclusions at the center of halos caused by the radioactive decay of polonium. Until recently, all known lead was categorized as primordial, common, or radiogenic, according to the abundances of the lead isotopes in terrestrial minerals and ores. The new spectrometer has revealed a form of lead with isotopic abundance ratios never before seen in nature.

What future surprises may be in store cannot be foretold, but it is indeed a coincidence that the ion microprobe, the one instrument capable of solving the problem of the genesis of the dwarf and giant halos as well as the polonium halos, has only recently come into operation. For the progress of science in this field one could hardly ask for a more fortunate circumstance.

Radiation Chemistry and the HO_2 Radical

How does lightning make ozone? How does light produce a visible image on photographic film? How does it convert (with the aid of chlorophyll) two normally very stable molecules, carbon dioxide and water, into sugars and oxygen? These are the kinds of question that are the everyday concerns of the radiation chemists.

During the course of a chemical reaction, many transient species may form and then disappear before the overall chemical change is completed. In order to be able to understand and control chemical reactions, it is necessary to identify these intermediates and to learn the nature and rates of their reactions (chemical kinetics). The types of intermediates produced depend principally on the way in which energy is introduced into the system — for example, whether the reaction is stimulated by heat, as in ordinary chemical reactions (thermal chemistry), by light, as in photography or photosynthesis (photochemistry); or by high-energy ionizing radiations such as x rays or high-velocity charged particles (radiation chemistry). Many of the intermediates can be produced in a variety of ways, and often they are common to all branches of chemical kinetics. Generally, these transient species are very reactive, and they may disappear in millionths or even billionths of a second. The trick in studying them is to produce a high concentration in a time that is short compared with their lifetime and, by some means, observe their behavior after formation. Two methods that have proved very fruitful in recent years and that are used by the radiation chemists at ORNL are flash photolysis and pulse radiolysis.

In these experiments the energy is supplied either by a bright flash of light (usually millionths of a second) or an intense pulse of high-velocity charged particles (millionths or billionths of a second). Very often the transient species absorbs light in a characteristic way, and, therefore, with a suitable combination of optical and electronic equipment, it can be studied on this short time scale.

One important transient species is the HO_2 radical, which appears in many reaction systems involving oxidation. It was first proposed almost 50 years ago as an intermediate in the combustion of hydrogen. In those days, direct observation of such transient species was not feasible, and their existence and functions were inferred from purely kinetic arguments, that is, arguments based on

how the rate of the reaction was affected by changing concentrations of the reactants. With the advent of pulse methods of producing intermediates in high concentrations and the improvement in sensitivity of detection methods, it became possible to detect various species whose existence had only been surmised. The HO_2 radical was one of these; its absorption spectrum in water solution was observed some eight years ago. However, in spite of much effort, no one had observed it in a gas reaction until this was achieved almost at the same time by radiation chemists at ORNL and by two chemists at Berkeley. The ORNL chemists also made accurate measurements of the rates at which these radicals reacted with each other to give oxygen and hydrogen peroxide, or with a different radical, hydroxyl (OH), to give oxygen and water. These are important reactions not only in radiation chemistry but also in combustion and other oxidation reactions and in atmospheric chemistry, including the normal surface atmosphere, polluted atmospheres, and the upper atmosphere. Atmospheric modeling calculations require accurate information on the reactions occurring, especially the values for rates of reactions such as those mentioned above.

These observations of the HO_2 radical are only a part of a much broader study of the radiation chemistry of atmospheric gases. Prominent among the molecules of interest is ozone. It can be formed by the action of either ultraviolet light or high-energy radiations on oxygen; the source of the ultraviolet light may be the lamp in the clothes dryer or light from the sun, and the high-energy radiation may be supplied by an atomic reactor or the radiations in space. The ozone layer in the upper atmosphere is a blessing, since it protects us from the damaging ultraviolet radiation from the sun, but the ozone in polluted atmospheres is a curse, since it is a key intermediate in the photochemical formation of the irritating and dangerous molecules produced from the hydrocarbon and nitrogen oxide pollutants. The radiation chemists have been studying mechanisms for ozone formation, including sensitized formation by energy transferred from irradiated nitrogen, helium, or argon, and also the inhibition of ozone formation by water, ammonia, hydrogen, and sulfur hexafluoride. The results have obvious implications in many modern technological problems — for example, the effect of the SST on the ozone layer.

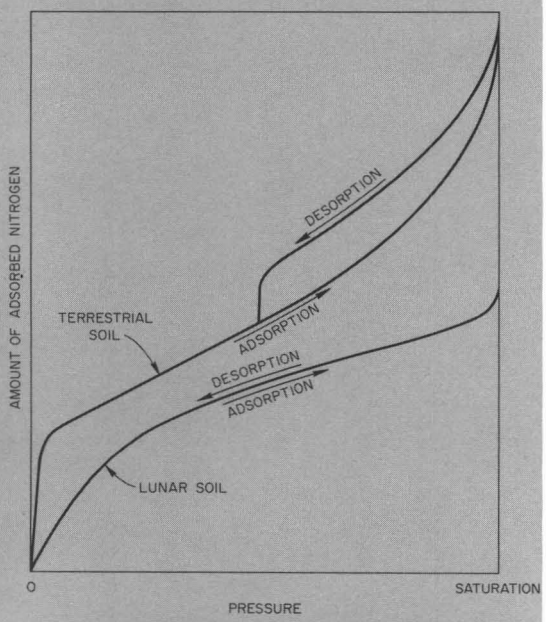

The adsorption of nitrogen on terrestrial and lunar soils shows the contrasting nature of the surfaces of the soil particles in the two cases. Absence of porosity in the lunar soil particles is evidenced by the coincidence of the adsorption and desorption data. This is not the case for the terrestrial soil. The greater surface energy of the terrestrial soil particles causes the isotherm to rise more steeply at low pressures than is the case for adsorption of nitrogen on lunar soil. These isotherms are not drawn to scale, since at any given pressure, terrestrial soil adsorbs approximately 100 times as much nitrogen as the same weight of lunar soil.

Interaction of Gases with Lunar Soil

Vapor adsorption studies at ORNL have proven to be of appreciable aid in revealing the nature of the disordered surface layers on particles of lunar soil. This aluminosilicate regolith has been subjected to eons of bombardment by solar wind and cosmic radiation, which have rendered the outer 40 to 200 atomic layers quite amorphous. Nitrogen and carbon monoxide are weakly adsorbed, whereas the less reactive argon and oxygen are attracted to the surface only by extremely weak forces at −196°C. The data for

all of these vapors are consistent with an area of 1.1 m^2 per gram of soil, compared with the value of about 100 m^2/g for terrestrial, "back-yard" soils.

Water vapor shows a somewhat limited uptake initially but does penetrate into the amorphous region through various avenues at higher relative humidities. There is, however, a very distinct group of routes (probably radiation damage tracks) where water enters at a relative humidity of 90% and is removed at 80%. In addition, there is a slow reaction of water at the internal ends of these routes to form a stable state that cannot be removed at ambient temperatures in a vacuum. Water vapor seems uniquely to penetrate these tracks via a hydration mechanism, whereas the other gases are completely excluded.

Elevated temperatures (500 to 600°C) are needed to heal these penetration avenues with no concomitant loss of surface area. At 800°C the material sinters appreciably, and the specific surface area decreases to less than 0.05 m^2/g. Thus we can conclude that the lunar temperature has not exceeded 500°C since the nearly saturated damage condition (about 10^{12} tracks/cm^2) was achieved. Nor has the temperature been above 800°C since the formation of the small grains of soil.

New Uses for Liquid Scintillation

High-Resolution Spectrometry for Alpha Radiation

Liquid scintillation counting — photoelectronic monitoring of the flashes of light caused by radioactive disintegrations of a radionuclide incorporated in a fluorescent liquid — has long been known and used primarily as a sensitive method of detecting and counting weak beta radiation. By far its largest use is in the assay of biological materials for carbon-14 and tritium. Alpha radiation can also be counted effectively by liquid scintillation methods (with 100% efficiency, in fact, compared with 5 to 50% efficiency by the more usual methods), but liquid scintillation has been little used for alpha counting because of (1) interference from beta and gamma radiation in the sample, (2) difficulties in introducing the usually

High-resolution energy spectra of alpha particles obtained with a liquid scintillation spectrometer.

(a) Thorium-232 and four of the daughters in its natural decay chain show the alpha-particle energy resolution of which the new liquid scintillation system is capable.

(b) Natural uranium shows the normal ratio of uranium-238 and uranium-234. The peak for uranium-235 can be found between these two peaks by computer analysis.

(c) Alpha activity detected in routine urinalysis monitoring was identified as californium-252, energy near 6.1 MeV, at a count rate of 2.2 dis/min by this method.

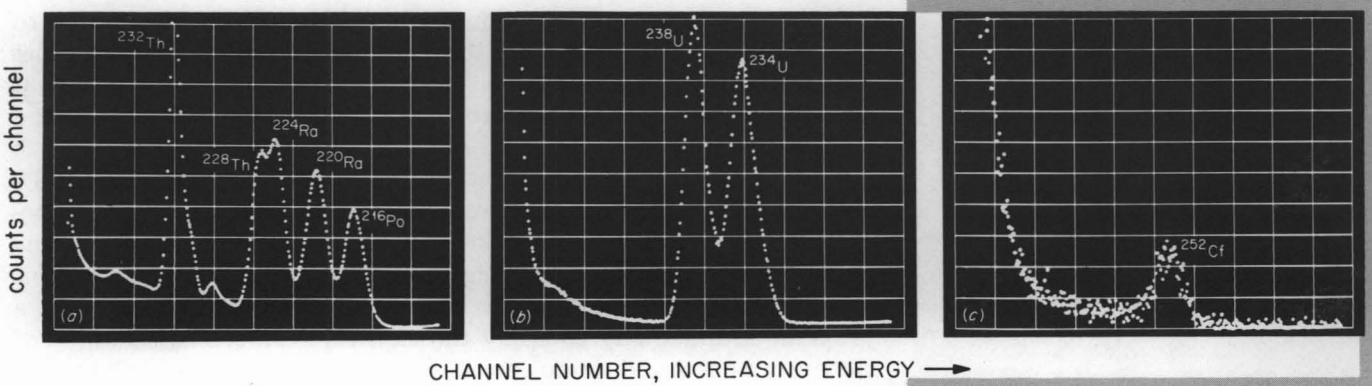

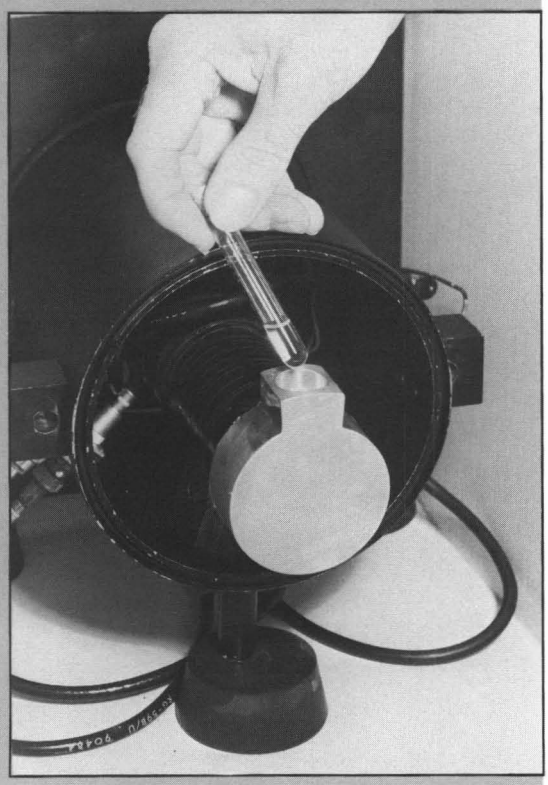

The source of alpha particles, in a solution of extractive liquid scintillator, is placed in a reflecting cavity attached to a photomultiplier tube inside a lightproof canister, the whole contained within a box made of lead 3 in. thick. By combining the techniques of solvent extraction with those of liquid scintillation, very high resolutions in alpha-particle counting have been achieved.

metallic nuclides into the primarily organic scintillator, and (3) "quenching." The term "quenching" covers a multitude of problems. In general it means any interference with the production of light in the scintillator or with its transmission to the detector, a multiplier phototube. In the case of alpha counting, variable quenching changes the amount of light produced by an alpha particle of a given energy. Since the introduction of almost anything into the scintillator mixture changes its quenching characteristics, the same alpha-emitting nuclide in different media (containing different amounts of water, salts, etc.) would show different light outputs and appear at different places on the energy scale of the spectrometer. Thus, used in the customary manner, liquid scintillation counting was not a reliable way to identify alpha energies.

New developments last year at ORNL virtually eliminated the problems associated with quenching (for alpha-emitting nuclides) as well as those encountered in introducing the nuclide to be counted into the scintillator. Large improvements have also been made in the alpha energy resolution capabilities of liquid scintillation, with a corresponding decrease in the interference of beta and gamma radiation with the alpha-particle spectra.

In the past year, ORNL chemists have applied a number of techniques to liquid scintillation. Perhaps the greatest success comes from combining the technology of solvent extraction with liquid scintillation: Either the nuclide is added to the scintillator in an organic extract from a separate solvent extraction step, or the extraction reagent is added to the scintillator, thus making the scintillator itself the extractant. These techniques provide methods of introducing the nuclide of interest into the scintillator without adding variable amounts of quenching materials such as water, acids, or salts. The scintillator system is thus reproducible and can be calibrated so that it is a reliable way to identify alpha-particle energies. Other improvements have been made in scintillator mixtures, light collection and detection equipment, and electronic instrumentation.

These developments in liquid scintillation counting appear to have important applications in the analysis of alpha-emitting nuclides in plant processes and in the laboratory. Of particular interest at present is the application to the simultaneous detection and identification of alpha-emitting nuclides in environmental and health physics surveys. The characteristics of low background, 100% efficiency in alpha-particle counting, and production of an alpha-particle energy spectrum make the method ideal for identifying alpha-emitting nuclides in samples of very low count rate. This method has proved useful for health physics survey work, and a program is under way to apply the method to an ecological study of the movement and distribution of certain alpha-emitting nuclides.

Mathematics

Canonical Analysis

Canonical analysis is a technique used by statisticians for reducing the collection of several measurements in an experiment to a number of components that can be plotted.

The capability for canonical analysis in the Mathematics Division was put to use last year on a research program in the ecological sciences. In the study of the effects of elevated water temperatures on fish, measurements on five proteins were made from blood sera taken from fish that had been subjected to thermal shock by being placed in warmer water for 5 min and then returned to their original habitat. Fish that had been acclimated at 16°C were placed in water at 26, 28, or 30°C as well as an additional 16° temperature for a control group. After 5 min they were returned to the 16° water, and the sera were collected 5, 30, 60, or 240 min later. Each of these samples was then tested for the five proteins.

The five measurements from each blood sample constitute a vector of multivariate data. The vector from fish shocked at 28°C may or may not be different from the vector from fish shocked at 30°C, for instance. It is hard to tell how much difference there may be by just looking at the vectors, because there are five different protein measurements to compare at one time. Moreover, the measurements are interrelated.

By using the technique of multivariate analysis called canonical analysis, the vector of five measurements may be reduced to a vector of only two that are independent of each other. The elements of this new vector can then be plotted, and, to acknowledge the fact that the measurements of the proteins are subject to statistical variation, a "circle of uncertainty" can be drawn around the resulting point.

From the data on the fish removed for examination 5 min after reacclimation, a plot of two canonical variates for the four different temperatures revealed a general overlapping of the circles of uncertainty, indicating that there was no clear-cut temperature effect. However, a similar plot for fish treated in the same manner but allowed to reacclimate 4 hr before being examined showed a distinct separation of the four different temperature groups. Thus, a significant effect of temperature shock can be seen after a longer recovery time.

A plot of the canonical variates was examined for the control fish kept continuously at 16°C. Here there was an overlapping of the circles of uncertainty, indicating no essential difference due to the amount of "recovery" time. A similar plot for the fish shocked at 28°C showed that the groups allowed to recover for 5 min and for

The upper plot is for control fish that were kept continuously at 16°C. Here the overlapping of the circles of uncertainty indicates no significant difference due to the amount of "recovery" time. Below, for fish subjected to thermal shock at 28°C, the picture changes considerably. The 5-min and 30-min recovery times are significantly different from the rest, but the 1-hr and 4-hr recovery times are not different from each other.

The top graph is a plot of variates for fish subjected to thermal shock at three different temperatures (26, 28, and 30°C) and removed for examination 5 min after reacclimation, together with a control group held at 16°C. The general overlapping of the circles of uncertainty indicates no clear-cut effect of temperature. The plot below, however, is for fish treated in the same manner but allowed to reacclimate 4 hr before being examined. Here there is a distinct separation of the points, indicating a significant effect of temperature on the blood sera of the fish when they are allowed a longer time to recover.

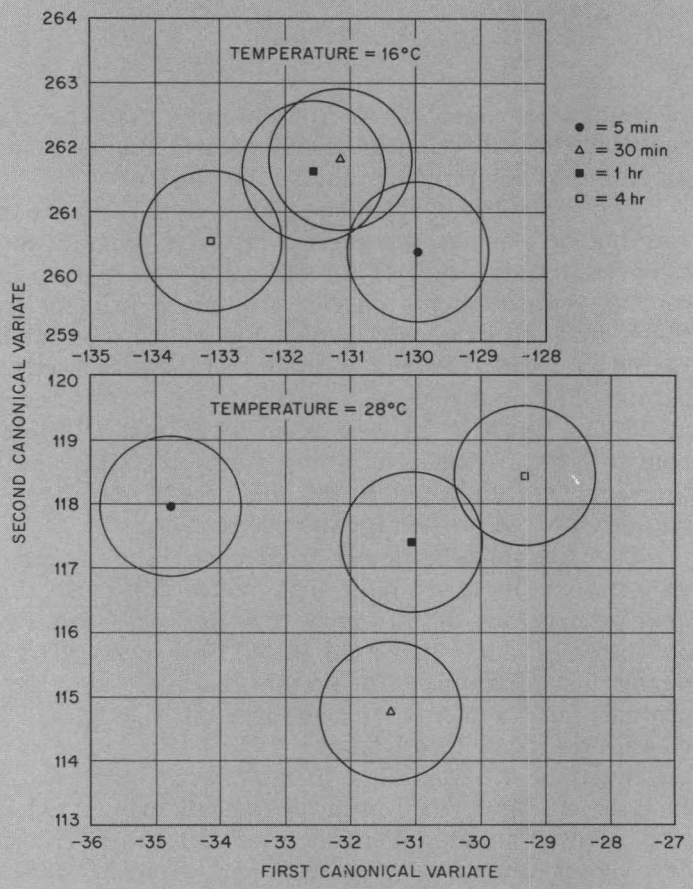

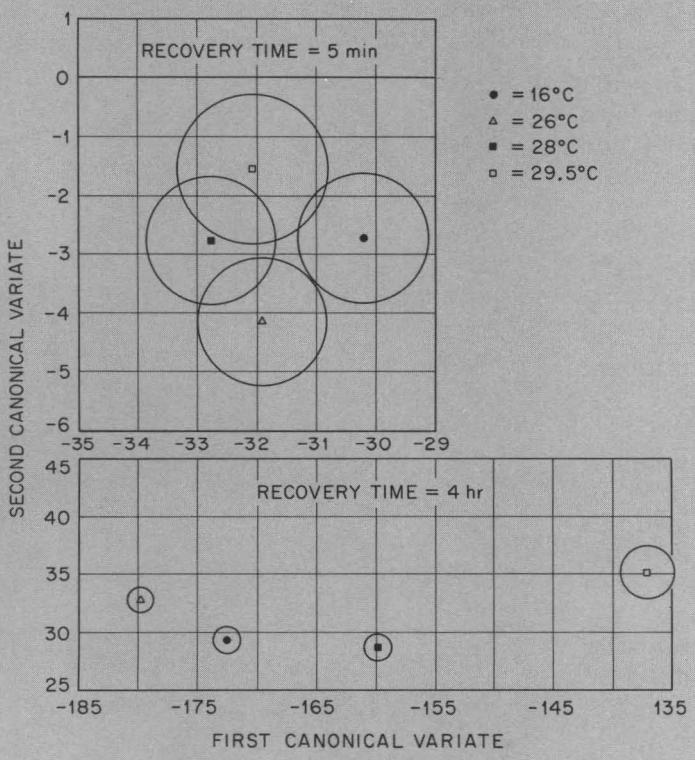

30 min were significantly different from the rest but that the groups allowed to recover for 1 hr and for 4 hr were not different from each other.

An experimenter could not be expected to detect phenomena of this kind by examining sets of five interrelated measurements. The social sciences, too, might well use the techniques of canonical analysis with profit in their experiments and studies. The reduction to two independent canonical variates permits a useful evaluation of the phenomena.

Life Sciences

Mutagenesis in Young Male Mice

Previous work in the Mammalian Genetics Section of the Biology Division has demonstrated the degree of sensitivity of germ cells present in adult male mice to the induction of gene mutations by ionizing radiation. This knowledge is useful in estimating the genetic hazards of radiation to man. The work has also shown that different germ-cell stages in the adult can have different degrees of sensitivity to the induction of gene mutations. The mouse testis is known to undergo great changes both in size and cell stages present between birth and adulthood. The Mammalian Genetics Section is exploring the possibility that the germ cells present in the testes of newborn or young male mice might have a sensitivity to the induction of gene mutations different from adult germ cells. A much higher sensitivity in young animals would be of considerable importance in the estimation of genetic hazard to man.

A large enough experiment is being done on newborn male mice to produce a reliable estimate of the mutation frequency for comparison with that found in adults. Male mice irradiated within 9 hr after birth with 300 R of x rays delivered at 80 R/min have sired 55,000 offspring, which have been observed for gene mutations. The point estimate of the frequency of mutations is only half as high as that found previously for similarly irradiated adult males, and the difference from adults is statistically highly significant.

Groups of male mice have also been irradiated with 300 R delivered at the rate of 80 R/min at 2, 4, 6, 8, 10, 14, 21, 28, and 35 days of age. The closer intervals at the earlier ages were chosen because of more rapid changes in the testes of the very young mouse. Thirty-five days was chosen as the latest age at irradiation, because by this time the testis resembles the adult testis histologically.

The reason for screening these nine ages was the possibility that the testis might pass through some stage during development in which its germ cells were highly susceptible to mutation induction. It was felt that a slightly increased mutational sensitivity during some stage of development would be of no great consequence in estimating the genetic hazard to man, since such a stage would be exposed for a short period of time relative to the germ cells present in the adult testis. (Maturation of the human testis is complete at about 12 years of age.) The experiments at these nine ages were therefore designed to determine whether the upper 95% confidence limit of the mutation rate at any one of the nine ages exceeded the point estimate of the adult rate by a factor of 4.

Paul Selby examines approximately one-quarter of a cup of half-day-old mice that are participating in the metagenesis program.

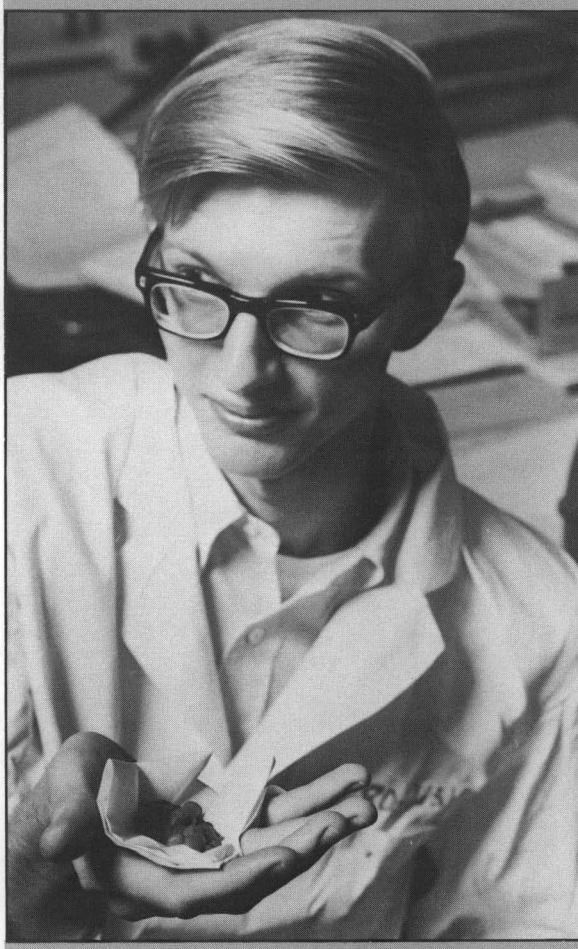

WILDLIFE AT ORNL LONG-TAILED WEASEL

To date, about 8000 offspring sired by each of the nine groups of irradiated males have been observed for gene mutations. Of the nine groups, seven have point estimates of the mutation rate lower than that of the adult. The highest has a point estimate 1.8 times that of the adult. However, neither this group nor the other group with a higher point estimate has a mutation rate statistically significantly higher than the adult mutation rate. Even the upper 99% confidence limit for each of the nine ages screened is less than four times the adult mutation frequency. It therefore appears highly unlikely that the mouse testis passes through any stages of development between birth and adulthood during which the germ cells in it are very much more sensitive to the induction of gene mutations than those of the adult.

Combining the data for the nine ages screened gives a mutation rate slightly less than that of the adult. Since the germ cells present in the newborn testis do show a markedly lower mutational sensitivity than those of the adult, the obvious question arises: When does the transition from the lower mutational sensitivity of the newborn testis to the higher mutational sensitivity of the adult testis occur? The present data suggest that the change has occurred by day 8, but further experimentation will be necessary to determine the exact time of the change and whether it is abrupt or gradual. Further work will also be necessary to determine the cellular basis for this change in mutational sensitivity.

Work at Harwell, England, had shown that the mutational sensitivity of the germ cells present in the male fetus at $13\frac{1}{2}$ and $17\frac{1}{2}$ days after conception could not be much higher than that of the adult. (The gestation period of the mouse is 19 days.) The point estimate of the mutation rate for each of these small experiments is lower than the point estimate for the adult.

The work at ORNL will constitute a part of the special report, now in press, on genetic effects by the United Nations Scientific Committee on the Effects of Atomic Radiation. The new data have filled in the gap in our knowledge of the mutational sensitivity of the developing testis between birth and adulthood. No stage in development has shown a statistically significant increase over the sensitivity of the adult. On the other hand, in at least one stage — the newborn — the testis clearly has a lower sensitivity to the induction of gene mutations than the testis of the adult mouse.

Viral Enzymes and Carcinogenesis

Certain types of RNA viruses are known to cause cancer in animals, including cats, mice, and monkeys, and are strongly suspected of inducing cancer in humans. Although the ability of these RNA tumor viruses to transform normal cells into genetically stable cancer cells has long been recognized, it was not until 1970

that we had a satisfactory explanation of how this transformation occurs. In that year, biologists at the University of Wisconsin and the Massachusetts Institute of Technology, working independently, showed that oncogenic (tumor-forming) RNA viruses contain an enzyme ("reverse transcriptase") that uses the viral RNA as a template for the synthesis of double-stranded DNA, which in turn is integrated into the chromosomal DNA of the host cell. This addition of viral DNA to the host's genetic material permits the production of new virus and is thought to be responsible for the cell's transformation into a cancer cell. The researchers' demonstration of genetic information flow from RNA to DNA completely reversed the entrenched dogma that the direction of flow is always from DNA to RNA and thus had wide implications for cancer research. If, for example, a way could be found to disrupt the transcriptase-catalyzed reaction required for the synthesis of viral DNA, then it might be possible to control the induction of cancer by these viruses.

This work, then, stimulated, at ORNL and elsewhere, studies aimed at characterizing the structure and behavior of this viral DNA polymerase, or reverse transcriptase. Experiments performed in the Biology Division by members of the ORNL Carcinogenesis Program have recently produced several promising results in connection with these efforts. When reverse transcriptase was isolated from a leukemia virus and placed in a reaction mixture containing synthetic single-stranded polyribonucleotides, it was strongly inhibited by these long chains of sequentially linked uridylate (U), guanylate (G), adenylate (A), or cytidylate (C). Inhibition of the enzyme resulted from competitive binding with a polyribonucleotide. The term "competitive" means that both the viral RNA and the polymers, because of their structural similarities, compete for binding sites on the viral enzyme. Sufficient amounts of the enzyme can become bound to a polymer instead of the viral RNA to inhibit the enzyme.

Significantly, none of the four polymers inhibited DNA polymerase from normal cells — which indicated that the inhibition was specific for the viral enzyme. This finding provided a simple means of distinguishing between viral and cellular forms of DNA polymerase, a task that can seriously complicate research with reverse transcriptases.

Once the inhibitory activity of the polyribonucleotides was established in a reaction mixture, it became important to determine whether they would inhibit virus function in whole cells and tissues. Mouse cells growing in tissue culture were therefore infected with a leukemia virus, and each of the polymers was added to the culture medium at different times. The results showed that only poly(A) significantly affected virus function — specifically, by inhibiting the production of new viruses within the infected cells. Inhibition of virus replication was seen only if poly(A) was added to the medium just before or just after the cells were infected with virus, which implies that the polymer was acting on reverse transcriptase, as it had in the synthetic reaction mixture. The reason that only poly(A) appreciably affected virus replication was probably that the other polymers were not getting inside the cells in sufficient quantity to be effective. The short duration of poly(A)'s effectiveness can be attributed to its degradation by normal cellular enzymes called nucleases.

WILDLIFE AT ORNL GOATSBEARD

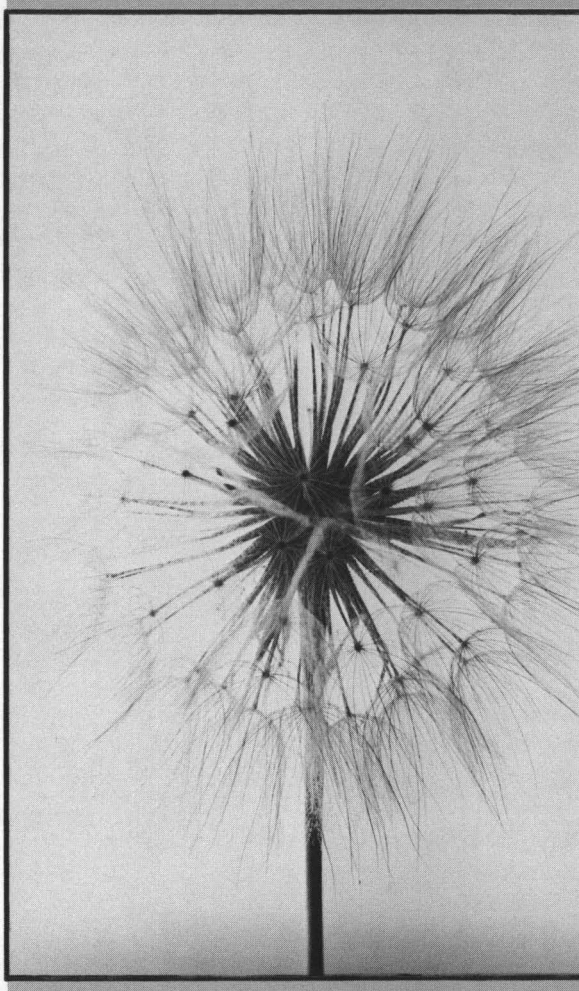

Pathology and Repair Mechanisms

Scheme for detecting defective repair of lesions in cell DNA. Cells from patients with the hereditary disease xeroderma pigmentosum are incapable or only minimally capable of carrying out DNA repair. This disease results in high sensitivity to ultraviolet light, including the induction of skin cancer upon chronic exposure to sunlight, and is invariably fatal. The following method was developed at ORNL to detect human fetuses that are incapable of repairing damage caused by ultraviolet radiation.

When normal human cells, capable of carrying out the repair of ultraviolet-induced lesions in their DNA, are incubated in the thymidine analog 5-bromodeoxyuridine after ultraviolet irradiation, the analog is incorporated into the regions being repaired. If such cells are subsequently exposed to 313-nm radiation and then placed in alkali, breaks appear in the DNA at the sites of incorporation of 5-bromodeoxyuridine, inducing a dramatic downward shift in the sedimentation constant of the DNA. Under the same conditions, xeroderma pigmentosum cells incorporate little 5-bromodeoxyuridine into their DNA and, upon 313-nm irradiation and sedimentation in alkali, exhibit only minor shifts in DNA sedimentation constants. When fibroblasts developed from biopsies of normal skin and of skin from patients with xeroderma pigmentosum are assayed in this fashion, unequivocal differences between normal and repair-defective cells are shown. The method can be used with cells taken from amniotic fluid for prenatal diagnosis of the disease.

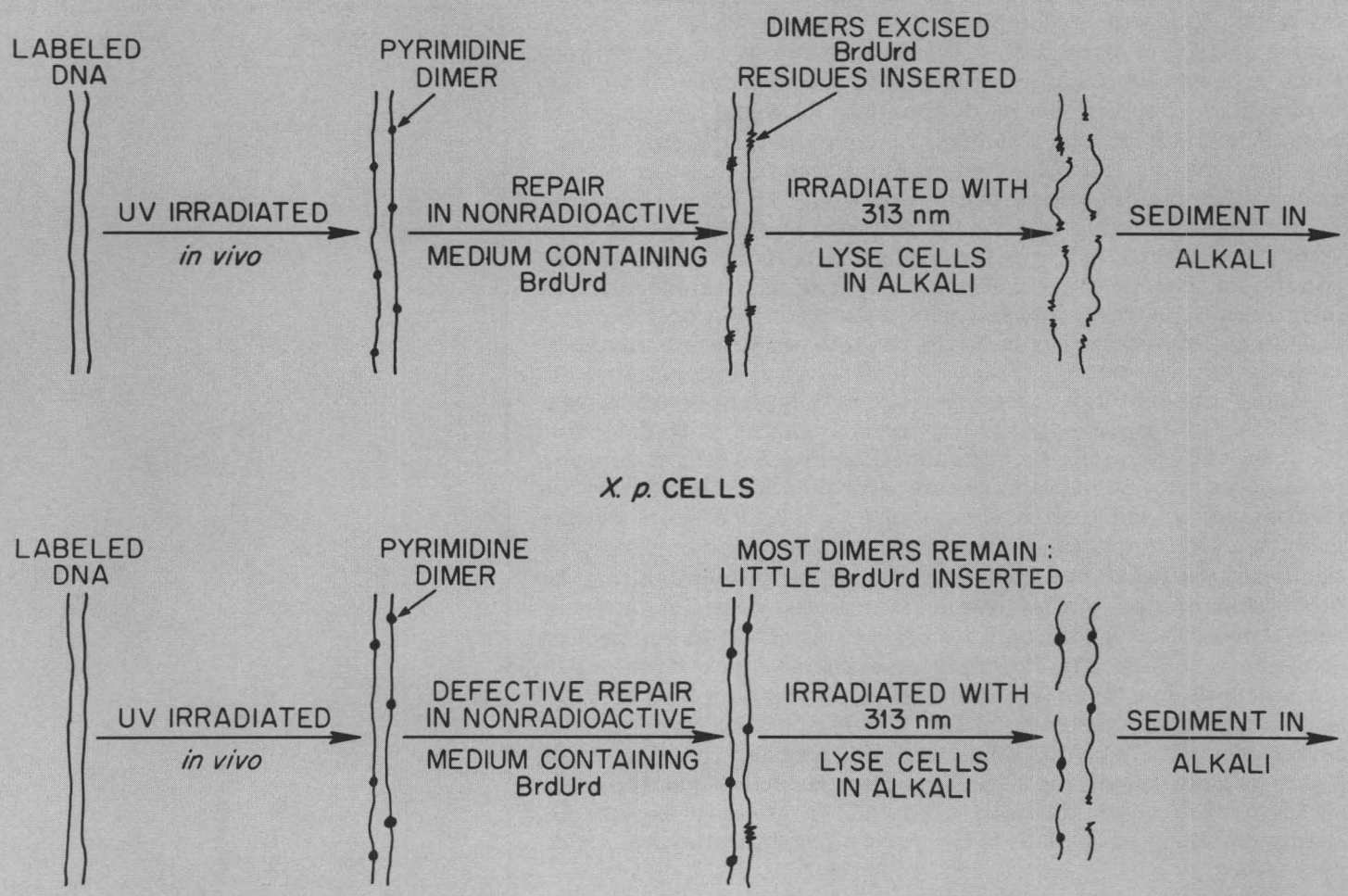

An intriguing aspect of this inhibition of virus function by a polyribonucleotide is that poly(A) appears to have no adverse effects on the cell. Should this be true, poly(A) would have a decided advantage over chemicals that halt virus production but injure the cell.

Efforts to develop a polyribonucleotide that is resistant to nuclease degradation are under way. Preliminary results indicate that certain methylated derivatives of poly(A) will resist nuclease activity while retaining the ability of their parent compound to inhibit the viral transcriptase. After additional characterization in tissue culture, these derivatives will be tested for their ability to block development of virus-induced malignancies in the whole animal. The outcome of these experiments will be critical to assessing the possibility that polyribonucleotides may someday be useful in cancer therapy.

It is not known whether reverse transcriptase is unique to cancer cells. Should it be, detection of the enzyme in an individual could signal the presence of a malignancy. Techniques to exploit this possibility are being developed in the Carcinogenesis Program. A special type of column, constructed of a cellulose-like material permeated with synthetic polyribonucleotides, is being tested for its ability to bind reverse transcriptase selectively. Results obtained thus far indicate that the reverse transcriptase from at least two types of cancer viruses can be isolated by this method.

Internal Dose Estimates by Age Groups

A concentration of gamma radioactivity in a particular organ of the body will, of course, affect neighboring organs. If the source is, for example, in the stomach, some of the radiation will strike the lungs and liver, and the dose rate in these organs will be determined by the inverse square effect and the amount of absorbing material that may intervene. In a child or infant, therefore, a higher dose rate would be expected in the lungs and liver per unit of source in the stomach than would be the case for an adult.

Quantitative estimates of this scaling effect have recently been made in the Health Physics Division by a computer study. With lungs and liver as target organs, dose per emitted photon was estimated by a Monte Carlo technique using photons of five different energies emerging from the stomach of a heterogeneous phantom. In this work the phantom previously developed to represent an adult was reduced by scale factors selected separately for the head section, the trunk section, and the leg section for five different age groups. When plotted vs age, the dose per photon was found to increase by more than a factor of 10 as the age decreased. A similar result is found when the lungs are the source organ.

Although these data are preliminary, they demonstrate the expected increase of dose for younger ages as well as a means of supplying the dose estimates for various age groups. Such dose correction factors are of great importance in nuclear medicine and in obtaining reliable estimates of dose for population exposure, since they are needed in obtaining an accurate estimate of dose, and the magnitude of the correction factor is quite large.

Environmental Monitoring

Recent concern over the radioactive pollution of aquatic, terrestrial, and atmospheric surroundings from operations of institutions engaged in nuclear enterprise has stimulated efforts to make accurate measurements of natural background radiation levels. Reasonable estimates of these levels have been possible for several years through the use of widely accepted techniques. Because of reductions in the maximum permissible levels of exposure to members of the general population, however, it is now necessary to make qualitative, as well as quantitative, measurements of natural background plus incremental amounts of radiation due to radionuclides deposited as a result of actions by man. In order to make

An interior view of the Health Physics Division's mobile low-level environmental monitoring laboratory. W. H. Shinpaugh is shown calibrating detectors in preparation for making measurements in the field.

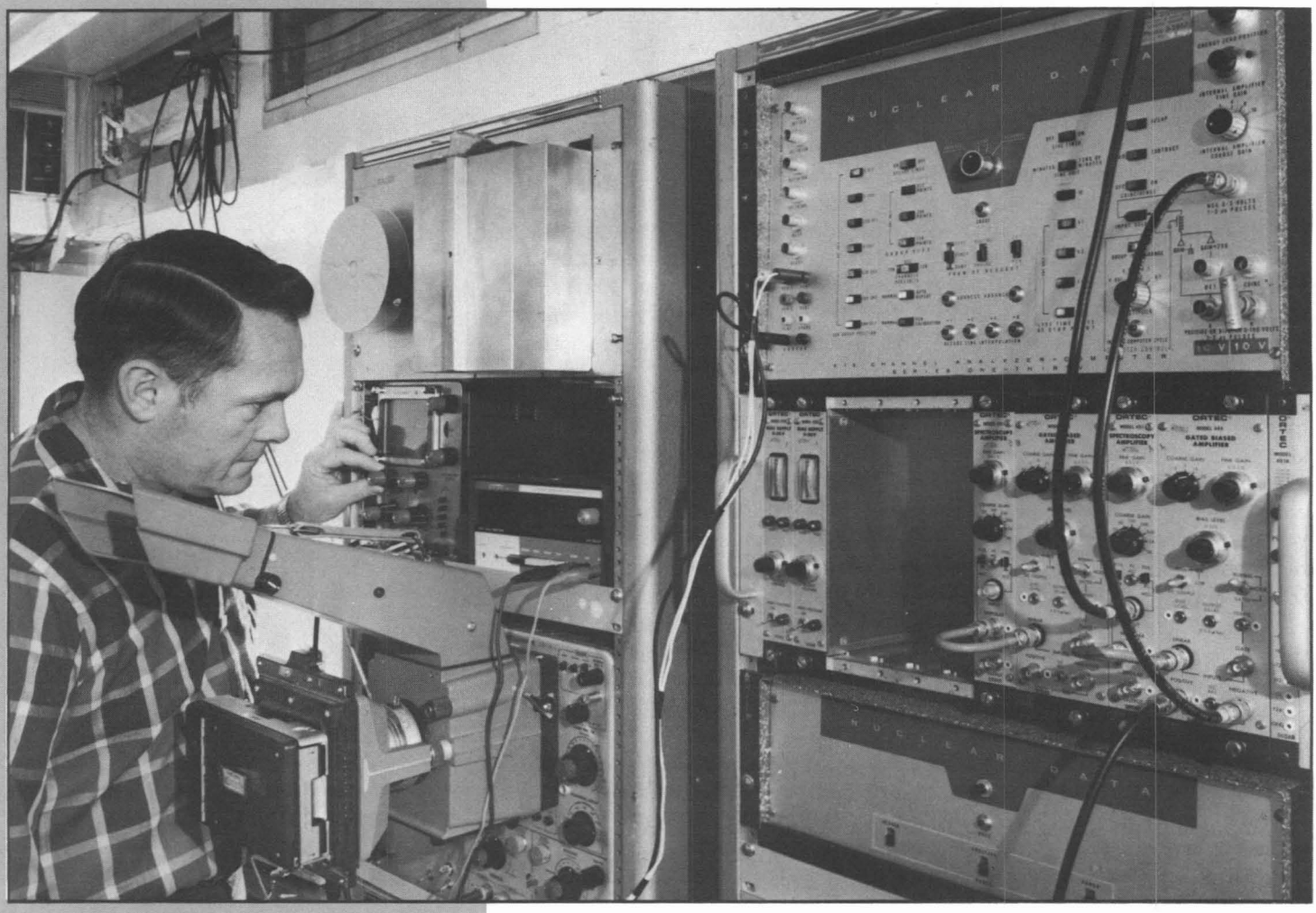

such qualitative measurements, specially designed equipment, in the form of high-resolution spectrometers for alpha particles and gamma rays, must be used.

A comprehensive program is now under way at ORNL to determine the contribution of natural background radiation to man's total radiation dose. The equipment is housed in a mobile laboratory and includes provisions for making measurements of background levels in situ, rapid measurements of both short-lived radionuclides (such as radon and thoron progeny) and those with longer half-lives, and detailed spectral measurements of nuclides contained in soil, surface water, waste, and by-products. This low-level monitoring system will be used in areas outside laboratory buildings and in areas of close public access outside ORNL's boundaries.

A typical detection system consists of a lithium-drifted germanium crystal, silicon diodes, fast charge-sensitive preamplifiers, a dual-parameter multichannel analyzer, and a selection of sampling equipment. Because of their sophistication and expense, it is not possible to deploy such systems in large numbers around a facility. It is therefore necessary also to use simpler detectors that integrate the exposure for fixed periods. Such detectors must be rugged and cheap and must possess a high sensitivity in order to measure natural background levels. Ceramic beryllium oxide is a candidate for meeting this need, using the principle of thermally stimulated exoelectron emission (TSEE). In the TSEE method, heating the ceramic disks after radiation exposure causes the emission of low-energy electrons at charcteristic temperatures, their number being proportional to the radiation dose. The ceramic beryllium oxide is cheap, tough, nontoxic, and near tissue equivalence in its absorption of radiation, and it is the most sensitive exoelectron emitter found to date. However, the exoelectron phenomenon involves the actual surface and near surface layers for both trapping of the latent exoelectrons and their escape. Ultrasensitive thermoluminescent dosimeters of calcium sulfate activated by addition of rare-earth ions are also being utilized in these same problem areas. Thermoluminescence is essentially a bulk phenomenon unplagued by surface effects; hence, although calcium sulfate is less rugged than beryllium oxide ceramic, it will complement the TSEE detectors in areas where the surface of the beryllium oxide may become damaged.

Medical Exposures to Ionizing Radiation

It is well established that x rays, particularly medical and dental x rays, contribute the largest exposure to the population of any man-made source of ionizing radiation. The fundamental objective of the medical use of radiation is to obtain optimum diagnostic information with minimum exposure of the patient, radiological personnel, and the general public. To achieve this objective in specific situations requires knowledge and understanding of many technical factors and clinical considerations.

There is an urgent need to couple the results of nationwide surveys of medical exposure (e.g., the U.S. Public Health Service

X-Ray Exposure Survey) with dosimetric information in order to estimate doses to selected organs. The geometrical complexities and inhomogeneities of the body and the various organs make experimental simulation of the human body extremely difficult and usually unsatisfactory.

Monte Carlo techniques in use on high-speed digital computers have greatly facilitated the solution of problems like these. They have gained wide use in the field of radiation protection, because the method allows one to simulate actual exposures on a computer. Many experimental arrangements and physical parameters can be described mathematically and handled by the computer to produce the required results. Calculations can be compared with available measurements to assure their accuracy.

The Laboratory has developed a Monte Carlo routine that calculates the dose in 22 organs and 100 subregions of an adult human phantom exposed to external photon beams. The phantom contains all the major organs as well as a skeleton with both yellow and red bone marrow. Results from these calculations are expected to provide information that will allow the assessment of the radiobiological effects in individual organs. Another hoped-for advantage is that these calculations from simulated clinical procedures using monoenergetic x rays will lead to reduced exposures and better estimates of the genetically significant dose.

Viable Frozen Embryos

It is not only of academic interest that we learn how to freeze and reuse complex mammalian systems, but of practical medical interest as well — for example, in organ transplantation.

Prior to 1971, attempts to freeze mammalian embryos were unsuccessful. In that year, a paper from Cambridge University described the successful freezing of certain stages of early mouse embryos to $-80°C$ for 30 min by suspending them in $7\frac{1}{2}\%$ solutions of polyvinylpyrrolidone (PVP) and freezing them at $60°$/min. However, none survived longer than 30 min, and two-cell embryos did not survive at all. The ORNL Biology Division, therefore, in collaboration with the Cambridge investigator, launched a series of experiments designed to explore the cryobiological factors that might affect the ability of embryos to survive freezing. In the most recent of these experiments, unfortunately, the embryos were not able to survive freezing in PVP.

The work was then repeated using another protective additive, dimethyl sulfoxide (DMSO). Previous thermodynamic and kinetic analysis at the Laboratory had indicated that objects the size of these embryos (80 μm in diameter) would have to be cooled at about $1°$/min or less to avoid intracellular freezing, nearly always a lethal event. First attempts to freeze eight-cell embryos in 1 *M* DMSO at rates of 0.4 to $40°$/min yielded 10% survival or less. Suspicious that deleterious osmotic events might be injuring these large multicellular objects during rapid thawing (used because it has almost always been better than slow thawing), the biologists tried slow thawing at 4 or $20°$/min. This solved the problem. If cooling was between 0.4 and

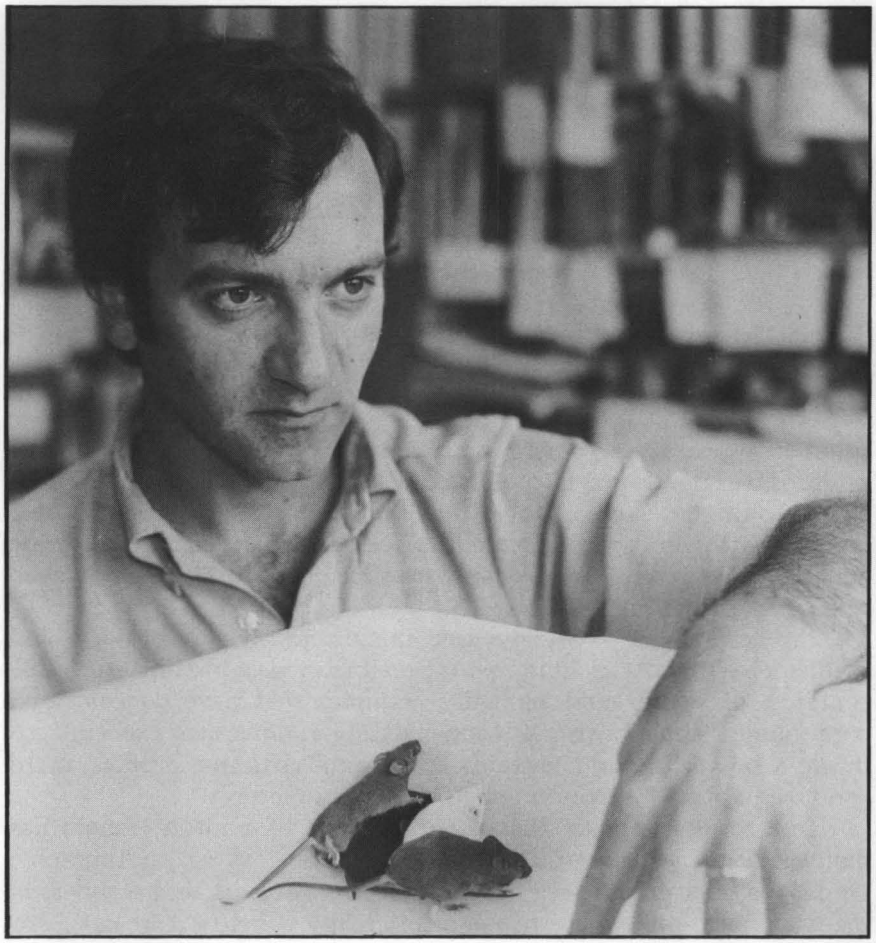

S. P. Leibo exhibits the mother mouse (white) with the black, brown, and gray offspring that were frozen as embryos, then unfrozen and implanted in her for eventual normal birth.

2°/min and warming was at 4 or 20°/min, over 50% of the embryos of one, two, or eight cells or of blastocysts survived freezing to −78, −196, and −269°C for up to eight days. Cooling at 6°/min or faster killed all embryos, even if the warming was slow. The above survivals are based on the ability of more than 2500 frozen and thawed embryos to undergo embryological development in culture. In addition, about 1000 frozen and thawed embryos were transferred into foster mothers. About two-thirds of the recipients became pregnant, and in these, 43% of the embryos developed into mature living fetuses or living mice. Some pregnancies were terminated to learn how many embryos had developed into mature fetuses and how many had become implanted but had not developed further.

One implication of these findings is that it is now possible to store mutant strains of mice that are not in use but are of potential interest. When desirable, the stored embryos could be transferred to foster mothers and the resulting offspring used to reestablish the mutant strain. A second implication is that if these procedures prove applicable to embryos of large domestic animals, they would facilitate worldwide dissemination of stock with an optimal genetic background for a given use or a given geography. Finally, and more generally, the success of cryobiological theory in suggesting the proper approach to the successful freezing of these sensitive embryos increases the likelihood that ways can be found to freeze complex mammalian systems that are of direct medical interest.

WILDLIFE AT ORNL BALD-FACED HORNET

Instruments

Proportional Counter Photon Camera

A new prototype camera that picks up an image from low-energy photons was developed in the Instrumentation and Controls Division. The photon detector is a gas-filled position-sensitive proportional counter with multiwire electrodes. The electronic signal-processing and imaging systems apply the "rise-time method," recently developed in the Division.

Photon imaging is widely used in nuclear physics, biology, and medicine. With this technique it is possible to visualize and study the function of organs and biological samples that have concentrated compounds labeled with photon-emitting radioactive elements, to image x-ray diffraction patterns for crystal structure studies, or to produce photon absorption images like x-ray pictures.

Test results indicate that this new type of photon camera has many advantages over such other image devices as photographic emulsions, scintillation and image intensifier cameras, and scanners in many applications where the photon energy is below 150 keV. For example, the pulse shape and energy of individually detected photons are measured to allow pulse shape and energy discrimination for background reduction. The electronic signal-processing and image storage permit image enhancement and background subtraction. The dimensions of the sensitive area of the camera can be adapted to image large subjects, since the length of the multiwire electrodes and the number of spaces between the wires are practically unlimited. The counter-gas mixtures and pressures can be selected to detect a wide range of photon energies with adequate detection efficiency and good spatial resolution. The camera can be adapted to detect and image other types of ionizing radiation, such as neutrons, electrons, or other charged particles. The absorbed radiation dose required for imaging with this camera can be kept extremely low (an x-ray absorption picture of a human hand was taken with less than 10^{-6} rad of absorbed dose), which is important where low radiation dose is essential and the high resolution of x-ray film is not required.

The prototype camera, built mainly for demonstration purposes, was of reduced size (200 mm square) and operated at low gas pressure (less than 150 cm Hg). The imaging was limited to photons with energies below 30 keV. Using only four amplifiers, the camera was able to resolve 40,000 picture elements, each a square millimeter, and a photon flux of 20,000 counts/sec did not appreciably affect the spatial resolution. The camera was tested in a series of imaging experiments that clearly showed the adaptability and advantages of this type of photon imaging device.

Signal flow diagram of the new proportional counter photon camera. As an example of its capabilities in medical use, the imaging process of a standard phantom of a human thyroid is shown. The phantom was filled with a radioisotope that emits 29-keV x rays. The intensity of the x-ray emission from the phantom was governed by several plastic absorbers incorporated in the phantom to simulate "hot" and "cold" nodules. The left lobe and the 11-mm-diam "hot" nodule in the right lobe had about twice the intensity of the rest of the right lobe. The 4-, 8-, and 11-mm-diam "cold" nodules did not emit x rays. A channel collimator, placed between the subject and the proportional counter, transmits only those x rays that have a perpendicular trajectory with respect to the window plane of the proportional counter; it absorbs all other x rays. Thus the image of the subject is projected onto the sensitive area of the proportional counter. This image, in the form of electronic signals, is decoded by the signal processing system and subsequently stored and displayed by the display system, in this case a TV monitor. An actual image of the thyroid phantom taken with the new photon camera is shown. As is typical in medical imaging, some contrast was lost by x-ray scattering in the plastic that surrounds the phantom cavities to simulate scattering in human tissue. However, all nodules were resolved in the image, and the differences in x-ray emission intensity are clearly shown.

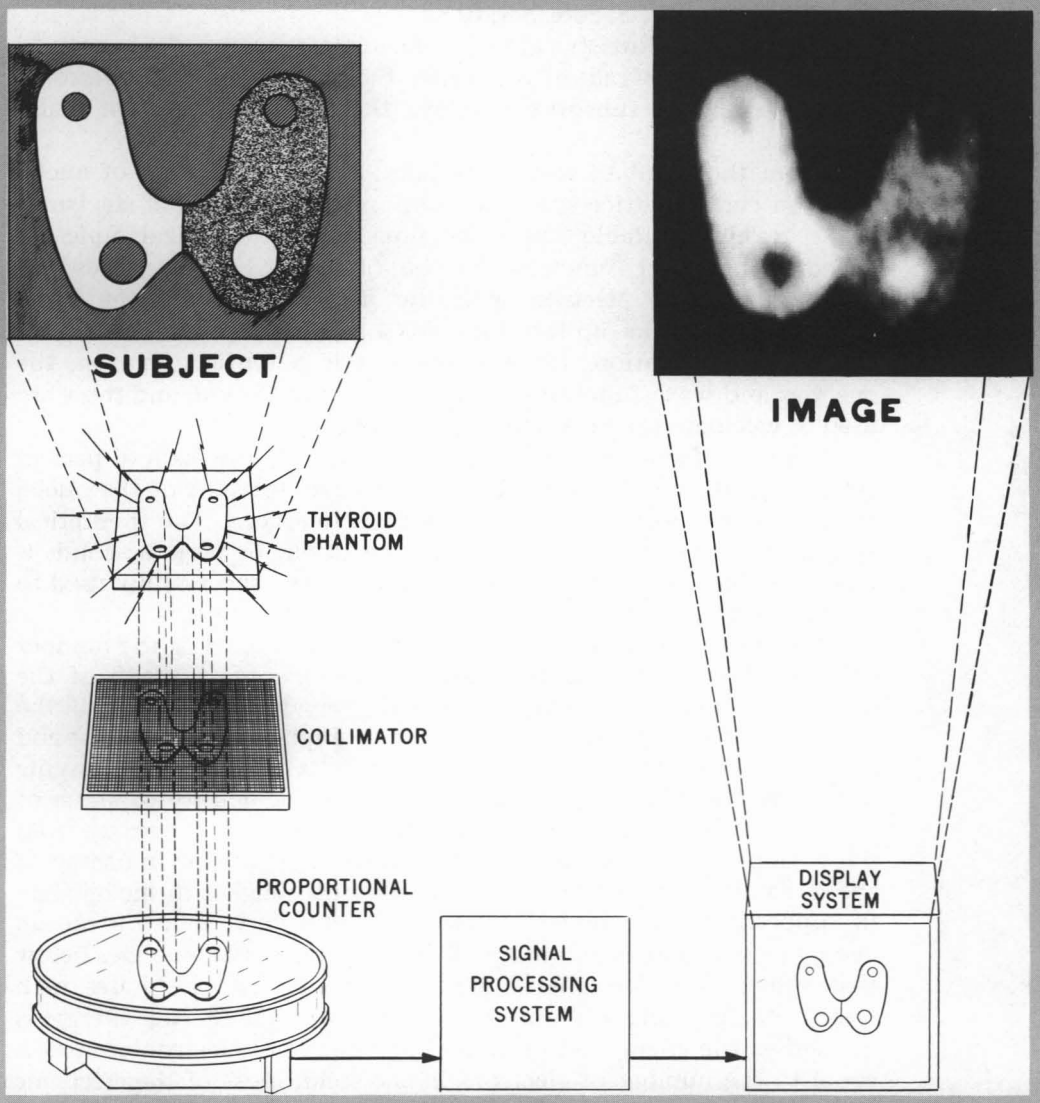

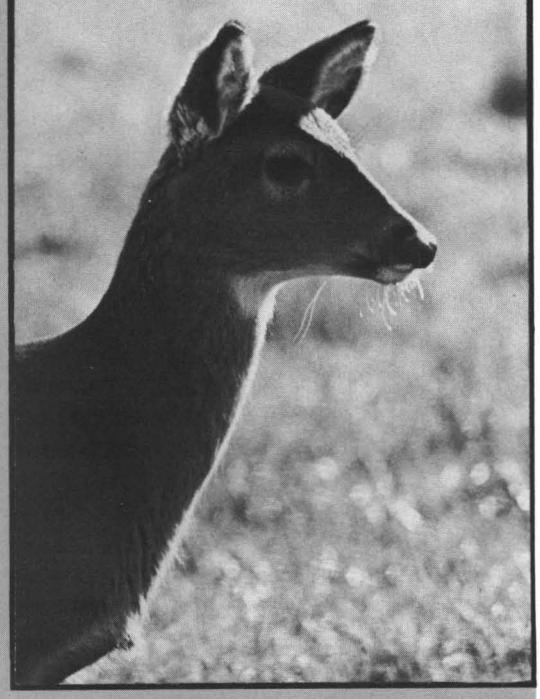

WILDLIFE AT ORNL WHITE-TAILED DEER

Materials

Density of States vs Energy in Copper-Nickel Solid Solutions

As the problems faced by materials scientists become more complex, a fundamental understanding of the properties of solids on the basis of the calculated dynamics of their constituent electrons becomes more useful. Although it is generally much easier to measure a property than it is to calculate it on this basis, the picture obtained from representative calculations leads to an understanding of the interrelation between properties that would not be apparent from more superficial considerations.

ORNL metallurgists are in the forefront of a theoretical movement that is radically altering the picture of the electronic states of random substitutive alloys that has been held for many years.

From the point of view of physics, a solid is an array of nuclei fixed on certain lattice sites and surrounded by a cloud of electrons. After making suitable approximations, a mathematical function called a potential function can be obtained that describes the interaction of an electron with the nuclei and all of the other electrons that make up the solid. By solving an equation called the Schroedinger equation, which contains this potential function, the energies and wave functions of the electrons are found, and these are used to calculate the properties of the solid.

Samples of some materials can be obtained in the form of perfect single crystals, and the periodicity of the arrangement of the nuclei in these solids leads to periodic potential functions. The theoretical approach to solving the Schroedinger equation for periodic solids is known as band theory, and this theory has been successfully used to calculate many properties of single crystals in recent years.

The density of states at a given energy is defined as the number density of electronic energy levels at that energy. A graph of the density of states vs energy is a concise way to show some of the results of a band theory calculation. Such graphs for pure copper and nickel appear along with some other results in the accompanying drawings. There is a high peaky structure in the density of states of both these metals caused by the so-called *d* bands, which rises up from a low smooth curve caused by the *sp* band. The position in energy of the *d* bands relative to the *sp* band is slightly higher in nickel than in copper. The area under a density-of-states curve below a certain energy gives the total number of electronic states with energies below that value. The electrons in a solid normally fill the states with lowest energy, one electron to a state, and the Fermi energy is defined as the energy below which the number of electronic states is equal to the number of electrons in the solid. Most of the electrons

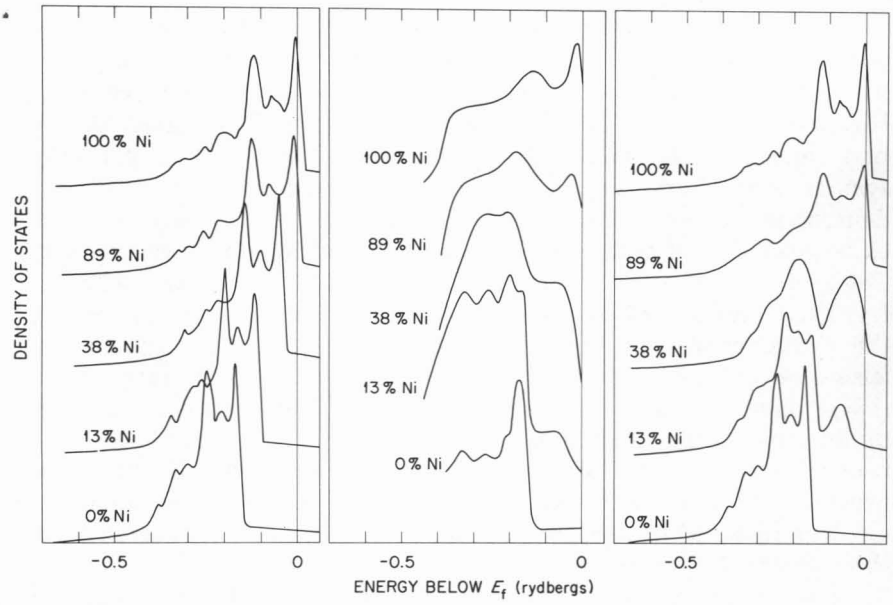

The densities of electronic states of pure copper, pure nickel, and several copper-nickel alloys, obtained three ways. Left: Calculated at ORNL from the virtual crystal approximation. *Center: Obtained from the photoemission experiments of Seib and Spicer,* Phys. Rev. B 2, *1676 (1970). Right: Calculated at ORNL with the recently developed coherent potential approximation.*

are localized about the atomic nuclei in a "rare-gas core," like the electrons in the very stable monatomic gases such as argon. Since these core electrons show very little interaction, they are usually ignored in band theory calculations. Without this core, there are 11 electrons per atom in copper and 10 in nickel. These numbers cause the Fermi energy of nickel to fall in the *d* band structure, while that of copper falls above that structure. The difference in density of states at the Fermi energy of copper and nickel is the reason for the difference between many of the properties of the two metals. For example, this is why nickel is ferromagnetic and copper is not.

A microscopic picture of a random substitutive copper-nickel alloy is obtained by first imagining a pure copper crystal and then substituting nickel atoms for copper atoms on a set of the copper lattice sites chosen at random through the crystal. The alloy has the same lattice sites as pure copper (or nickel), but the probability that a copper or nickel atom will be found on a given site is given by the copper or nickel concentration in the alloy.

The techniques of band theory cannot be used to calculate the electronic states of a random alloy because the potential function is not periodic. The earliest theory of alloys is the rigid band model, which assumes for the example we are considering that the density of states is the same in copper and nickel and any copper-nickel alloy. As nickel is substituted for copper in the alloy, the Fermi energy moves toward the *d* band structure simply because the average number of electrons per atom is reduced. This process continues with increasing nickel concentration until the Fermi energy reaches the position corresponding to ten electrons per atom for pure nickel. The density of states for alloys calculated by a slightly more complicated theory called the virtual crystal approximation is shown in one of the accompanying figures. In this theory the nonperiodic potential function is replaced by a periodic function that is the weighted average of the potential functions of pure copper and pure nickel. This approximation gives the correct density of states for pure copper and nickel, but it leads to a picture of the density of states for the alloys that is essentially the same as the rigid band model.

The coherent potential approximation evolved through the contributions of many scientists, but it was most clearly enunciated by Soven in 1967 and later put in a more usable form by Kirkpatrick, Velický, and Ehrenreich. This theory was used for the first time at ORNL to obtain the densities of states for a real alloy system across the entire range of concentrations, and it was demonstrated that, contrary to previous beliefs, it explains the experimental results for copper-rich copper-nickel alloys very nicely. The picture that arises from the ORNL calculations is very different from the one described above. As nickel is substituted for copper, the Fermi energy moves very little relative to the copper *d* band structure, but rather a bump appears in the density of states above this structure. With the further increase in nickel concentration this bump grows larger, and at the same time the copper *d* band structure becomes smaller and loses its peakiness. For nickel-rich alloys the process continues, with the structure that started as a bump evolving into the nickel *d* band structure, while the structure that arose from the copper *d* bands becomes insignificant.

The coherent potential approximation is obtained by the application of multiple scattering theory to the nonperiodic potential of the alloy and is better established theoretically than the rigid band model or the virtual crystal approximation. A rather crude measure of the density of states of these alloys obtained from photoemission experiments is shown. These experimental results are detailed enough to show that the picture of the electronic states given by the coherent potential approximation is the correct one.

These calculations are only a part of the studies of the electronic states of nonperiodic solids at ORNL. In addition to calculations on other alloy systems, the coherent potential approximation is being extended to treat liquid metals. Efforts are being made to extend the theory beyond the level of the coherent potential approximation and to use the knowledge that has been gained about the electronic states to explain the properties of alloys.

This simplified diagram shows the contrasting behavior of two samples of thorium oxide differing only in their specific surface area, which is determined by the temperature at which the samples were originally heated. Samples originally calcined at temperatures below 1000°C have unique "nonideal heterogeneous" heat curves, whose outstanding feature is the very high initial heat of adsorption. The heterogeneous nature of the oxide surface causes the heat of adsorption to decrease continuously as more water is adsorbed. In contrast, samples that were originally calcined at 1200°C or above have a common heat curve characteristic of an "ideal homogeneous" oxide surface. Water is adsorbed in three distinct layers, the heat of adsorption being constant throughout each layer. The three steps can be identified with the successive reactions of (a) hydroxylation to form surface hydroxyls, (b) hydration to give one water molecule for two hydroxyls, and finally (c) hydration to give one water molecule for each hydroxyl.

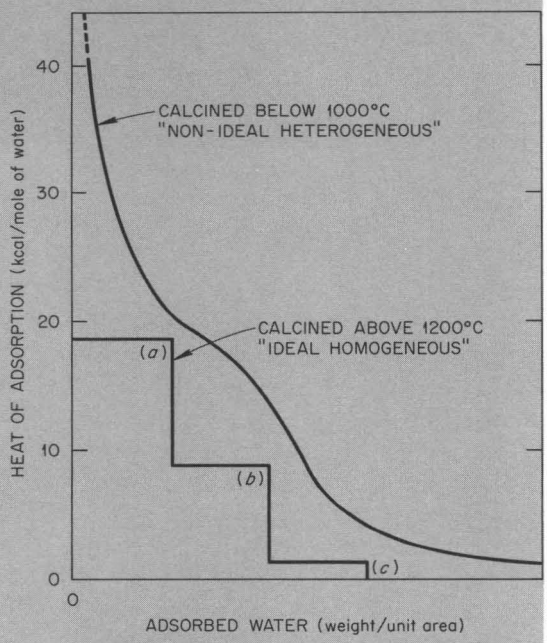

Heat of Immersion of Metal Oxides

The surfaces of insoluble metal oxides interact strongly with water, an ever-present component of the normal atmosphere. A quantitative measure of the strength of this interaction is important in any process involving oxide surfaces. Examples are nuclear fuel production and processing, catalysis, sorption processes in general (such as those used to remove contaminants from the atmosphere), corrosion, and production of ceramics. A convenient way to obtain this information is to measure, by means of a suitable calorimeter, the heat liberated when insoluble oxide particles are immersed in liquid water. This heat of immersion is normally quoted as energy per unit area of oxide surface. Oxide surfaces are covered with irreversibly adsorbed water under normal atmospheric conditions. Removal of this water (which can only be done by heating in a high vacuum) before the immersion experiments leads to an increase in the heat of immersion, because the irreversibly adsorbed water is replaced, with a corresponding release of energy. By means of this

and complementary experiments, the heat of immersion can be related to the quantity of water involved in the process to give an important quantity called the heat of adsorption.

Measurements at ORNL have been made of the heat of immersion of the oxides of thorium and zirconium for samples outgassed at temperatures ranging from 25 to 500°C. The data clearly indicate that the surfaces of both oxides (if outgassed above about 300°C) interact chemically with water to form surface hydroxyl groups. Additional interaction with water occurs by means of hydrogen bonding to the surface hydroxyl groups and by reversible physical adsorption. If the oxide surface is flat and planar on a molecular scale, the interaction with liquid water is rapid, reaching completion in less than 4 min. However, if the oxide particles contain pores about the size of molecular dimensions, the interaction extends over several hours, because of the hindered diffusion of water molecules into these tiny pores.

For samples of comparable surface area (surface areas are normally compared in units of square meters per gram), a thorium oxide surface is more energetic than a zirconium oxide surface. The heat of immersion of both oxides decreases with increasing particle size (decreasing specific surface area) to a point where it is independent of particle size. Some samples of zirconium oxide show a maximum in the heat of immersion as a function of the outgassing temperature. This is possibly due to an increase in hydrophobicity (water removed during the outgassing period is not completely replaced in the time interval of an immersion experiment) at the higher outgassing temperatures. Thorium oxide does not show this maximum. Zirconium oxide exists in two crystal forms, a monoclinic form, which is stable up to about 1100°C, and a tetragonal form, stable above this temperature. However, when the crystals are small (diameter less than about 300 Å), they always occur in the tetragonal form even at room temperature. The heat of immersion results show that the monoclinic form has a much higher surface energy than the tetragonal form. This difference in surface energy is the stabilizing factor for small crystallites of zirconium oxide. Although the chemistry of the thorium oxide—water interface is quite complex, a comparison with the zirconium oxide—water system and other systems described in the literature clearly indicates that it is one of the simplest of such systems.

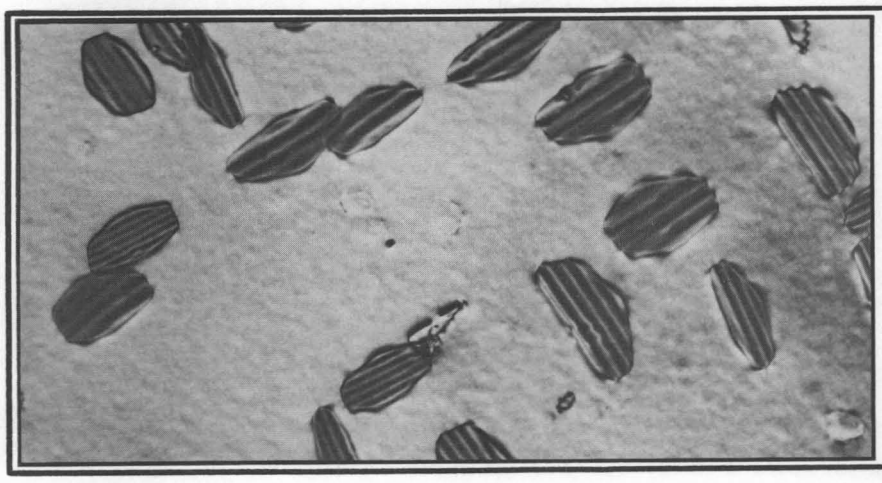

Electron Bombardment from Microscope
In specimens examined in the high-voltage electron microscope, electrons occasionally strike atoms and eject them from their lattice sites. These displaced atoms migrate through the lattice and form clusters similar to those produced by neutron irradiation. Since only a small fraction of the electrons collide with lattice atoms, the microscope image is not seriously impaired, so the evolution of the damage structure can be observed. This micrograph shows disks of displaced atoms (the striped objects) formed in nickel irradiated for 1 hr at about 475°C by 650-kV electrons.

ENVIRONMENT

NSF Environment-Energy Studies

Strip Mining

Energy, especially electricity, is an essential input to all sectors of the American economy. Unfortunately, each step in the energy cycle, from resource extraction to final use, contributes to environmental degradation. The energy vs environment conflict is worsening as fuel resources become more scarce while the demand for energy continues to grow exponentially. Three approaches to these problems have been suggested: to develop new energy sources, to devise improved methods for pollution control, and to consider methods for moderating growth rates in energy consumption.

Work on new energy sources, both nuclear fission breeders and thermonuclear fusion, is going on in many parts of ORNL. The ORNL-NSF Environmental Program is analyzing pollution control ideas and ways to affect energy demand. A particularly serious source of pollution arises in strip mining for coal.

This activity has increased more than fivefold in the U.S. during the past three decades and now accounts for nearly one-half of the total coal production. Ultimately, an area covering 71,000 square miles — nearly twice the area of the state of Tennessee — will be affected. Serious proposals have been made to prohibit stripping altogether, but in the light of current fuel shortages and expected increases in energy consumption, the value of the coal to the nation may call for an investigation of credible alternatives. One such alternative is to require full restoration of the land areas affected by strip mining. This option has been adopted in West Germany, and their successful land reclamation program constitutes a measuring stick, or standard, against which strip-mining practices in the United States can be compared.

The German reclamation approach is characterized by planning and carrying out the mining process as one continuum from early planning to final restoration of the land and its succeeding use. Sometimes, whole villages lying in the path of the mining operations must be evacuated and relocated. Before mining begins, the new landscape is designed and specified to fit into the planned overall land-use pattern of the region. Such early and detailed planning makes it possible to coordinate mining activities and concurrent land reclamation work. The comprehensive approach makes it possible to treat the overall problem effectively instead of dealing with its separate aspects on a piecemeal basis. For a cost that may increase the price of coal by 10 to 15%, it appears possible to make use of the mineral resources without destroying the usefulness of the land.

WILDLIFE AT ORNL FALSE INDIGO

WILDLIFE AT ORNL FLYING SQUIRREL

Energy Use in the U.S.

During the past two years, the Energy Group in the ORNL-NSF Environmental Program and similar groups elsewhere have begun to investigate energy consumption in the U.S. This work seeks to answer two basic questions: What are the historical and present energy consumption patterns within the various sectors of the U.S. economy — who uses energy, for what purposes, and how much? What policies might be used to reduce growth rates in energy consumption, such as technological improvements in the efficiency of energy utilization, economic changes that affect energy prices, public education, and new government policies?

This work, still in its early stages, can as yet offer but a preliminary discussion of some of these issues.

Transportation, of both people and freight, consumes about one-fourth of all U.S. energy, primarily as petroleum. The energy efficiency among various transport modes is calculably variable. For example, automobiles are twice as efficient per passenger-mile as airplanes, and buses twice as efficient as automobiles. For freight traffic, trains are four times as energy efficient as trucks and 60 times as efficient as airplanes. Shifts in the modal mix for both freight and passenger traffic could substantially increase the energy efficiency of our transport system.

Almost 20% of U.S. energy is devoted to space heating of homes, offices, stores, and factories, placing a premium, both economic and energy-conservative, on improved building insulation.

Industry is a major consumer of both primary and electrical energy. Three industries — primary metals, chemicals, and paper — account for over half the industrial consumption of electricity. Thus, studies on the economies of increased recycle of these materials are called for in the interest of saving energy, as well as reducing solid waste problems and conserving material resources.

Toxic Element Studies

Today's agricultural and industrial technologies release a variety of toxic and potentially toxic substances to rapid and wide circulation in the environment. Of the chemical compounds in commercial use, 9000 have a level of usage of over 1000 lb/year. Many of these materials, in different chemical and physical forms, enter food chains through various pathways. In some instances they have already reached concentrations deleterious to man. Mercury-contaminated fish and shellfish have caused illness and death at Minimata Bay and Niigata in Japan, and nearly a hundred deaths have resulted from cadmium contamination of rice caused by mine waste discharges in the Jintsu Valley of Japan. There are also reports of the lethal and sublethal effects of these substances on natural populations of wild species.

We are, for the most part, ignorant of the sources, sinks, and environmental pathways of these materials. Likewise, we know little about the long-term effects on man and other organisms resulting from chronic low-level exposures to hazardous materials discharged into the environment. The problem is further complicated by the chemical changes that can occur after toxic substances enter the environment. These materials may become more or less toxic because of their modification in the ecosystem or as a result of the synergistic and antagonistic effects of two or more materials.

Work on toxic materials at ORNL is part of the NSF-sponsored Environmental Program. An initial effort toward assessment studies has culminated in the publication of the report "Mercury, the Human Element." A similar document, "Cadmium, the Dissipated Element," is currently being reviewed in draft form. These reports attempt to analyze, as completely as data permit, the problems associated with management of these elements, first, in order to avoid environmental damage, and second, to promote conservation.

The analyses have stimulated research into a number of problem areas, such as the identification of potential sources of toxic elements; identification of the movement, translocation, and fate of mercury and cadmium in aquatic and terrestrial ecosystems; development of improved analytical methods, such as a high-sensitivity x-ray fluorescence technique for measurement of heavy elements in environmental specimens; and treatment by solvent extraction of aqueous effluents containing mercury.

The effectiveness of assessment activities, as well as that of laboratory research, depends on collecting and organizing a very large body of information ranging from the biological and physical aspects of the flow of each element, to the legal, political, and economic aspects of pollution control. This task is being accomplished through the Environmental Information System, which has combined the work of a number of specialized information centers at the

WILDLIFE AT ORNL COTTONTAIL

Laboratory into a single system. Access to pertinent external information centers and data bases will also be available. Not only does this computer system of retrieval provide the investigator quickly with available published literature, but it also informs him of current research efforts around the country.

A large part of the work on toxic elements is being done in cooperation and collaboration with other institutions. For example, with TVA, the ORNL-NSF group is performing a mass balance for trace elements at the Allen Steam Plant in Memphis. The objective in this study is to determine the fate of the not inconsiderable amounts of toxic elements present in the coal burned in the plant — finding out how much remains in the ash, how much is trapped by the electrostatic precipitators, and how much is actually discharged from the stack. Also, with TVA, the Southeast Water Laboratory of the Environmental Protection Agency, and Vanderbilt University, the ORNL group is studying the problem of mercury in Pickwick Reservoir. The Laboratory's contribution has been to apply zonal centrifugation and other methods to the characterization of the contaminated sediments by looking at mercury content as a function of particle size, mineral composition, density, and chemical extractability. Iodide extraction and gas chromatographic separation are also helping to identify the organic complexes of mercury in fish and sediments. Similar investigations of cadmium-contaminated sediments in the Holston River near zinc mining and ore beneficiation operations are also in progress. Finally, with Purdue University, a comprehensive survey of cadmium and other trace elements in the environment has begun near the industrial area of Gary and southeast Chicago. One part of the work will be a study of the flow of trace elements through a large integrated steel plant in collaboration with Inland Steel Corporation. A major ORNL role will be to apply a battery of analytical techniques not available at Purdue. These joint efforts involving industry and the university community with a national laboratory are expected substantially to increase the effectiveness of toxic element research above that of any single group alone.

Some specific results achieved in 1971 are briefly abstracted below. The first three of these were done in the Environmental Sciences Division and the last in the Metals and Ceramics Division.

Relative Toxicities of Four Arsenical Compounds

A meadow katydid population was exposed to varying degrees of two organic and two inorganic arsenical compounds. Lethal dosages required to kill 50% of the population were determined at the end of 14 days. Whole-body concentrations of arsenic were determined by neutron activation analysis for those animals that died during the 14-day period. Whole-body arsenic concentrations 14 days after treatment were expressed as a function of dose for cacodylic acid, Phytar-560, arsenic pentoxide, and arsenic trioxide respectively. Dosages required to kill 50% of the population in 14 days were higher for the cacodylic acid (7.5 ppm) and the Phytar-560 (3.5 ppm) than for the arsenic pentoxide (2.8 ppm) and the arsenic

trioxide (0.2 ppm), showing the inorganic arsenicals to be much more toxic to the grasshopper population than the organic. There was not a linear relationship between whole-body arsenic concentrations and arsenic concentrations in the administered dose. For the less toxic organic arsenicals, whole-body arsenic concentrations reached levels twice those of the inorganic arsenicals for similar arsenic levels in the administered dose.

Microcosm Studies Using Cadmium Transport

In a controlled ecological system in minature (microcosm), cadmium introduced into the water compartment was subsequently followed into the biota and sediments. One week after the introduction of cadmium, the resident snail population reached chemical equilibrium with the cadmium in the water. In contrast, the algal population, which was undergoing rapid growth, did not reach chemical equilibrium within seven weeks. When both algae and snails were present in the microcosm, cadmium disappeared from the water at a faster rate than in microcosms in which either algae or snails were present alone. These experiments were conducted using quartz sediments, but comparable data are available for both organic and clay sediments, as well as for the absence of sediments.

In a larger and much more complex microcosm, the transfer of cadmium from a terrestrial to an aquatic system was studied. A

Microcosm analysis of heavy metals. A section of stream bank was removed intact and placed in this microcosm along with a water component and associated aquatic life. Cadmium was added to the terrestrial component of the system as cadmium chloride in a simulated rainfall. Subsequently the system was rained on once weekly for three weeks. The microcosm was then dismantled and analyzed by component for cadmium concentrations. The majority of the cadmium input remained in the soil fraction of the terrestrial system; only 4% was translocated to the aquatic component. Terrestrial vegetation accumulated very little cadmium. Fish and aquatic snails accumulated some cadmium, although both contained less cadmium than the bottom sediments.

section of a stream bank was removed intact and placed in the microcosm with water and a varied aquatic biota that included fish, snails, and watercress. Two such microcosms were set up with only the terrestrial system tagged with cadmium chloride in a simulated rainfall. The microcosms were kept in the greenhouse, and twice a week the average rainfall for the area was simulated. Measurements of the movement of cadmium in the system were taken after each rainfall. After three weeks the entire system was dismantled and the cadmium content of each component determined.

The data obtained from the two microcosms agreed satisfactorily. The majority of the cadmium was contained in the terrestrial system, the highest percentage being in the soil. Translocation of cadmium introduced into the system as cadmium chloride did occur, but the rate of bioaccumulation in plants was slow, particularly when the plants had to compete with soil or other organic matter for cadmium ions.

In the two microcosms, only 4% of the cadmium was transported from the terrestrial to the aquatic components. Bottom sediments accumulated the cadmium more rapidly than any of the organisms analyzed. Fish accumulated cadmium more slowly than snails. However, the fish did acquire enough to permit determining a percentage distribution by organs. When fish were dissected, the gastrointestinal tract contained the highest concentrations of cadmium. The study demonstrated that while most of the cadmium released to a simple land-water system in the form of cadmium chloride remains in different compartments of the terrestrial system, there is sufficient transport to the aquatic system to allow accumulation by fish populations.

Microcosm and Stream Experiments on Movement of Mercury

A major consideration in the problem of mercury in the environment is the concentration and transfer of mercury through aquatic food chains. It is known that fish will concentrate methylmercury from the water very rapidly, and it is generally believed that methylmercury in water is the source for contaminating fish. Aquatic insect larvae (bloodworms) were placed in water containing tagged methylmercury, where they remained until reaching equilibrium. The larvae were washed and assayed and then fed to mosquito fish (*Gambusia*), which in turn were fed to largemouth bass. The insect larvae concentrated the methylmercury to 3000 times the value for water. The transfer of methylmercury through the mosquito fish to the bass was very efficient. Mosquito fish retained 76% of the methylmercury obtained from feeding on the tagged insect larvae. Even after ten days the bass retained 54% of the mercury that was in the larvae. With such an efficient transfer through the food chain, it is apparent that the mercury in fish could be obtained via the food chain as well as by direct absorption from the water. Long-term feeding experiments now going on will tell us just how rapidly the bass concentrates mercury through the food chain.

Although there has been a great deal of sampling of the aquatic biota for mercury, almost nothing is known about the movement of

the different forms of mercury once they are released into the water. To provide information on natural systems, two similar streams at ORNL were tagged with different forms of mercury. White Oak Creek was tagged with methylmercury, $CH_3{}^{203}HgCl$, and Walker Branch, a similar stream, with mercuric nitrate, $^{197}Hg(NO_3)_2$.

About 40 min were required for the mercury tags to reach 100 m downstream. Water samples were taken at 5-min intervals and filtered to determine the mercury content of the particulate matter. Four hours after the release of mercury, collections were made of sediments and the biota. Collections were then made at regular intervals for nine days.

Twenty-five percent of the mercuric nitrate and twenty percent of the methylmercury passed through the first 100 m of the stream in 90 min. That is to say that 75% of the mercuric nitrate and 80% of the methylmercury were contained in the sediments and biota of the first 100 m of the stream below the input. After nine days, fish had concentrated methylmercury about 100 times as much as they concentrated mercuric nitrate. Also, there was a significant difference in methylmercury concentration between the fish species in the stream (dace and stone rollers). This could be due to differences in trophic level position. Gut content analysis showed that the dace fed on a variety of small invertebrates, while the stone rollers fed on algae (mostly diatoms). The decreasing order for concentration of methylmercury was fish > snails > periphyton > aquatic macrophytes > inorganic sediments.

The concentration ratios for mercuric nitrate were similar to those for methylmercury, except for fish and snails. The concentration ratio was the greatest in the snails; in the fish it was less than in any other component measured. This was a transient input into an oligotrophic stream. Since many organisms are known to have an affinity for methylmercury, it can be inferred that the relationships would be different in more eutrophic streams.

X-Ray Fluorescence to Detect Heavy Elements

Members of the Metals and Ceramics Division have improved the techniques of x-ray fluorescence analysis to a new order of sensitivity in the determination of heavy trace elements. The method is particularly applicable to the analysis of environmental samples because it is cheap, fast, and quantitative and does not demand a time-consuming prior chemical concentration. When solid-state detectors such as lithium-drifted silicon are used, the sensitivity has been limited by background to about 10 ppm by weight of heavy elements in water.

The main improvement has been effected by reducing the background. This has been done by using monochromators made of annealed pyrolytic graphite, made by a special compression process. Using a lithium-drifted silicon detector with two such monochromators, ORNL metallurgists detected mercury in water at a level of 1 ppm, in coal at 0.15 ppm, and in dried tuna fish at 0.5 ppm. Future work will aim for higher resolution, which should further reduce the interference.

WILDLIFE AT ORNL RUFFED GROUSE NEST

Water Research

Treatment of Industrial Wastes by Hyperfiltration

In the course of research in aqueous chemistry aimed chiefly at desalination, the ORNL Water Research Program has developed techniques that also appear promising for treatment of diverse industrial effluent streams. Among these techniques are hyperfiltration, often called "reverse osmosis," with dynamically formed membranes, and cross-flow filtration, a low-pressure filtration process that uses a turbulent flow of solution parallel to the filtering surface to hinder the formation of a thick, flux-reducing cake on the filter surface. To date, these techniques have been tested on some typical effluents from paper mills, textile mills, and municipal sewage treatment plants. Researchers in the program have begun to look at wastes from food processing, at cooling tower blowdowns, and at water contaminated with a low level of radioactivity. The potential of the techniques can be illustrated by a few results from laboratory experiments.

In a 1970 Water Quality Office—Environmental Protection Agency report, the pulp and paper industry was ranked No. 1 in priority for research and development efforts to develop or upgrade treatment of waste water. With the cooperation of the International Paper Company, the ORNL program has applied filtration techniques to several of the most troublesome waste streams resulting from the kraft wood-pulping process. Under investigation are three possible approaches: (1) to treat a given effluent stream to make it suitable for discharge, (2) to produce an effluent of high enough quality to recycle in the process, and (3) to separate from the waste effluent one stream bearing concentrated contaminants and another mainly containing recoverable processing chemicals.

One experiment directed toward the first two objectives consisted in combining acidic and caustic pulp bleaching wastes and hyperfiltering the highly colored neutral solution. The membrane, of hydrous zirconium(IV) oxide and polyacrylate layers, was formed dynamically on porous carbon tube supports, mounted in a prototype module. At the process temperature of 60°C, a temperature not compatible with commercially available hyperfiltration membranes, about 99.9% of the color, 95% of the carbon, and between 80 and 85% of the salt were removed. At a pressure of 950 psi, fluxes were initially about 60 gal/day per square foot of filter surface. The flux declined with time but could be restored by simple chemical washes. The product stream, after 80% water recovery, appeared to meet specifications for recycle at most stages in the pulping process and easily met present discharge standards.

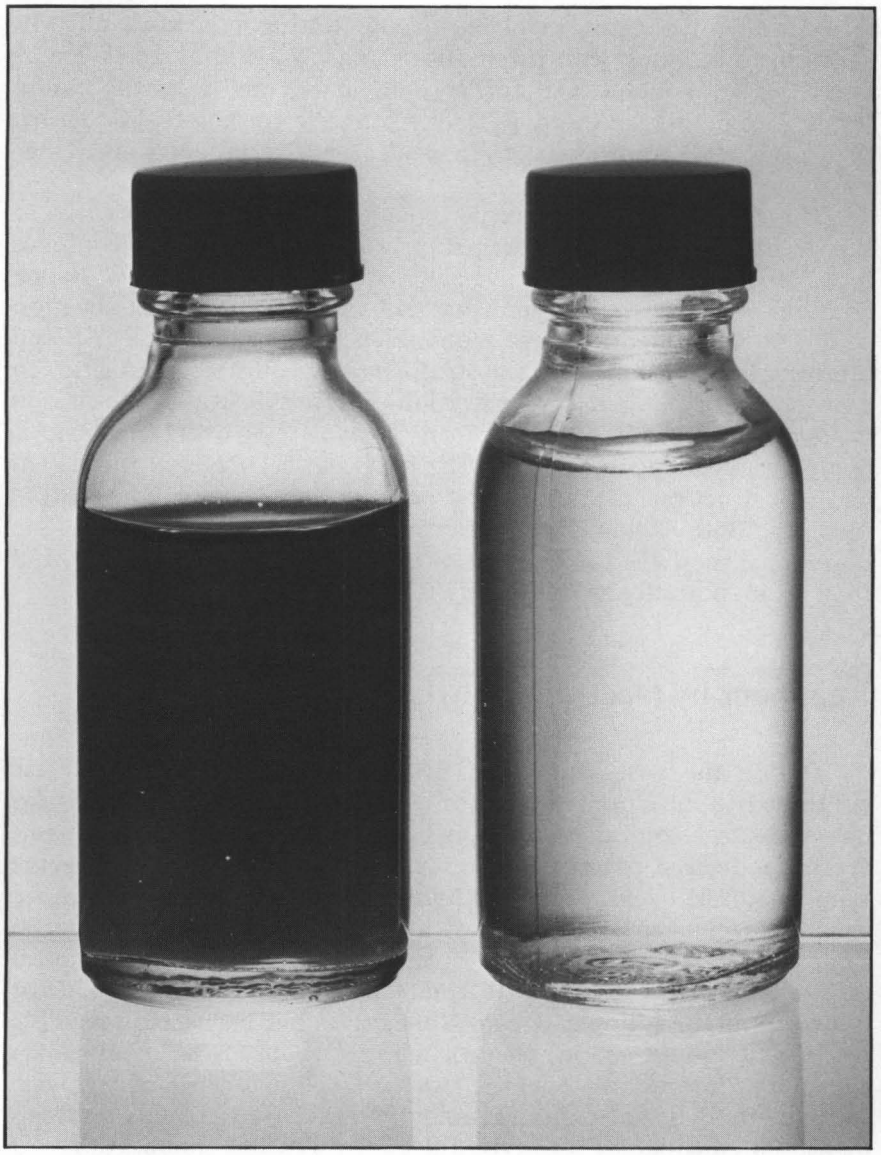

Samples of feed (left) and product (right) from the hyperfiltration of textile dyeing wastes by dynamically formed hydrous zirconium(IV) oxide—polyacrylate membranes on a porous ceramic support. The filtration was carried out at process temperature (about 60°C) and at 950 psig. The feed had been concentrated by hyperfiltration to 87% water recovery, and analyses of the product showed that 98% of the color and 90% of the carbon had been removed. A test dyeing was carried out at a textile plant with the filtrate, with no detectable differences from water customarily used. Test strips were successfully dyed with the concentrate.

To meet the third objective, the investigators treated a neutralized kraft waste by a single-layer hydrous zirconium(IV) oxide membrane at low pressure, around 200 psig. Under neutral conditions, the ion exchange capacity of this membrane is low, and therefore its salt rejection is also low. Low pressures also contribute to low salt rejection but have less effect on the rejection of the larger organic molecules. In this experiment, with fluxes at about 50 gal day^{-1} ft^{-2}, most of the color and carbon were filtered out, but, as desired, about 85% of the salt was in the permeate. A similar experiment with a neutral organic membrane, dynamically formed from polyvinylpyrrolidone, gave equally good results.

A number of other kraft waste experiments have been performed, using different membrane supports, different waste streams and combinations of them, and different operating conditions and different techniques, including cross-flow filtration. Several appear promising for practical application, and the International Paper Company is considering looking for government funding to continue

WILDLIFE AT ORNL LOBLOLLY PINE

a cooperative program, involving on-site testing at a kraft mill. In addition to working with International, the Water Research team at ORNL is in contact with other companies, and tests of "white water" from the Southern Extract Company (a Knoxville concern that makes paper products by a neutral sulfite process) are under way.

The experiments with textile dyeing wastes have been carried to the point that others are engaged in bringing the ORNL techniques into practice. Clemson University, which has long had strong relations with the textile industry and which pioneered application of ORNL-developed dynamic membranes to dye wastes, has received a favorable reception from the Environmental Protection Agency to a proposal for in-plant demonstration of hyperfiltration. The Gaston County Dyeing Machine Company, Stanley, North Carolina, is applying experience gained in early work with ORNL to the design and construction of hyperfiltration units for use in the textile industry. Both Union Carbide Corporation and Selas Flotronics are developing modules for hyperfiltration by dynamic membranes, and they also reportedly envision early tests with dye waste streams.

Treatment by Electrochemistry

During the past year the ORNL Water Research Program has continued to develop a number of electrolytic cell configurations for direct electrochemical production of chemicals for water treatment. Present industrial practice depends heavily upon the use of reagents such as sulfuric acid, lime, and hydrolyzable salts. Such procedures usually involve considerable cost and inconvenience in transportation, storage, handling, and dispensing of chemicals. Economical on-site generation of water-treatment chemicals, especially acids or bases, from the effluent streams themselves has been made possible by recent advances in electrochemical theory and cell design capability. Interest in this area arose originally because of the need for a method of softening seawater or brackish waters as pretreatment for distillation or hyperfiltration. Possible applications of on-site production of acids and bases, of course, cover a much wider field.

The ORNL prototype cells are capable of continuous efficient electrolysis of seawater and other natural, municipal, or industrial waters to produce a variety of products, depending upon the particular water composition, cell design, and mode of operation. One version removes essentially all bicarbonate ions from incoming seawater and acidifies the product stream, which can then be used for acidification pretreatment of larger volumes of feed. In another mode of operation it is possible to remove all hardness from brackish waters by precipitation of calcium carbonate and magnesium hydroxide. An outgrowth of this work that has immediate practical significance is a small unit to be field tested in pretreatment of brackish waters during hyperfiltration tests at Roswell, New Mexico. At present, various configurations of electrodes and other components are being tested, and several alternative modes of operation are being investigated, to identify options for other applications of direct electrochemical methods of water treatment.

The effluent from a small prototype cell for direct electrolytic treatment of seawater is being collected for analysis by Al Palko. The white material visible in the glass parts of the apparatus is a suspension of precipitated calcium carbonate and magnesium hydroxide that appeared in the seawater after it was pumped through the cathode compartment of the cell.

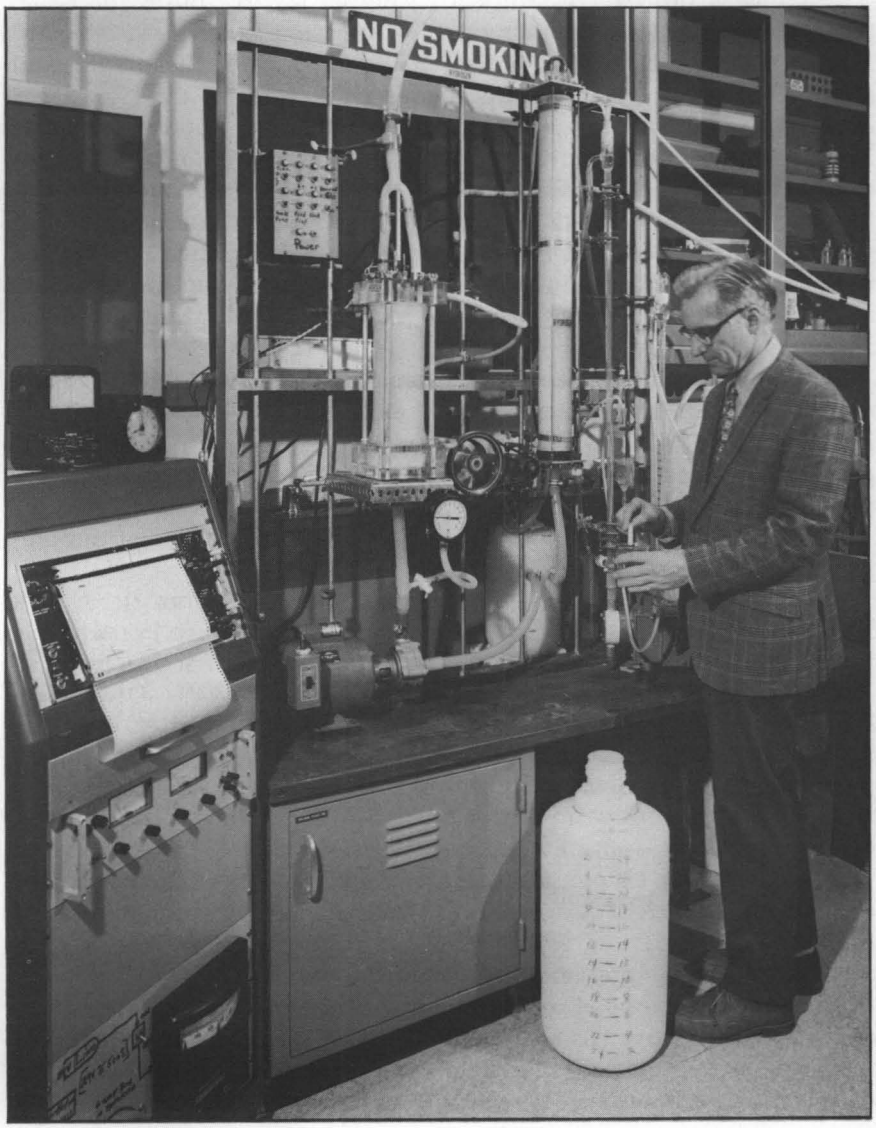

WILDLIFE AT ORNL WHITE-FOOTED MOUSE

Environmental Impact Statements

In its decision of July 23, 1971, the U.S. Court of Appeals for the District of Columbia Circuit, in litigation involving the Calvert Cliffs nuclear power plant, directed the Atomic Energy Commission to revise its rules for implementing the National Environmental Policy Act of 1969 (NEPA). Circuit Judge J. Skelly Wright ruled that (1) the AEC must consider the environmental consequences of all actions taken after the effective data of NEPA (January 1, 1970); (2) an environmental impact statement must accompany each application for a construction permit or operating license throughout the AEC's review process, regardless of whether a party raises the issue; (3) AEC regulations deferring to certification by other State and Federal agencies that environmental standards were satisfied violated NEPA; (4) certification of compliance with water quality standards devised and administered by State agencies and approved by the Federal Government under the Federal Water Pollution Control Act does not relieve the AEC of the responsibility for conducting an independent examination of the effects of a particular project on water quality. The court also found that AEC's "blanket policy" of refusing to consider the possibility of halting construction in plants in particular cases, pending a full NEPA review, was a violation of the act.

Over 100 nuclear power reactors are directly affected by the court's decision, representing a total electrical generating capacity of about 100,000,000 kW (about 25% of the current electrical generating capacity of the United States from all types of power plants). Also affected are three fuel reprocessing facilities.

The Commission set about promptly to revise its regulations and to gear up to prepare adequate impact statements.

Early in August the AEC asked three national laboratories — Oak Ridge, Battelle Northwest, and Argonne — for assistance in preparing the needed NEPA statements under administration of the Division of Radiological and Environmental Protection (DREP). ORNL responded immediately, organizing a new Environmental Reports (ER) Project consisting of six interdisciplinary task groups made up of personnel from 14 divisions. Over 60 staff members became involved in this sudden redirection of effort. Some are engaged full time, others part time; some are assigned to task groups, others serve as technical editors or consultants or reviewers in particular areas of concern in a full NEPA operation. Altogether about 130 members of the scientific staff and about 50 support personnel are involved to some degree in the preparation of impact statements.

The preparation of environmental impact statements requires consideration of five basic elements: (1) the environmental impact of the proposed action, (2) unavoidable adverse effects, (3) alternatives to the proposed action, (4) relationship between short-term uses and

long-term productivity, and (5) irreversible and irretrievable commitments of resources. Section 102 of NEPA also calls for the development of methods and procedures "which will insure that presently unquantified environmental amenities and values may be given appropriate consideration in decisionmaking along with economic and technical considerations." Thus, a discussion and balancing of the benefits and costs involved in the proposed action are also required in NEPA statements.

These NEPA reviews raise questions about potential impacts that may not be answered for many years. Here are a few examples: What are the impacts on aquatic organisms (phytoplankton, zooplankton, planktonic eggs and larvae of fish and invertebrates) entrained in cooling water on passage through the condenser and subsequent exposure to heated water in the discharge system? How can cooling-water intake and discharge structures be constructed and operated to minimize their impact on aquatic ecosystems? What are the lasting effects on anadromous and catadromous fish populations to be expected from steam-electric plants (nuclear fueled and fossil fueled) and hydroelectric plants proliferating along the shores of our major estuaries? What are the different impacts that may result from the operation of wet and/or dry cooling towers? What are the probabilities of and problems associated with major nuclear accidents or with accidents involving shipments of irradiated fuel to reprocessing plants? What impacts can result from the discharge of chemicals (chlorine, hydrazine, etc.) to a receiving body of water? Finally, what are the impacts on land and water uses from construction of the plant and development of its power transmission lines? In addressing these questions and considering the alternatives, the aim is to find a balance between costs and benefits that our society considers "acceptable."

To date the ER Project has completed eight NEPA reviews (Oconee 1, Farley, Palisades, Indian Point 2, Vermont Yankee, Surry 1 and 2, Hatch 2, and Fort St. Vrain), three of which have been incorporated in AEC draft statements (Oconee 1, Palisades, and Surry 1 and 2). Some of the material in the AEC draft (e.g., Accident and Transportation Impacts) is prepared by the Commission. The AEC draft statements are sent to other Federal, State, and local agencies for comments and are made available to the public for comments on the proposed action. After comments on the draft statement are taken into consideration, the AEC, in collaboration with the national laboratories, then prepares a final statement, which is filed with the Council on Environmental Quality at least 30 days before any action is taken. It is too early to tell if the AEC's post-Calvert Cliffs impact statements will withstand all challenges in the courts or stand the test of time. The next few months should provide a clue.

Recently the ER Project has assumed two additional assignments. One involves the computation of the release of radioactive material during normal operation for all proposed nuclear power plants — not just those assigned to ORNL for NEPA reviews. This work is done for the Commission's Division of Reactor Licensing. The other assignment involves technical input to DREP's impact statement on the Commission's proposed rule on "as low as practicable," on which hearings are now being held.

CIVIL DEFENSE PROJECT

Hasty Winter Shelters

Until quite recently the fast construction of any kind of expedient fallout shelters, either for summer or winter, received little attention in official U.S. civil defense circles. The reason for this may stem from a national civil defense policy that emphasized the identification and stocking of fallout shelter spaces in already existing buildings rather than the erection of new shelters. Recently, however, the evacuation of urban populations to rural areas, together with their protection in hastily constructed shelters, is being considered in the light of several present-day realities. Foremost among these are (1) strong evidence of a Soviet evacuation-based civil defense program, requiring several days to implement, and (2) increasing experience that international crises tend to take several days to escalate, a fact that greatly reduces the likelihood of an "attack out of the blue." Therefore, interest is developing in the construction of expedient shelters in areas away from cities, which would be likely targets in the event of a nuclear war. Even at Hiroshima and Nagasaki, timber-framed, earth-covered shelters survived intact as close as 90 m from ground zero, where buildings were completely demolished.

Research in the construction of hasty shelters has been conducted in the Civil Defense Project at ORNL for several years now. The initial goal was to develop written instructions and drawings that

A-frame log shelter being covered with snow, after being covered first with polyethylene. Vertical wooden duct serves as ventilator for the shelter.

WILDLIFE AT ORNL CHIPMUNK

would enable average rural Americans to build themselves high-protection-factor shelters within 48 hr of starting time. The criteria for these shelters included the use of local materials and tools, the erection of the shelter outside of preexisting structures, an adequate radiation protection factor (PF), a shelter sufficiently habitable to permit an average family to live inside it for a period of weeks under all weather conditions, and designs that allow for the improvement of both habitability and strength as time permits.

Five designs of such high-PF hasty shelters were developed, and shelters were built from them by Laboratory employees near ORNL in the fall of 1969. But the question remained whether average untrained rural Americans would be able to build such shelters, completing them within 48 hr of receiving written instructions. To learn the answer, several different groups of families and individuals were engaged to build shelters in the summer of 1970. The incentive of a bonus was offered for completion of the shelter within a 48-hr period.

As a result of this experiment, four hasty pole-type shelters were built in four localities in East Tennessee. Bonuses were awarded in three out of four cases for completion of the shelter within the 48-hr maximum, demonstrating that inexperienced people can build high-PF shelters from detailed written instructions within a two-day period, less time than it would take either for a typical crisis to escalate or for the Soviet Union to put its evacuation program into effect.

The shelters were built in unfrozen ground; so the research effort was resumed in February and March of 1972 to test the practicality of hasty winter shelters, both above and below frozen ground.

Since no records could be found of any winter shelter built in the U.S., guidance was provided by Russian designs appearing in the unclassified Soviet military publications and by the experience of people used to living in a cold climate. Further, since the practicality of the Russian designs was not established, men experienced in working in extremely cold weather were chosen for the initial stage of developing designs and instructions.

The shelters were almost all located on private land near Grand Junction, Colorado, at an elevation of approximately 2600 m in a predominantly wooded area of aspens, ponderosa pines, and scrub oak. Three types of snow-covered above-ground shelters were constructed: a log-tepee shelter (a strengthened version of a Russian design), a ridgepole shelter, and an A-frame log shelter. This last

WILDLIFE AT ORNL YELLOW POPLAR

appears to be one that can be built with little or no mechanized equipment in minimum time (4.8 man-hours per one-man shelter space).

To explore the practicality of constructing below-ground hasty winter shelters, three methods of breaking through frozen earth—by hand, machine, and explosives — were explored. The hand method was done most effectively with the combination of an ax, a heavy digging bar, and a shovel but was very laborious at best. Such machines as backhoes and bulldozers were effective in ground frozen to a depth of about 0.3 m. Where the frost extended deeper than this, however, it was not worth while to use the backhoe, and the bulldozer was found to be extremely inefficient unless equipped with a movable ripper, an attachment that enables a bulldozer to excavate deep-frozen earth and some softer sedimentary rock. For explosives to be effective, it was concluded that they must be detonated within a frozen layer of earth rather than on the surface, and even then a large amount of dynamite is required.

With the Russian designs serving as models, two types of narrow covered-trench shelters were built: a 1-m-wide trench shelter, covered with logs, and a wire-catenary-roofed shelter. The first of these could not be dug as deeply as planned, because massive slabs of rock were encountered at about 1.4 m. It was therefore finished as a stoop-in shelter rather than one with an overhead bunk. To complete this shelter required 15 min for using the bulldozer with a ripper plus 28 man-hours, or 5.6 man-hours per austere shelter space.

The plan to build a wire-catenary-roofed shelter according to the Russian model also had to be modified because of rocky digging. Again the plans for overhead bunks had to be abandoned. Moreover, in both these shelter-building efforts, it was difficult to limit the shelter width to 1 m, in accordance with the design. When the bulldozer with the ripper was used, large, irregular frozen chunks broke out, resulting in widths of up to 2.3 m in parts of the 5-m-long trench.

The third underground hasty shelter built with the help of a bulldozer was a wide, log-covered shelter with 42 m^2 of space. The width of the trench was 4.3 m — wide enough to enable standard American bulldozers to do the excavation. The greater availability of such bulldozers in the U.S., together with the availability in some areas of logs long enough to cover trenches this wide, makes it desirable to perfect plans for building large shelters of this type. More such work is planned.

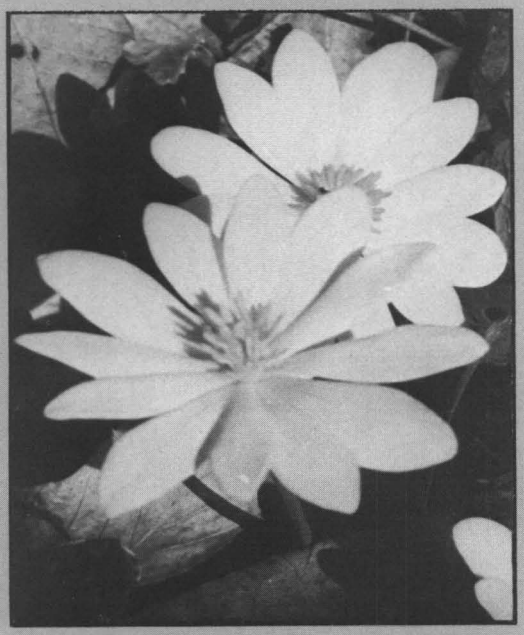

WILDLIFE AT ORNL BLOODROOT

Meetings:

Oak Ridge National Laboratory
P.O. Box X,
Oak Ridge, Tennessee 37830

MAJOR CONFERENCES SPONSORED OR COSPONSORED BY ORNL DURING 1972

Second Conference and Workshop on Embryonic and Fetal Antigens in Cancer — February 14–16

Co-Sponsor: National Cancer Institute
Chairman: N. G. Anderson

Fourth Annual Symposium on Advanced Analytical Methods for the Clinical Laboratory — March 9–10

Co-Sponsor: National Institute of General Medical Sciences
Chairman: C. D. Scott

Conference on Molecular Basis of Human Genetic Disease (Biology Research Conf.) — April 4–7

Chairman: J. D. Regan

Second Symposium on Sharing of Computer Programs and Technology in Nuclear Medicine — April 21–22

Co-Sponsors: Oak Ridge Associated Universities
Vanderbilt University
Society of Nuclear Medicine
Chairman: Betty F. Maskewitz

Health Physics Conference on Radiation Standards and Regulations — April 28

Co-Sponsor: Health Physics Society—East Tennessee Chapter

Immunology of Carcinogenesis Conference — May 8–11

Co-Sponsor: National Cancer Institute
Chairman: M. G. Hanna, Jr.

Blood Platelet Conference — June 1–2

Sponsor: ORNL
Chairman: T. T. Odell

International Woodlands Workshop on Ecosystem Analysis — August 14–27

Co-Sponsors: International Biological Program
University of Tennessee
Chairman: D. E. Reichle

12th USAEC Air Cleaning Conference — August 28–31

Co-Sponsors: Harvard Air Cleaning Laboratory
AEC's Division of Operational Safety
Chairman: M. W. First, Harvard Air Cleaning Laboratory

First Regional Workshop Seminar on State Emergency Planning in Relation to Licensed Nuclear Facilities — September 11–14

Co-Sponsor: U.S. Atomic Energy Commission
Chairman: Harold E. Collins, AEC-Washington

Germanium Crystal Growth and Detector Fabrication Workshop — October 2–3

Chairman: J. W. Cleland

16th Conference on Analytical Chemistry in Nuclear Technology — October 24–26

Chairman: L. J. Brady

AEC Conference on Pollution Control — October 25–27

Co-Sponsor: U.S. Atomic Energy Commission
Chairman: Frank Coffman, AEC-Washington

The Photosynthesis Conference listed in the Annual Report for 1970–71 was improperly titled. The listing should read: International Conference on the Photosynthetic Unit, Chairman: R. M. Pearlstein, ORNL.

Central
Research Library
Current Collection
DEC 28 1972